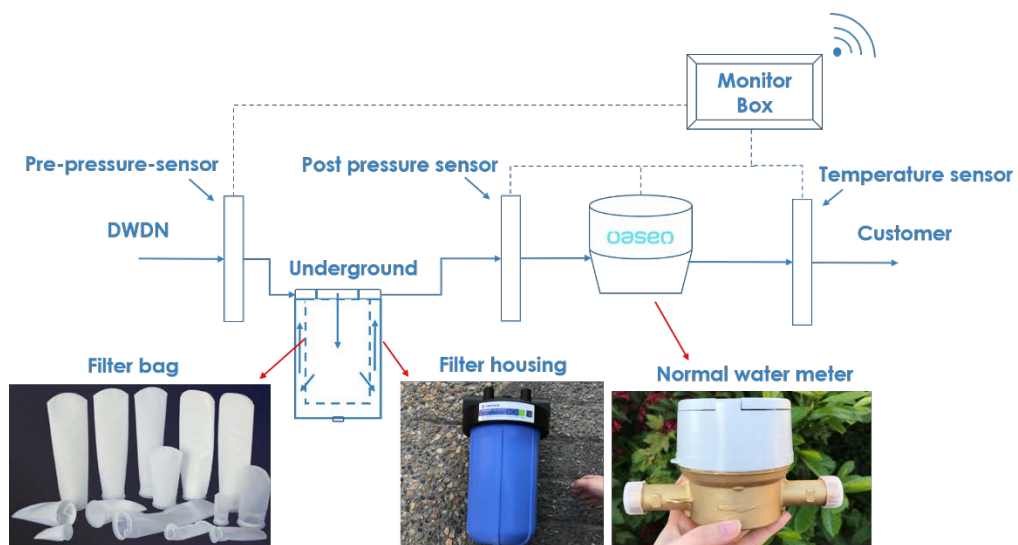


The Study of Potential Transition Effects on Water Quality During Distribution by Smart Water Meters (SWMs)



Jiaxing Fang
Master of Civil Engineering
Delft University of Technology

The Study of Potential Transition Effects on Water Quality During Distribution by Smart Water Meters (SWMs)

By

Jiaying Fang

Master of Science
in Civil Engineering

at the Delft University of Technology,
to be defended publicly on Monday May 28, 2018 at 3:00 P.M.

Committee:

Prof. dr. ir. J. P. Van der Hoek,
Assistant Prof. dr. ir. Gang Liu,
Assistant Prof. dr. ir. Edo Abraham,

Delft University of Technology
Delft University of Technology
Delft University of Technology

An electronic version of this thesis is available at <http://repository>.

Acknowledgement

Studying in TU Delft for a master's program offered me a great opportunity to enrich my knowledge on water treatment technologies as well as allowing me to unblock my potential to enrich myself. The critical thinking atmosphere and patient guidance from teachers here greatly encouraged my academic interests. My internship in the drinking water company Oasen provided me a wonderful chance to learn how to bridge the academic knowledge with real practice and allow me to experience how to efficiently work in a multi-lingual and cultural background environment. I would like to express my sincere appreciation to TU Delft and Oasen for their great support and tuition.

I am so grateful to be supported and helped during my thesis work. I would like to extend my gratitude first and foremost to Prof. dr. ir. J. P. Van der Hoek. Great appreciation not only for his patient supervision on academic aspects, but also for his kind response and warm encouragement when I was under struggling situation. I would like to give my sincere gratitude to my daily supervisor dr. ir. Gang Liu who helped me on building up critical thinking, scientific writing skills as well as how to take right actions in career life. I would also like to express my gratitude to dr. ir. Edo Abraham for his helpful comments during my thesis work. I would also like to acknowledge to my wonderful colleagues from Oasen, TU Delft, Vitens including Aaron Chan, Gang Liu, Harmen van der Laan, Dick van der Lagemaat, Harm Kien, Mariëlla Beker, Armand Middeldorp, Arjan Thijssen, Tea de Vries for their great efforts for field work help, experiment arrangement and coordination.

I would like to give my sincere thankfulness to my all dear friends both in the domestic and in Netherlands. Thanks for their continuous accompany and warm encouragement during my struggling period.

Finally, I must express my very profound gratitude to my parents providing me with unfailing support and continuous encouragement throughout my years of study and through the process of researching and writing this thesis. This accomplishment would not have been possible without their care and trust. Thank you and love you forever!

*Jiaying Fang
Delft, May 2018*

Abstract

Driven by the fast development of water purification technologies, tightening of water quality regulations and the increasing public concern on water-related health problems, drinking water companies have spared no efforts on treatment processes upgradation as well as striving on maintenance aspects. In the event of perturbation such as supply-water change in this study, historically harbored materials in drinking water distribution systems (DWDS), can potentially be converted into suspended materials and consequently delivered to end users, leading to a reduction on hygienic water quality.

In order to capture the potential occurrence of transition effects in a research area and figure out the impact as well as trace back its potential origination, Smart Water Meter is designed and developed with the integrated functions of on-line monitoring, sampling and real-time data communication detect and monitor potentially occurred physiochemical and microbiological water quality deterioration during supply-water change period. The improved Smart Water Meter consists of pressure sensors, temperature sensors, filter bag with 50-micron pore size, a normal water meter and a monitor box. Meanwhile, 3 batch of pipes sampling and 2 batch of filter bags sampling were carried out in time series to analysis and confirm the development and behavior of transition effect.

The results showed that new supplied water with low nutrients and particle load in the research area has triggered the occurrence of transition effects while the improved Smart Water Meters are capable to well capture the destabilized distribution network harbored materials (DNHM) in DWDS and prevent undesirable large particulate matter from reaching the consumers'. Besides, the triggered transition effect in this case was not violate and the temporal tendency of the microbiological and elemental parameters indicated the gradual settle-down of the transition effect. The cross comparison between the elements structure from pipe samples and filter bags, Ca and Fe are the dominate compounds in filtrates and indicates the destabilized DNHM could probably originated from detached biofilm and resuspended loose deposits since they the hotspots for calcium and iron respectively.

Key words: Smart Water Meter, supply-water change, drinking water distribution system, transition effect

Contents

ACKNOWLEDGEMENT	I
ABSTRACT	II
CONTENTS	III
LIST OF FIGURES	V
LIST OF TABLES	VII
LIST OF ABBREVIATIONS.....	VIII
1. INTRODUCTION.....	1
1.1 Project description.....	1
1.2 Drinking water distribution system.....	2
1.3 Bacteriology and water quality deterioration in DWDS.....	3
1.4 Transition effect.....	4
1.5 Objectives of this research.....	5
2. MATERIALS AND METHODS	7
2.1 Experiment area.....	7
2.2 Experiment tools.....	8
2.2.1 Smart Water Meter.....	8
2.2.1.1 Working principle.....	8
2.2.1.2 Pore size selection	9
2.2.2 Pipes.....	10
2.2.3 Filter bags.....	11
2.3 Experiment methods.....	12
2.3.1 Sampling timetable	12
2.3.2 On-line data monitoring.....	12
2.3.3 Data analytical methods.....	13
2.3.3.1 Pressure drops	13
2.3.3.2 Pipe samples.....	14
2.3.3.3 Filter bags	14
3. RESULTS.....	16
3.1 Pipe samples.....	16
3.1.1 Biological analysis.....	16
3.1.1.1 ATP.....	16
3.1.1.2 HPC.....	18

3.1.1.3	Aeromonas.....	20
3.1.2	Elemental analysis.....	23
3.2	Filter bags.....	27
3.2.1	Visual observation.....	28
3.2.2	Biological analysis.....	29
3.2.2.1	ATP.....	29
3.2.2.2	HPC.....	31
3.2.2.3	Aeromonas.....	32
3.2.3	Elemental analysis.....	34
3.2.4	ESEM.....	36
3.3	On-line monitoring.....	39
3.3.1	Pressure difference.....	39
4.	DISCUSSION	42
4.1	Comparison between filter bags.....	42
4.2	Comparison between pipe samples.....	43
4.2.1	Microbial.....	44
4.2.2	Elemental.....	46
4.3	Elemental comparison between pipe samples and filter bags.....	47
5.	CONCLUSIONS AND RECOMMENDATIONS.....	49
5.1	Conclusions.....	49
5.2	Recommendations.....	50
	BIBLIOGRAPHY.....	51
	APPENDIX A. MICROBIOLOGICAL PARAMETER DATA FOR PIPES AND FILTER BAGS	53
A.1	Pipe samples.....	53
A.2	Filter samples.....	54
	APPENDIX B. PRESSURE DROP RESOLUTION.....	56
	APPENDIX C. ESEM AND EDS RESULTS.....	59

List of Figures

Figure 1.1 Water purification processes at ZS Lekkerkerk before upgradation. (Conventional)	1
Figure 1.2 Comparison of purification procedures before and after upgradation.	2
Figure 1.3 Processes related to microbial growth in drinking water distribution system.	4
Figure 2.1 Location of pumping station and 4 sampling points in Lekkerkerk area.	7
Figure 2.2 Schematic of Smart Water Meter.	8
Figure 2.3 a) Smart Water Meter set-up; b) Smart Water Meter was installed in the ambient in a household.	9
Figure 2.4 Particle distribution in water samples from 3 locations in Lekkerkerk area.	10
Figure 2.5 a) Main pipe(PVC-U) sample with diameter of 110mm; b)Household connection pipes(HGPE) with a diameter of 25mm	11
Figure 2.6 a) Philips XL30 environmental scanning electron microscope instrument ; b) Tested filter bag pieces in the chamber.	12
Figure 2.7 Timeline for supply-water quality shift and sample activities	12
Figure 2.8 On-line data visualization of Smart Water Meter.	13
Figure 3.1 Biofilm ATP concentration for 1st batch pipe samples in June, 2017	17
Figure 3.2 Biofilm ATP concentration for 2nd batch pipe samples in September, 2017	17
Figure 3.3 Biofilm ATP concentration for 3rd batch pipe samples in December, 2017.	18
Figure 3.4 Biofilm HPC concentration for 1st batch pipe samples in June, 2017	19
Figure 3.5 Biofilm HPC concentration for 2nd batch pipe samples in September, 2017.	19
Figure 3.6 Biofilm HPC concentration for 3rd batch pipe samples in December, 2017	20
Figure 3.7 Biofilm Aeromonas concentration for 1st batch pipe samples in June, 2017	21
Figure 3.8 Biofilm Aeromonas concentration for 2nd batch pipe samples in September, 2017	22
Figure 3.9 Biofilm Aeromonas concentration for 3rd batch pipe samples in December, 2017	22
Figure 3.10 Biofilm metal elements concentration for 1st batch of pipes in June, 2017	23
Figure 3.11 Biofilm metal elements content proportion for 1st batch of pipes in June, 2017	24
Figure 3.12 Biofilm metal elements concentration for 2nd batch of pipes in September, 2017	25
Figure 3.13 Biofilm metal elements content proportion for 2nd batch of pipes in September, 2017	26
Figure 3.14 Biofilm metal elements concentration for 3rd batch pipe in December, 2017	27
Figure 3.15 Biofilm metal elements content proportion for 3rd batch pipe in December, 2017	27

Figure 3.16 Visual observation of 1st and 2nd batch filter bags sorting in distance order from L1 to L4.....	28
Figure 3.17 ATP concentration for 1st batch filter bags in September, 2017.....	29
Figure 3.18 ATP concentration for 2nd batch of filter bags in November, 2017.....	30
Figure 3.19 HPC concentration for 1st batch filter bags in September, 2017.....	31
Figure 3.20 HPC concentration for 2nd batch of filter bags in November, 2017.....	32
Figure 3.21 Aeromonas concentration for 1st batch filter bags in September, 2017.....	33
Figure 3.22 Aeromonas concentration for 2nd batch of filter bags in November, 2017.....	33
Figure 3.23 Metal elements concentration for 1st batch of filter bags in September, 2017..	34
Figure 3.24 Metal elements concentration for 2nd batch of filter bags in November, 2017..	35
Figure 3.25 Environmental Scanning Electron Microscope (ESEM) image for the 1st batch filter bags from 4 sampling locations.....	37
Figure 3.26 Environmental Scanning Electron Microscope (ESEM) image for the 2nd batch filter bags from 4 sampling locations.....	38
Figure 3.27 Comparison of pressure drop cross the filter bags during the operation of the 1st filter bag.....	39
Figure 3.28 Comparison of drop cross the filter bags during the operation of the 2nd filter bag.....	40
Figure 3.29 Comparison of temperature variation monitored by SWM within one day (2017/08/01) and the avergae temerature during a period (2017/07/27~2017/08/31).	41
Figure 4.1 Comparison of different batch of filter bag samples.....	42
Figure 4.2 Comparison of temporal ATP variation on main pipes from 4 sampling locations.....	44
Figure 4.3 Comparison of temporal ATP variation on household connection pipes from 4 sampling locations.....	45
Figure 4.4 Comparison of temporal elements contents and structure variation on main pipes from 4 sampling locations.....	46
Figure 4.5 Comparison of temporal elements contents and structure variation on household connection pipes from 4 sampling locations.....	47
Figure 4.6 Cross comparison on elements contents and structure between a) pipe samples and b) filter bags.....	48

List of Tables

Table 3.1 Biofilm metal elements concentration for 1st batch of pipes in June, 2017	23
Table 3.2 Biofilm metal elements concentration for 2nd batch of pipes in September, 2017	25
Table 3.3 Biofilm metal elements concentration for 3rd batch pipe in December, 2017	27
Table 3.4 Metal elements concentration for 1st batch of filter bags in September, 2017	34
Table 3.5 Metal elements concentration for 2nd batch of filter bags in November, 2017	35

List of Abbreviations

SWM	Smart Water Meter
DN	Distribution network
DWDS	Drinking water distribution system
ZS	Treatment plant (Dutch: Zuiveringsstation)
DNHM	Distribution network harbored material
PVC	Polyvinyl chloride
HDPE	High-density polyethylene
RO	Reverse osmosis
ATP	Adenosine triphosphate
HPC	Heterotrophic plate count
Ca	Calcium
Fe	Iron
Al	Aluminum
Mn	Manganese
As	Arsenic
P	Phosphorus
ESEM	Environmental Scanning Electron Microscope
EDS	Energy Dispersive Spectrometer
SS	Suspended solids
ICP-MS	Inductively coupled plasma mass spectrometry

1. Introduction

1.1 Project description

Supplying better water quality to customers is the everlasting aim of every drinking water company to strive efforts to and so do the Dutch drinking water utility Oasen. To further achieve this goal, they have launched a project called 'Oasen West' which involved Reverse Osmosis and aim at improving water quality as well as supply-water biological stability in one of the Oasen's western supplying areas. Actually, since the source water quality in the Netherlands is usually good enough that it is readily available, implementation of RO for drinking water production has not been widely applied in Netherlands. However, due to the fact that an increasingly raised chlorine concentration observed in western part resulting from saline water intrusion from North Sea and the assignable hard water problem in the supplying area, Oasen had finally made their decision to upgrade the purification process to RO after a pilot feasibility investigation at ZS Lekkerkerk.

The conventional water purification process at ZS Lekkerkerk (Figure 1.1) comprises of sprinklers responsible for aeration after anaerobic groundwater extracted from intake well Schuwacht and Tiendweg, followed by a two-step filtration process; pre-filtration (first filter) consists of a double layer of sand and anthracite while post-filtration (second filter) is a single media sand filter. Afterwards, filtrated effluent flow through the activated carbon to remove odor, taste, color producing compounds as well as organic micropollutants. UV disinfection destructs cell DNA at the final step to block potential micro-organism multiplications during Distribution network (DN) transportation.

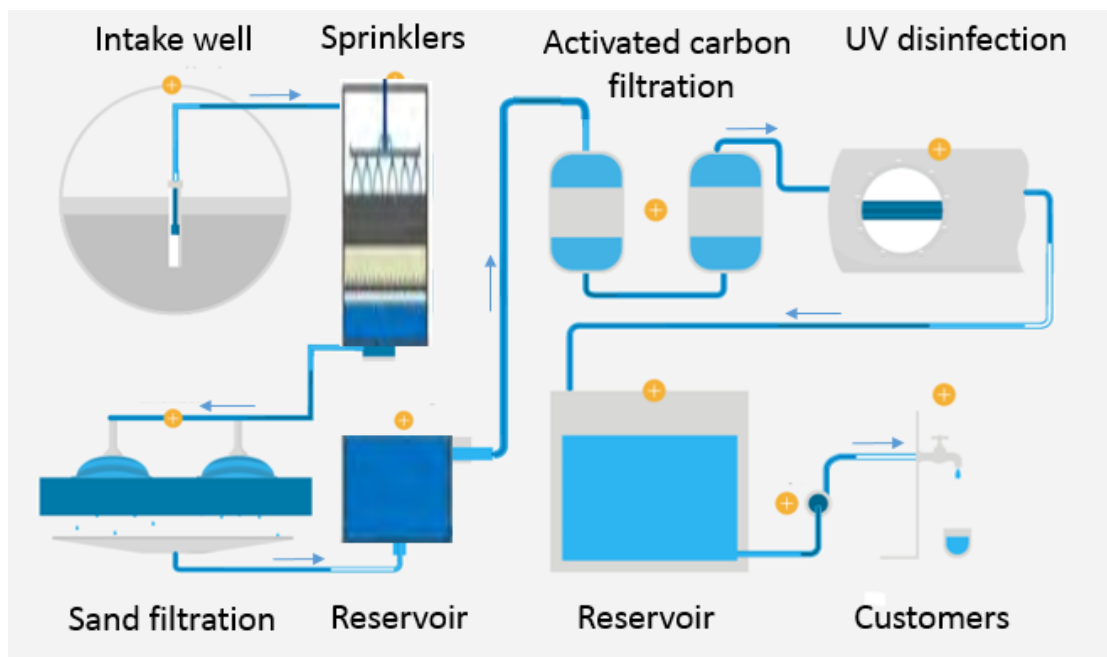


Figure 1.1 Water purification processes at ZS Lekkerkerk before upgradation. (Conventional)

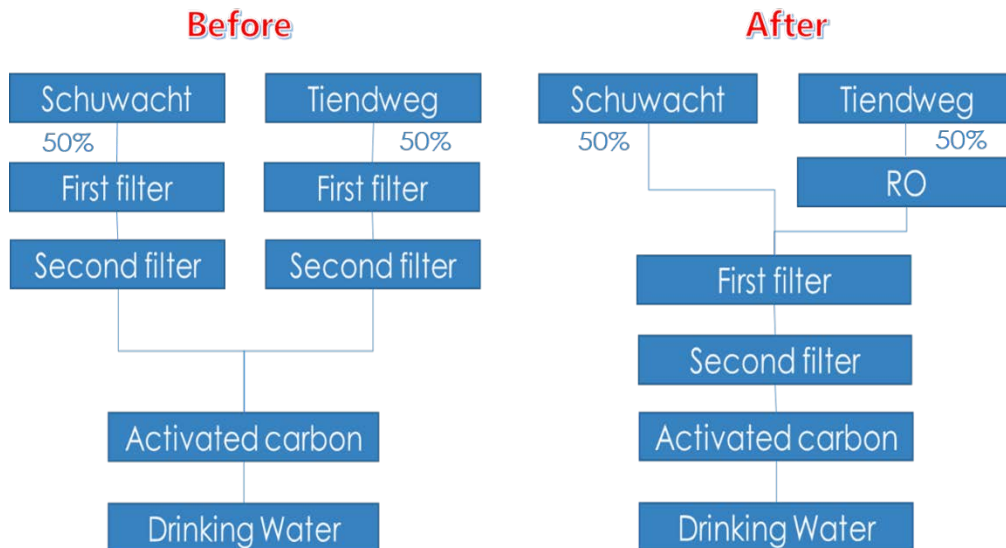


Figure 1.2 Comparison of purification procedures before and after upgradation.

Since June 2017, ground water from Tiendweg well, counting for 50% raw water, was first treated by RO before mixing with the other half raw groundwater extracted from Schuwacht. The mixed was then treated by the conventional treatment processes at ZS Lekkerkerk before injecting into the distribution system. Comparison of treatment procedures before and after upgradation is shown in Figure 1.2.

Previous study had convinced that RO application at ZS Lekkerkerk dramatically reduced the food source (nutrient load) for bacteria and positively improved biological stability (Dusseldorp, 2013). This is of course a desirable progress from the perspective of ensuring safe and high-quality water supply, but dramatic change in supply-water quality will in turn cause inevitable destabilization/restabilization of DWDS ecology. As a consequence, though water quality is promoted at treatment plants, it might still be deteriorated at customers' facets after distribution. Water meter clogging used to happen in one of Oasen's supplying areas and discourage the consumption experience on quality and pressure.

Additionally, Dutch drinking water is considered as a typical oligotrophic environment with the characters of extremely low nutrient load to hinder bacteria regrowth under the absence of disinfectant residuals (G. Liu, Verberk, & Van Dijk, 2013a). Such unique feature poses special difficulties to capture dynamic changes in DWDS, especially for particulate materials such as detached biofilm and resuspended solids, mainly related to low amount of material and the tremendous dilution effect brought by the countless water flushing through pipelines (X. Li, 2017).

In order to better understand the phenomenon and prevent it at an early stage, a solution could be to develop special devices that can sensitively seize changes as well as allowing for ex situ sampling and in situ monitoring.

1.2 Drinking water distribution system

Drinking water quality is not only subjected to source water quality and applied treatment processes. The well-treated drinking water is delivered to household via premise plumbing

and distribution mains and therefore, the drinking water distribution network(DN), as the final barrier, is responsible to ensure safe and high-quality drinking water at the end tap (G Liu, Van der Mark, Verberk, & Van Dijk, 2013). In general, a distribution network consists of drinking water distribution system (DWDS) and premise plumbing, basically including pipes, valves, meters, fittings, storage tanks, reservoirs and other hydraulic appurtenances (J. H. G. Vreeburg, Schippers, Verberk, & van Dijk, 2008). DWDS are usually multi-loop pipes buried underground with different materials, diameter and length. Many processes observed in DWDS such as pipe-wall biofilm formation and detachment, loose deposit formation as well as microbial growth are microbial in nature. Moreover, treated water injected into the distribution system is with a particle load, a microbial load and a nutrient load which means water quality at the customers' taps can only be as good as it in a water treatment plant, as a consequence of physiochemical and biological activities in DWDS(G. Liu et al., 2013a; I. J. H. G. Vreeburg & Boxall, 2007). Premise plumbing refers to the portion of potable water pipelines beyond the property line and in buildings including water meters, faucets, sprinkles, etc. Comparing to DWDS, premise plumbing is characterized as periodically stagnant environment with relative warmer temperature, higher surface to volume ratio, longer retention time and closer contact with water (Wang et al., 2017).

1.3 Bacteriology and water quality deterioration in DWDS

In accordance with previous studies, there is a broad consensus that ecology inside a DN can be subdivides as bulk water, pipe wall biofilm, suspended solids and loose deposit. Although water quality, as an everlasting heat public concern, has been substantially improved by emerging and updated treatment processes at plants over the recent decades, water entering the distribution systems flows inevitably with particles, microorganisms and nutrients(Gang Liu, Tao, et al., 2017; Proctor & Hammes, 2015). Thus, four niches including bulk water, suspended solids, loose deposits, pipewall biofilm, functioned as harbors (providing surface and nutrients to support microorganism growth) for microbial activities and particle accumulation in one sealed and pressurized DWDS and turned out to achieve an equilibrium after lengthy stable operation (Boe-Hansen, Albrechtsen, Arvin, & Jørgensen, 2002). Although environment inside a DWDS is considered as relatively stable, contents harbored subdivisions possess potential to reduce water quality when released under irregular operation and further leading to water quality deterioration at customers' sides. Every year, there were lots of such undesired water problems happened all over the world, such as the discolored water (I. J. H. G. Vreeburg & Boxall, 2007), deterioration of taste and odor(Dietrich, 2006), proliferation of opportunistic pathogenic bacteria(Emtiazi, Schwartz, Marten, Krolla-Sidenstein, & Obst, 2004; Feazel et al., 2009) and high inorganic compounds concentration(Gauthier, Barbeau, Millette, Block, & Prévost, 2001). Such water deterioration problems had pose threats to both food safety (if food industry is included in the area) and public health and were believed to be attributed to the accumulation of distribution network harbored material(DNHM) as well as the ongoing physiochemical and microbiological processes during pipe transportation. Figure 1.3 provided the related microbial activities happened between different niches during supply-water distribution(G. Liu, Verberk, & Van Dijk, 2013b; Proctor & Hammes, 2015).

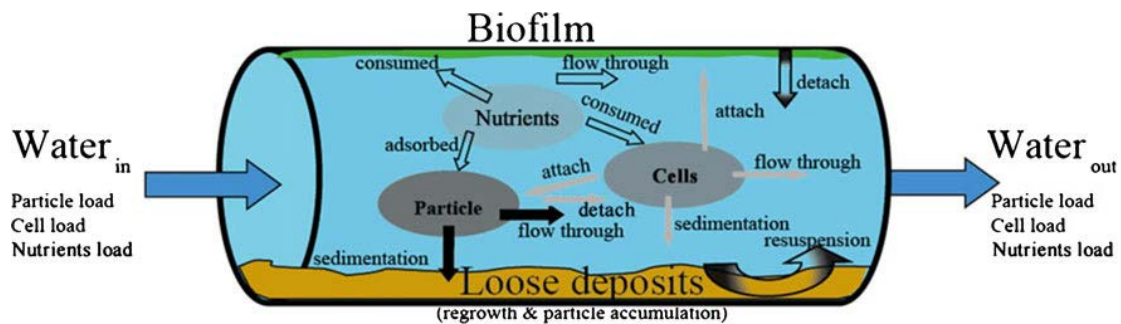


Figure 1.3 Processes related to microbial growth in drinking water distribution system.

1.4 Transition effect

It is widely believed that though the environment and ecology within a DWDS after decades operation is quite stable, while such stability is a dynamic equilibrium with parameter varying within acceptable range. Supply water quality change constitutes one of the attributions for the dynamic change. Furthermore, supply water quality change comprise of regular changes subjecting to daily fluctuation of feeding water, performance of treatment procedure, operationally related variations such as filter backwash, seasonally quality fluctuation of surface water (if applied as source water), annual switching of supply-water source as well as adjustment of mixing ratio of multi water sources (Gang Liu, Tao, et al., 2017; Gang Liu, Zhang, et al., 2017), and irregular changes, referred as promoted supply-water quality (Gang Liu, Zhang, et al., 2017), switch to an alternative source water (D. Li et al., 2010; Zhang, 2009) as well as implementation of a distinct disinfection strategy (Wang et al., 2014). Generally, fluctuations caused by regular changes still fall under the rubric of dynamic equilibrium. On the contrary, irregular changes usually come out with situations that are significantly differentiating from normal operation conditions and turned out to be undesirable esthetic or even public health issues under extreme conditions. Correspondingly, such consequence is accordingly denoted as transition effect referred as physiochemical and microbiological water quality problems attributed to the destabilization and mobilization of drinking water network harbored material (DNHM) and its release into bulk water (Gang Liu, Zhang, et al., 2017). It is noteworthy that since regular change of supply-water quality is considered as part of the cultivating environment for DNHM stabilization when the supply-water is continuously flushed out, fluctuations led by regular changes were not counted as transition effect.

Any external disturbance that could break the microbiological equilibrium in DWDS have the potential to trigger transition effects. These disturbances include but not limited to water quality change due to source water shift, treatment processes change, pipe material change, hydraulic condition change in DWDS (resulting in excessive flushing or depositing), etc. There are a lot of adverse consequences resulted from transition effect. For instance, the clogged water meter and insufficient water pressure at taps could undesirably affect customers' consumption experience and in turn, damage the reputation of water utilities; the leaching heavy metal elements such as Fe, Mn, Pb could pose health threats to customers, especially to some susceptible groups such as infants and the pregnant (Inkinen et al., 2014); the pathogenic microorganism enriched loosen biofilm or resuspended loose deposits might lead to high cell densities in tap water (Falkinham, Pruden, & Edwards, 2015; Feazel et al., 2009),

etc. Nowadays, increasing crisis of water resources, the tightening of water quality related regulations as well as the improvement of water purification technologies make transition effect more frequently observed all around the world. Discoloration led by source water switch in Tucson(Gang Liu, Zhang, et al., 2017) and Tampa(Tang, Hong, Xiao, & Taylor, 2006) in USA, extensive precipitation of iron oxides and iron-related bacteria caused by source water switch in Beijing(D. Li et al., 2010) as well as the famous 'Flint Water Crisis', resulting in high Pb and Legionella concentration, caused by both source water and purification procedure shift (Schwake, Garner, Strom, Pruden, & Edwards, 2016) are all typical witnesses of transition effect's adverse impacts. Therefore, it is of great importance to make effective evaluation for underlying transition effect before supply-water switch and set early-warning plans to cut down or even prevent adverse effect. However, so far only few researches have given insight into transition effect because the investigation requests for both the involvement of whole DWDS and an occasion of irregular water quality change. Opportunities to meet both access to a DN facing potential transition effect and the feasibility of taking spatially comprehensive pipe samples are quite limited. On second thoughts, almost all available studies include the abovementioned explored transition effect by batch sampling method after visible or noticeable indication observed at the end-users. Not to mention the time-consuming and money-costing analysis methods, the afterwards and discontinuous sampling method itself has a potential of losing valuable information since transition effect is an ongoing process. Therefore, developing an effective monitoring tool that is capable for online monitoring and easy operation at end users' is of urgent demand to better assess and understand transition effect.

1.5 Objectives of this research

Driven by the fast development of water purification technologies, tightening of water quality regulations and the increasing public concern on water-related health problems, drinking water companies have spared no efforts on treatment processes upgradation as well as striving on maintenance aspects such as aged infrastructure, cross connection, permeation and leaching, pipe repair, etc. (Gang Liu, Zhang, et al., 2017). In the event of perturbation, historically balanced microbiological environment can potentially be converted into suspended materials while carried to end users, leading to a reduction on hygienic water quality. However, as an emerging issue, transition effect potentially posing a consequence of water quality deterioration and accompanying public health problems, has so far been poorly documented. The available reports mainly focus on the features of the materials developed and harbored in DWDSs via batch sampling approaches because the destructive sampling methods make implication of measurement impossible and usually, access to real full-scale DWDSs are limited. Furthermore, all of them were post-investigations that conducted after the transition-effect-led phenomenon was obviously witnessed from wide aspects and to a large extent, missed valuable information on the formation and development of transition effect performed at an early phase.

The main objective for this study is to capture and study transition effect by employing Smart Water Meter throughout whole restablization process after supply-water change in Netherlands as well as giving possible indications for the origin of the destabilized DNHMs.

Smart Water Meter was first developed and commissioned as a reliable on-line detection and monitoring set-up to fulfill the call for on-site monitoring followed by installation at 4 individual dwellings in Krimpen aan de Lek and Krimpen aan de IJssel, responsible for physical parameters updating as well as periodical sampling throughout the whole process. Filter bags and pipe specimens from DWDS and premise plumbing before and after supply-water quality switch were collected as well to replenish a premise description. In general, all efforts were strived to answer the following research questions:

1. How can a Smart Water Meter be improved to ensure sampling under premise of no disturbance on water pressure regarding actual operation?
2. Will transition effect appear after supply-water switch in studying area?
3. What will the impact be on water quality and water meter clogging brought by transition effect?
4. Where do the entrapped particulate material originated from?

2. Materials and Methods

This chapter mainly focuses on what the Smart Water Meter looks like and how it works, the applied tools including filter bags, pipes and on-line monitoring system, how the pore size of the filter bag was selected as well as how the samples were taken and analyzed.

The Smart Water Meter study briefly consisted of 3 stages: preparation for formal experiments which was also denoted as pre-selection of filter pore size, on-site set-up operation as well as samples collection including both district distribution pipes and household connection pipes as well as filter bags replacement.

2.1 Experiment area

4 individual households located in Lekkerkerk in Netherlands, one of the supplying area of Oasen, had Smart Water Meter installed in their ambient for on-site experiments. Figure shows the locations where the experiments were conducted. These 4 locations, in accordance with distance from pumping station, were labelled as L1, L2, L3, L4 from proximal to distal shown in Figure 2.1.

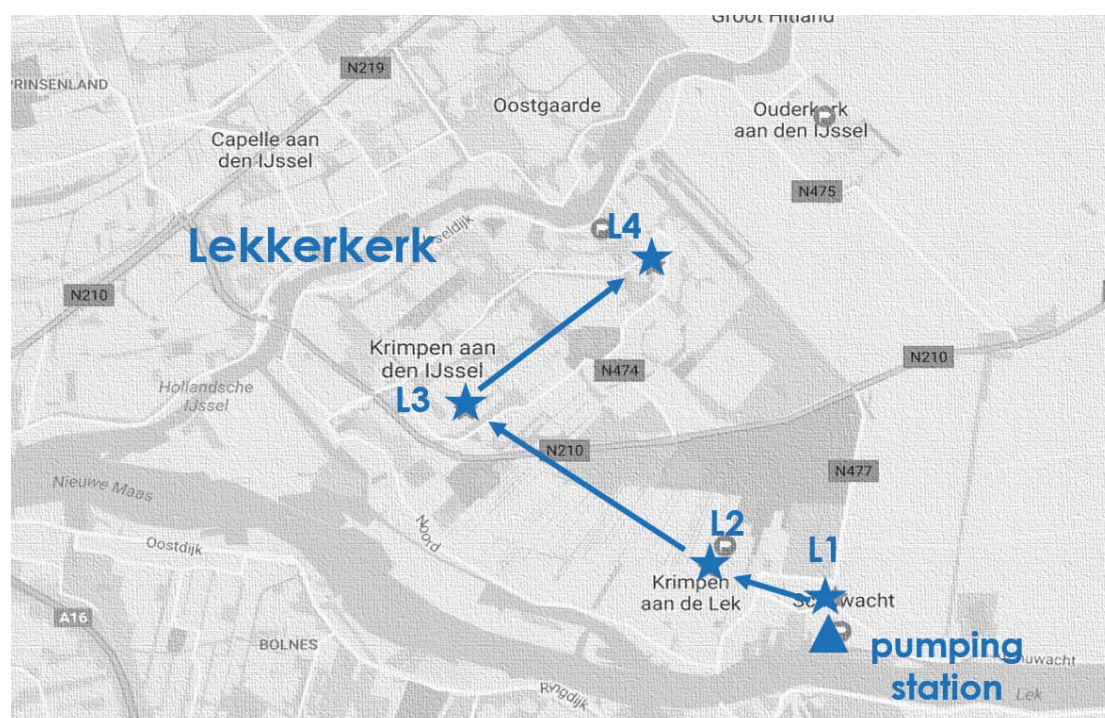


Figure 2.1 Location of pumping station and 4 sampling points in Lekkerkerk area.

2.2 Experiment tools

2.2.1 Smart Water Meter

2.2.1.1 Working principle

Smart Water Meter is an on-line equipment integrated the function of monitoring water temperature, pressure and consumption rate as well as intercepting the unexpected particles larger than the pore size during the transition effect period. In general, each Smart Water Meter consists of 2 parts, one is the monitoring system and the other one is the on-line updating system. As for the monitoring system, one Smart Water Meter is assembled with conventional water meter, a temperature sensor, two pressure sensors installed individually before and after the filter bag as well as a filter bag contained in a filter housing. There are also three valves included for sampling, filter bag replacement and maintenance. One of the highlight of the Smart Water Meter is its on-line updating system also known as monitor box. This panel is able to precisely log data for every 8 seconds and once accessing to an available internet such as Wi-Fi at customers', it can continuously update the logged data to our on-line data pool (with approximately 2-hour delay) and made it visualized through the website <https://oasen-monitor.nl/> to achieve a 24/7 monitoring without disturbing our customers. Figure 2.2 showed the schematic of the improved Smart Water Meter.

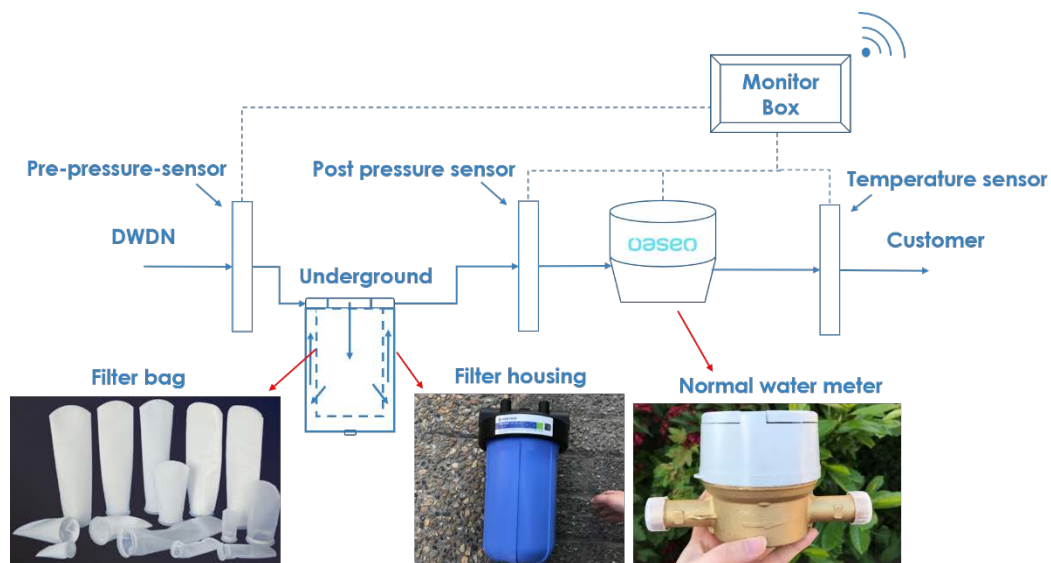


Figure 2.2 Schematic of Smart Water Meter.

The Smart Water Meter developed and applied in this study is shown in Figure 2.3. One set-up was operated in Water Lab at Tu Delft as pilot test for the influence from flow rate and water usage on pressure drop build-up while four set-ups were individually installed in the underground ambient at four households in one of the supplying areas of Oasen. In TU Delft, the monitor box connected to the internet via a router with a SIM card inside for portable and flexible installation while for the ones at sampling locations, monitor boxes got connected by accessing the household WiFi network.



Figure 2.3 a) Smart Water Meter set-up; b) Smart Water Meter was installed in the ambient in a household

2.2.1.2 Pore size selection

The main idea of a Smart Water Meter is to seize the detached biofilms under abnormal conditions while let most of the particles passing through the filter during normal operation to guarantee that residents' daily water consumption would not be disturbed. Therefore, choosing an appropriate pore size of the filter bag turned out to be an important premise for on-site operation. In order to pick an appropriate pore size that will smooth the subsequent experiment, water samples taken from the Lekkerkerk area from 3 households' taps were then analyzed for the particle distribution. The particle counter HIAC Royco 9703, working together with the Pharm Spec Version 2 software, was applied for particle counts and size distribution analysis. Based on light obscuration principle, HIAC Royco 9703 is able to accurately detect particles fall in the range of 2 to 400 micron. In this research, HIAC 9703 was set twice rinsing with ultrapure water before each measurement, and each measurement was conducted twice automatically twice with a 10ml sucked volume for each run time. For the sake of even distribution in volume, a magnetic bar under power rate 5 was applied for stirring. Figure 2.4 provided information about the distribution of particle size before the supply-water has been changed. According to the results, under normal condition more than 99.5% particles were distributed under 50 microns, only few large particles could be observed in Lekkerkerk's supply water. Since the purpose of Smart Water Meter was to seize potentially occurred large DHNM triggered by water quality change, hence the pre-selection of the filter bag pore size was determined as 50 microns. Adoption of filter bag instead of other filter medias such as filter disk was out of the concern of an appropriate run time. This is because comparing to the filter disk, the filter bag has larger surface for filtration and relative larger pore size, hence the run period for a filter bag can be longer. Moreover, the health certificate of the filter media has also been taken into account.

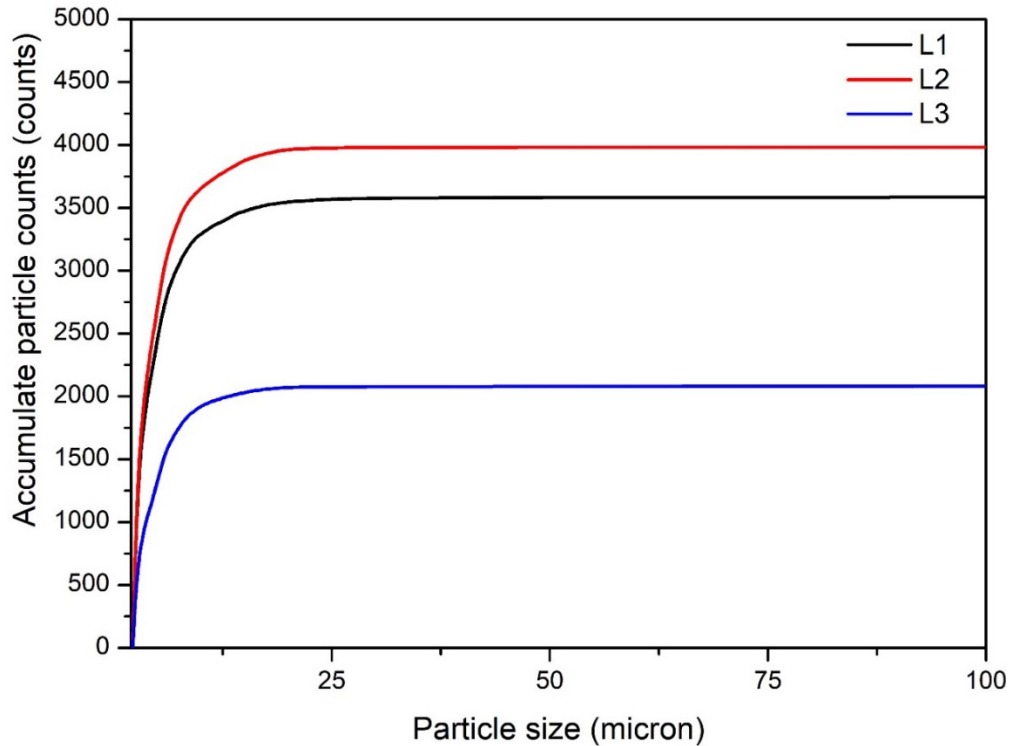


Figure 2.4 Particle distribution in water samples from 3 locations in Lekkerkerk area.

2.2.2 Pipes

Two groups of sampling were performed at each location. One for pipe sampling and the other for filter bag sampling.

For pipe samples, both district distribution pipes and household connection pipes at and/or near sampling location were dug out. Distribution pipes are pipes buried under district street responsible for water distribution within a certain area, and usually made of PVC with a typical diameter of 63~110mm while household connection pipes are those connect the distribution networks with water meters at the customers', most HDPE pipes with a relative small diameter of 25~32 mm (Figure 2.5). All district distribution pipes collected were 110mm PVC pipes except for a 50mm HDPE pipe at L1. All household connection pipes were 25mm HDPE pipes placed right in front of the water meters. These pipe wall biofilm samples were cut into 20~40cm specimens in duplicates and were closed with end caps as soon as they were removed from the distribution systems. Tap water (flushed until stable temperature) from customers' houses was filled in each specimen to maintain a humid. There were two batches of pipe sampling, before and after supply-water switch in Lekkerkerk area. For each batch of experiments, sampling time difference between distribution pipes and household connection pipes at each location was no more than 1 day.



Figure 2.5 a) Main pipe(PVC-U) sample with diameter of 110mm; b)Household connection pipes(HGPE) with a diameter of 25mm

The pipe specimens were pretreated with ultrasonication, which was 2mins each time, 3 times in total as well as emptying and refilling the pipe with DNA free water, to detach the biofilm from the pipe wall. The obtained suspensions were applied for further analysis including microbial measurements as Adenosine Triphosphate (ATP), Heterotrophic Plate Counts (HPC), Aeromonas, DNA extraction as well as 5 metal elements, Fe, Al, Mn, Ca, As, measured by ICP-MS. Pretreatments and measurements were conducted by Vitens Lab.

2.2.3 Filter bags

In order to track the influence of the supply-water switch in DWDSs, filtrates on filter bags were replaced approximately every 8 weeks depending on the customers' condition (the availability of each household, for example some of customers might be on vacation so the previously scheduled time could be delayed). Filter housing together with the old filter bag contained was to be replaced, after water was emptied, by a set of new filter housing and filter bag pre-rinsed by ultrapure water. The taken filter housing was then sealed with its original cap as sample deliver container. 30ml DNA free water was evenly poured over on a filter bag to keep filtrates from drying-out. All samples were delivered to the laboratory within 3 hours while pretreatment and analysis were conducted no more than 24h.

Pretreatment for microbial and chemical test were done separately for filter bags. Concerning the filtrates' uneven distribution on surface, 2 x 1cm² pieces of samples cut from each part, upper, middle, bottom, were prepared as 2 groups for pretreatment. For microbial analysis, each piece was filled with DNA free water till 90ml followed by sonification for microorganism detaching. Afterwards, the acquired suspension was used as 20µl for ATP, 1ml for colony number as well as 10ml for Aeromonas. For chemical analysis, the filter piece was placed in a 50 ml DNA free water and nitric acid mixture for ultrasonication. Then waiting 24h for all attached material falling into the liquid phase and the obtained suspension was ready for Fe, Mn, Al, Ca, As measurement accomplished by ICP-MS. All analysis was carried out in Vitens

Lab.

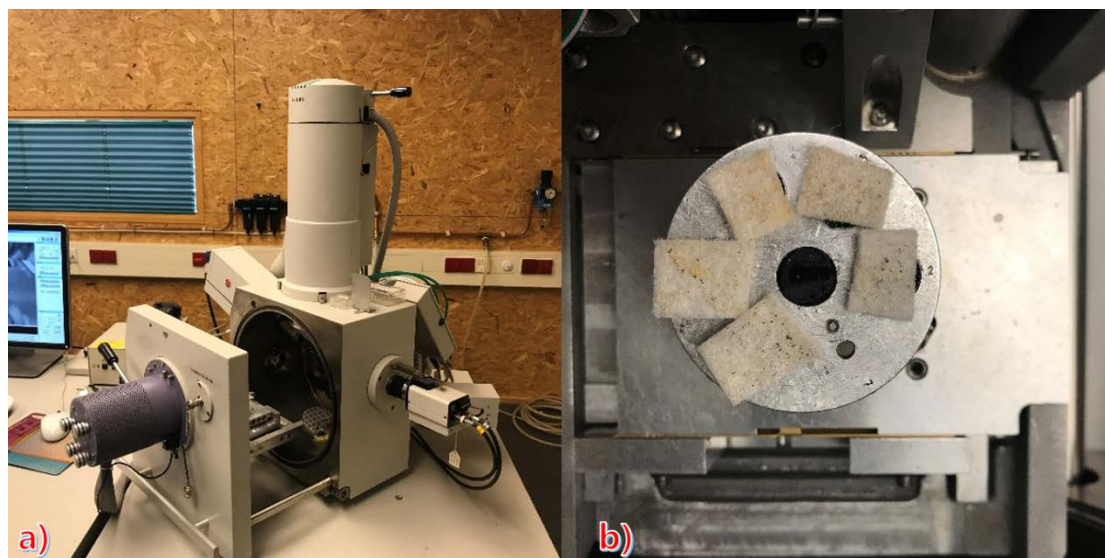


Figure 2.6 a) Philips XL30 environmental scanning electron microscope instrument ; b) Tested filter bag pieces in the chamber.

Besides, one piece for each filter bag was cut and reserved for ESEM and EDS test to gain an insight of the particle morphology and the elements distribution on the filter bag surface. The instrument is a Philips XL30 ESEM Tungsten filament electron microscope (Figure 2.6) with a magnification of 100 x ~50000 x that can work humid samples.

2.3 Experiment methods

2.3.1 Sampling timetable

For a better understanding, a timeline of supply-water switch, different batch of samples was provided in Figure 2.7.

	June	July	August	September	October	November	December
PS	1 st pipes			2 nd pipes			3 rd pipes
FB		Filter bags installation		1 st Filter bags		2 nd Filter bags	
	Supply Water Switch						

Figure 2.7 Timeline for supply-water quality shift and sample activities

2.3.2 On-line data monitoring

Besides all the equipment, an on-line monitoring website for real-time data visualization,

offering observers with on-site conditions including pressure, consumption and temperature, that can be easily told even just as a quick glance. The monitor took a measurement every 8 seconds and sent it to the website every minute which, as a consequence, amounted to an outrageous amount of data. Curves were displayed as automatically averaged data which is 1 minute for daily plots, 15 minutes for weekly plots, 2 hours for monthly plots and 1 day for yearly plots. Moreover, raw data download was also available via this page for further analysis. Figure 2.8 gives a direct look website for the data visualization for Smart Water Meter.

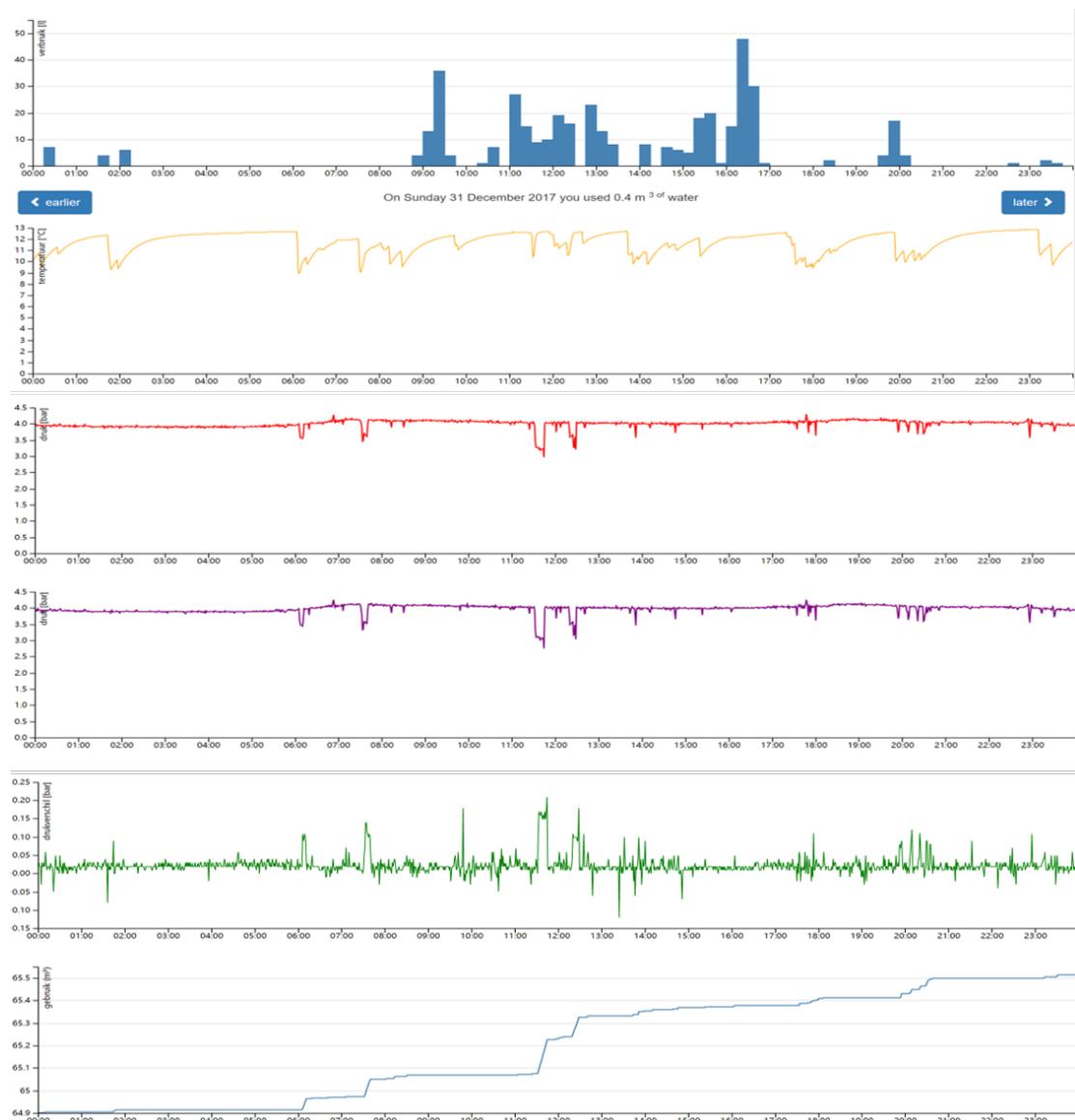


Figure 2.8 On-line data visualization of Smart Water Meter.

2.3.3 Data analytical methods

2.3.3.1 Pressure drops

For smooth visualization, monitored data from Smart Water Meter from all households were averaged on a 2-hours-base every operation period.

Water was only allowed one-way flow from DWDS to household and pressure difference before and after the filter bag was supposed to build up as particles accumulated on media surface. The pressure difference can be calculated by Equation 2.1.

$$\Delta P = P_{in} - P_{out} \quad \text{Equation 2.1}$$

Where: ΔP - water pressure difference

P_{in} -water pressure before filter bag

P_{out} - water pressure after filter bag

2.3.3.2 Pipe samples

Based on the pretreatment described above, the acquired suspension volume after biofilm detachment can be calculated by Equation 2.2.

$$V_s = \frac{4}{3}\pi d^2 \cdot l \quad \text{Equation 2.2}$$

Where: V_s - volume of suspension obtained after ultrasonication pretreatment

d - diameter of a pipe sample

l -length of a pipe sample

Total item content can be calculated by Equation 2.3.

$$T = V_s \cdot R \quad \text{Equation 2.3}$$

Where: T - total content of a certain measured parameter

V_s - volume of suspension obtained after ultrasonication pretreatment

R -volumetric content of a certain measured parameter in suspension

Specific surface area content can be acquired by Equation 2.4.

$$C = \frac{T}{\pi dl} = \frac{4}{3}\pi dR \quad \text{Equation 2.4}$$

Where: C -specific surface content of a certain measured parameter

d - diameter of a pipe sample

l -length of a pipe sample

2.3.3.3 Filter bags

Microbial and chemical analysis were separate for filter bags but sample size for both test was 1cm^2 . For each analysis, 3 pieces originated from top, middle and bottom respectively were measured and thus, the final result was presented as an average value.

Total accumulated amount of a tested item:

$$N = \left(\frac{R_t + R_m + R_b}{3}\right) \cdot V \quad \text{Equation 2.5}$$

Where: N -Total content of a certain measured parameter

R_t - volumetric content for the top of a certain measured parameter in suspension

R_m - volumetric content for the middle of a certain measured parameter in suspension

R_b - volumetric content for the bottom of a certain measured parameter in suspension

V - volume of suspension obtained after ultrasonication pretreatment

In this study, $V=90\text{ml}$ for microbial analysis, $V=50\text{ml}$ for chemical analysis.

Assuming all trapped filtrates come with water while taking water consumption into account, filtrates content can be calculated as:

$$C = \frac{N \cdot S}{Q} \quad \text{Equation 2.6}$$

Where: N-Total content of a certain measured parameter.

S- Inner surface area of the filter bag, constant as 480 cm^2 in this study.

Q- Water consumption volume of the corresponding household.

3. Results

The Smart Water Meter research was launched in March 2017 and is still in progress so far. Up to now, 23 district distribution pipe specimens and 22 household connection pipe specimens as well as 8 filter bag samples were successfully collected from 4 locations in Lekkerkerk area in 3 batches and 2 batches respectively from June to December in 2018. Meanwhile, physical parameters as pressure, pressure difference, temperature were continuously recorded and uploaded for each household. Biological and elemental results for pipe samples and filter bags will be displayed in section 3.1 and 3.2. In section 3.3, on-line monitoring data for 4 locations will be analyzed in 2 periods in terms of filter bag replacement.

3.1 Pipe samples

Pipe samples comprised of 110mm PVC district distribution pipes (except for L1, 50mm HDPE) and 25mm HDPE household connection pipes immediately before water meter. 7 distribution pipes and 8 household pipes were obtained in June before purification technology upgradation in ZS Lekkerkerk. Afterwards, duplicate specimens were collected for each type at 4 locations in September and December (no household samples at L4), respectively. District distribution pipes referred as main while household connection pipes referred as household in the following discussion.

3.1.1 Biological analysis

3.1.1.1 ATP

Adenosine triphosphate is an energy-rich compound existing in active biomass closely related to TCC and thereby is often adopted to determine active microorganism concentration. The ATP for 3 batch pipe samples were shown in Figure 3.1.

1st batch

The first batch of pipe samples taken before supply-water switch in DWDS and can be regarded as historical equilibrium. Both ATP in main and household pipes remained under 0.4 ng/cm^2 with main higher than household at all locations. No obvious trend was seen for main, only little fluctuation comparing to average. However, ATP on household pipes demonstrated a downwards trend along distance which could be attributed to the low nutrient load at the end of the system.

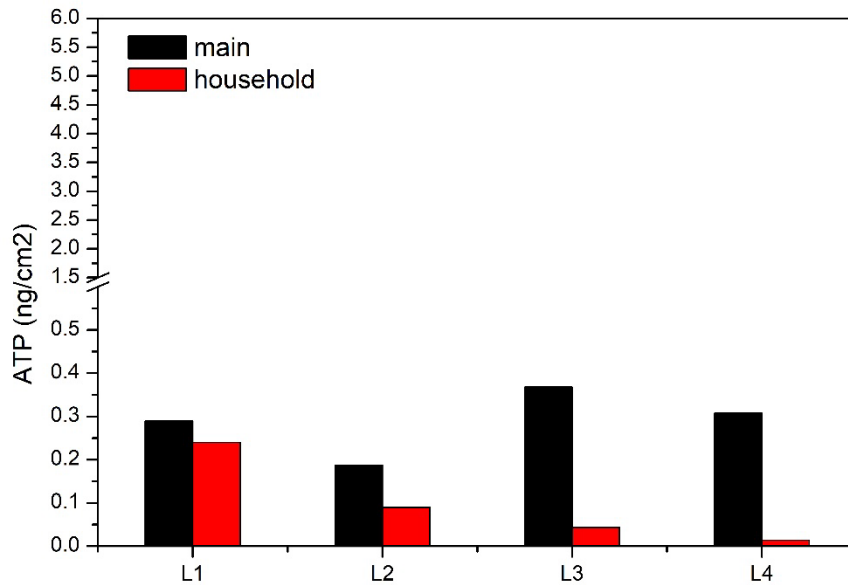


Figure 3.1 Biofilm ATP concentration for 1st batch pipe samples in June, 2017

2nd batch

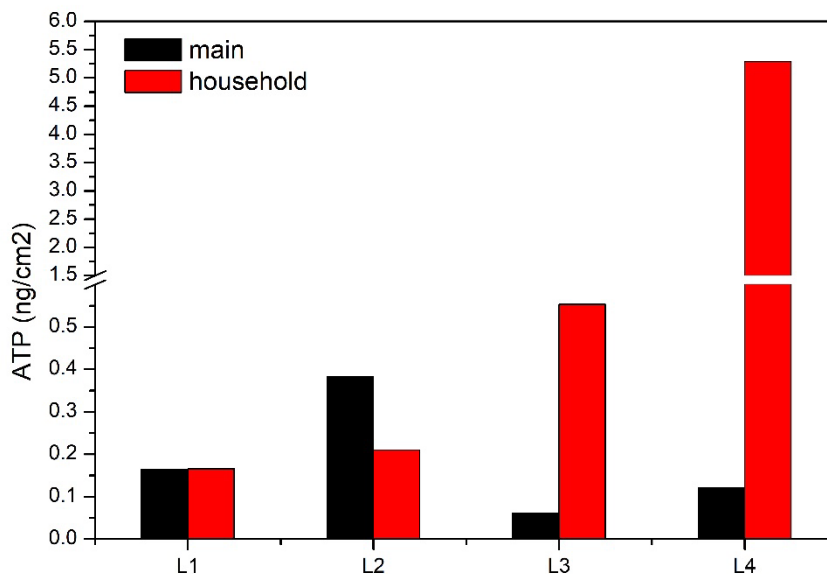


Figure 3.2 Biofilm ATP concentration for 2nd batch pipe samples in September, 2017

After 15 weeks' operation under the upgraded water quality, ATP varied significantly on both pipes. Main pipes still maintained its ATP level under 0.4 ng/cm^2 with a peak of 0.38 ng/cm^2 observed at L2 and the rest under 0.2 ng/cm^2 . For household pipes, a dramatic increase was witnessed from 0.17 ng/cm^2 to 5.29 ng/cm^2 along distance indicating the further the location, higher the microbial activity. This could also be attributed to the distinct hydraulic condition and water temperature due to independent water consumption habits of each household such as the different water consumption volume due to distinct family member number and different water consumption period.

3rd batch

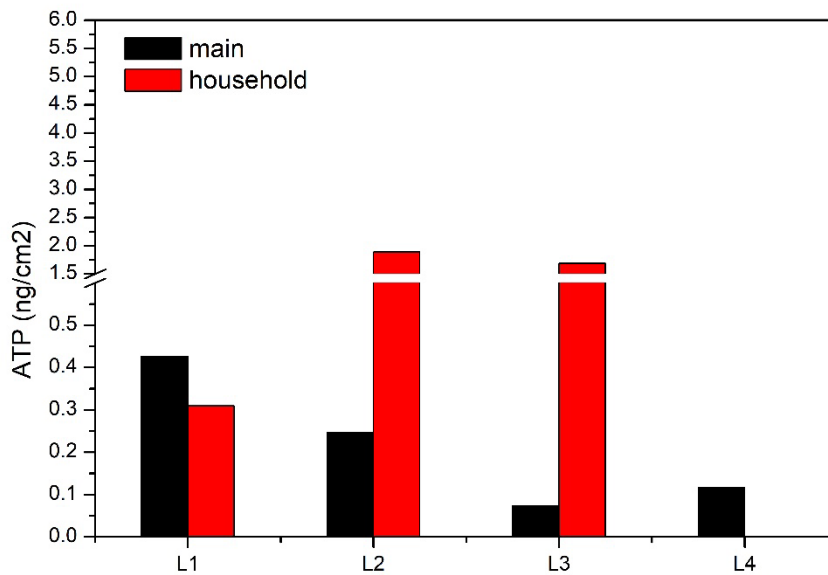


Figure 3.3 Biofilm ATP concentration for 3rd batch pipe samples in December, 2017

The 3rd batch of pipe samples were collected 5 months after supply-water switch and could to some extent, represented microorganism activity after restabilization. This is because normally 5 months is expected to be sufficient for a DWDS to gradually adapt to new conditions. Comparing to previous batch, ATP for main pipes remained almost the same low level expect for L1 slightly exceeded to 0.43 ng/cm². On contrast, ATP in household pipes increased in all collected samples indicating an increased active biomass concentration in household-pipe attached biofilm after restabilization.

3.1.1.2 HPC

Heterotrophic plate count (HPC) is a primary parameter for assessing the general microbiological quality in drinking water study via culture-based methods and targeting at cultivable microbial biomass which only amount for a small proportion (0.001~6.5%) in drinking water. HPC value for 3 batch of pipe samples were displayed in figure 3.4~3.6 and table 3.4~3.6.

1st batch

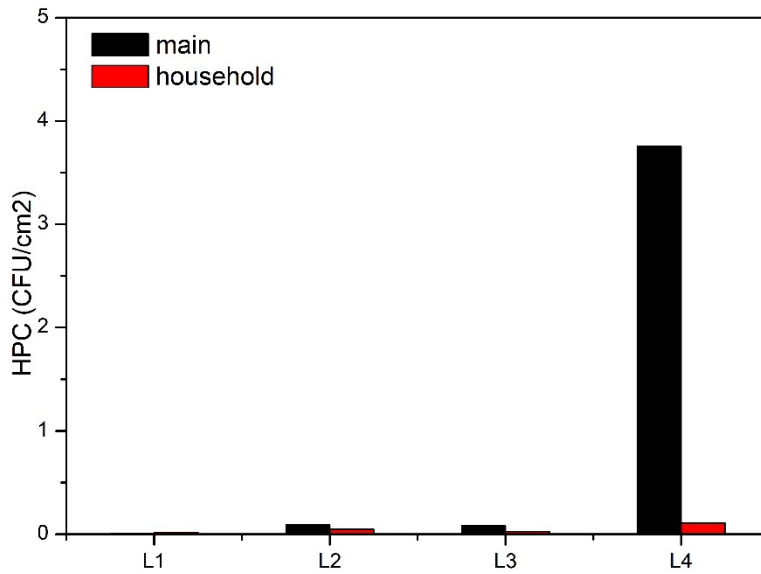


Figure 3.4 Biofilm HPC concentration for 1st batch pipe samples in June, 2017

As shown, HPC were rarely detected (most around 0 CFU/cm²) with exception to the distribution pipe at L4, though the value was still low. Household pipes were characterized for distinct hydraulic conditions such as frequent stagnation subject to customers' water consumption. So generally, the stagnation-occurred household connection pipes were supposed to possess higher HPC value than distribution with continuous water flow because stagnation can lead to HPC rise (Inkinen et al., 2014).

2nd batch

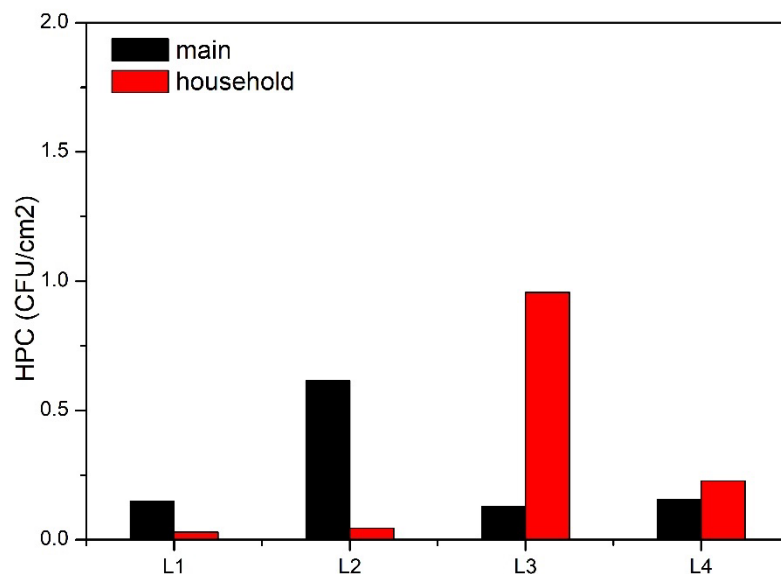


Figure 3.5 Biofilm HPC concentration for 2nd batch pipe samples in September, 2017

After flowing with upgraded supply-water for a while, main at L2 and household pipe at L3 were detected with a 1CFU/cm² value while the rest remained around 0 CFU/cm². Compared with the previous batch, though still maintained low, increase of HPC value was seen in terms of an average level and this is especially true main pipes and household pipes at the last 2 locations. However, the attribution of this unobvious variation might be the influence of the occurred physiochemical and biochemical processes during transitional period, but it might also resulted from the unevenly distributed microorganism communities either in the distribution pipelines or on the sample specimens. Household pipes was supposed to suffer more from latter since these samples of each batch were not collected from the exactly same household dur to the limited pipe replacement cycle.

3rd batch

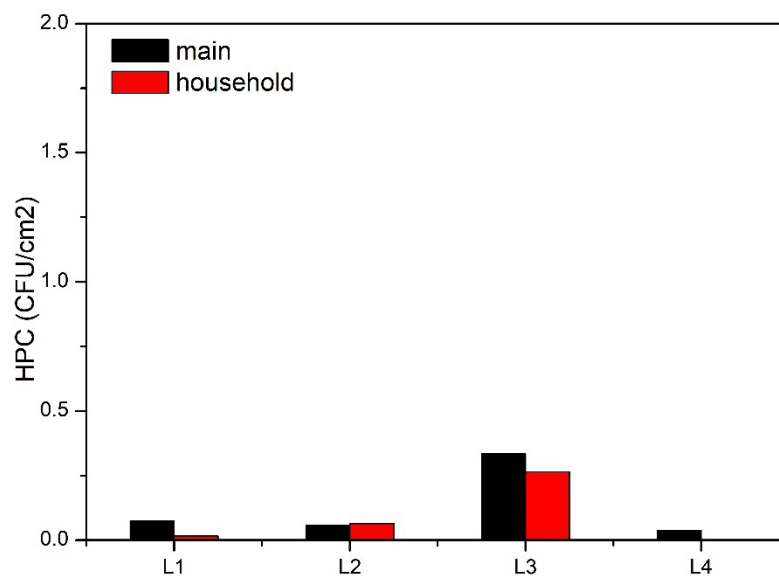


Figure 3.6 Biofilm HPC concentration for 3rd batch pipe samples in December, 2017

When it came to 5-month steady operation after RO application in Lek, both type of pipes was observed with low HPC value as close as 0 CFU/cm² manifesting that a new equilibrium of the microbial ecology was likely to be achieved under the upgraded oligotrophic environment.

3.1.1.3 Aeromonas

Aeromonas used to be an indicator for regrowth in DWDS. The detection limits in this study is 10 CFU/100ml. As shown in the figure, only some of the samples were detected by Aeromonas and pipes without detected Aeromonas were not of the same type, consisting both distribution pipes and household connection pipes. Moreover, it is corroborated in a previous research that loose deposits are hotspots for harboring Aeromonas in DWDS. Aeromonas(Gang Liu, Tao, et al., 2017).

1st batch

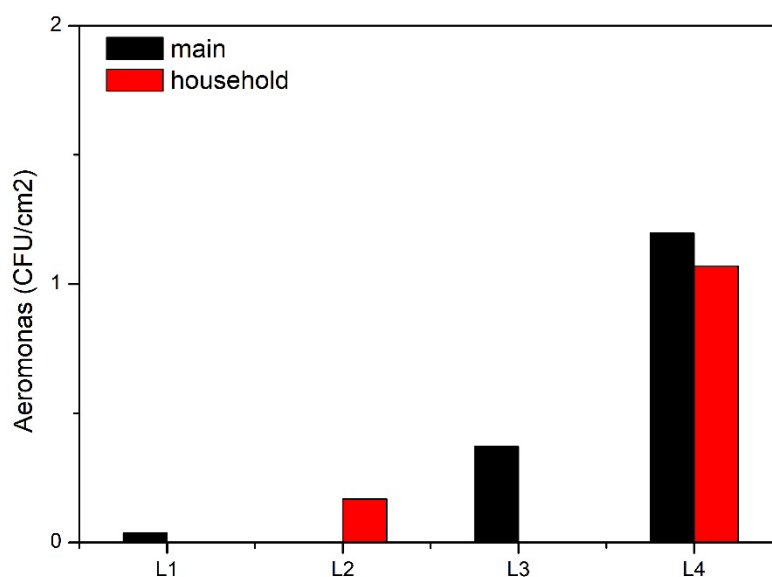


Figure 3.7 Biofilm *Aeromonas* concentration for 1st batch pipe samples in June, 2017

In order to cater to the unit request of the bacteria count, the calculated *Aeromonas* was rounded as integer. Therefore, as the level of pristine equilibrium, *Aeromonas* was detected as 1 CFU/cm² at L4 whereas that of main at L2, household at L1 and L3 was below detection line and the rest were observed with low level that can be regarded as 0 CFU/cm². An investigation has reported that loose deposits were the only niche for *Aeromonas* accumulation in an unchlorinated Dutch DWDS where *Aeromonas* was found under detection limit on biofilm attached either on PVC-U (referred as main) or HDPE (referred as household) pipe specimens (Gang Liu, Tao, et al., 2017). Thereby, the detected *Aeromonas* in this study was considered as an interference who could be either originated from water and loose deposits niches in filling-in water from consumers' taps or attributed to the residual loose deposits that was not fully gotten rid of.

2nd batch

After flowing with water of elevated quality with less particle load, nutrient load for 3 months, even less *Aeromonas* was witnessed at different location. Only three samples, who were main at L2, household at L3 and L4 were detected to possess low concentration under 0.2 CFU/cm² (rounding to 0 CFU/cm²). *Aeromonas* was below detection limit at L1. From a low-level perspective, *Aeromonas* decreased on an average level in all samples comparing to the 1st batch. However, *Aeromonas* has a low content in DWDS even before the supply-water switch and taking tap water as filling water from customers' taps have the possibility to introduce loose deposits (hotspots for *Aeromonas* in DWDS). Hence, the pristine low *Aeromonas* contents in pipe wall biofilms and their small variation as well as the inevitable disturbance of *Aeromonas* origin have made it hard to figure out the cause of this fluctuation.

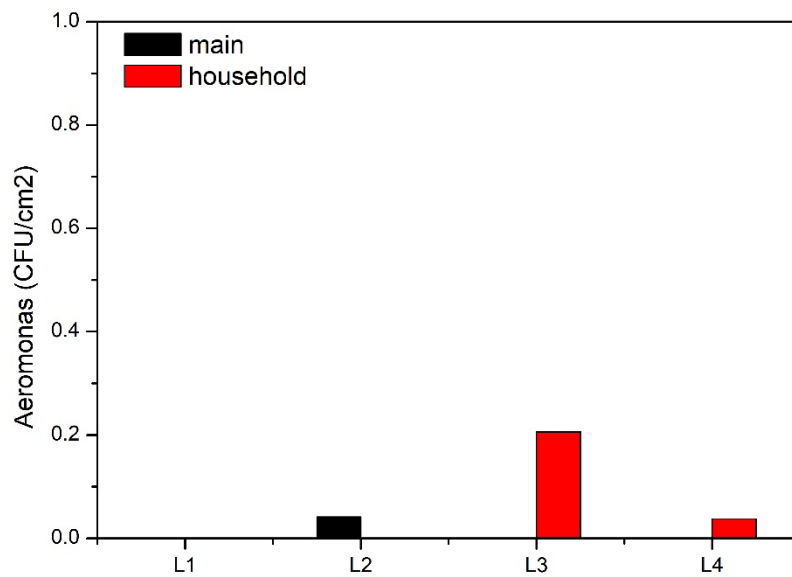


Figure 3.8 Biofilm Aeromonas concentration for 2nd batch pipe samples in September, 2017

3rd batch

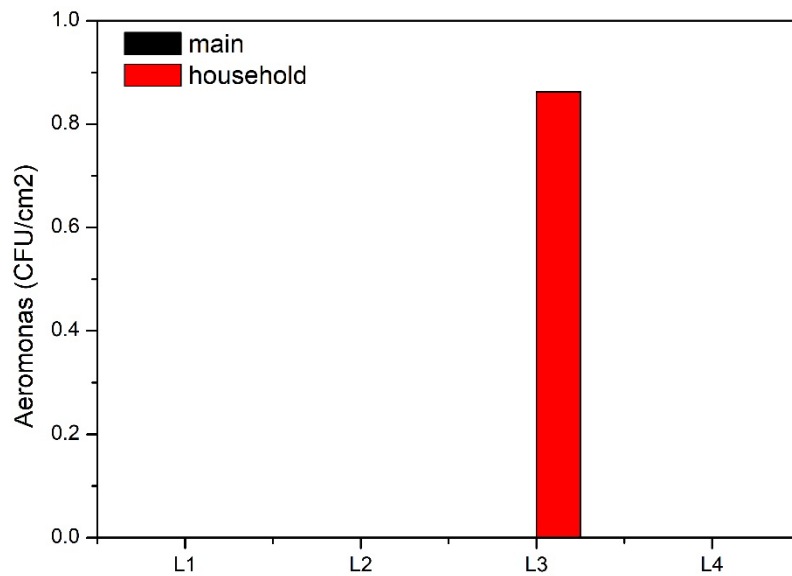


Figure 3.9 Biofilm Aeromonas concentration for 3rd batch pipe samples in December, 2017

As time went by, when it came to 5-months after supply-water switch, no Aeromonas was identified in biofilms excepted for household pipes at L3 with a content of 1 CFU/cm². Since DWDS has been pumped with improved water for quite a long period, new bio-chemical equilibrium was postulated to be established among different niches. The restablized biofilm niche in the research area reached a quite good agreement with that biofilm is not a Aeromonas hotspot. The 'outliner' in household at L3 was not caused by deviation between duplicate, but might a consequence of bulk water or loose deposits contamination from the

filling-in water utilized for maintaining biofilm humid.

3.1.2 Elemental analysis

For each location, the left and right stack column manifested the total metal elements for (main) distribution pipe and household connection pipe. There are 5 metal elements, including Fe, Mn, Ca, Al, AS, analyzed for the inner pipe wall biofilms from sampling area.

1st batch

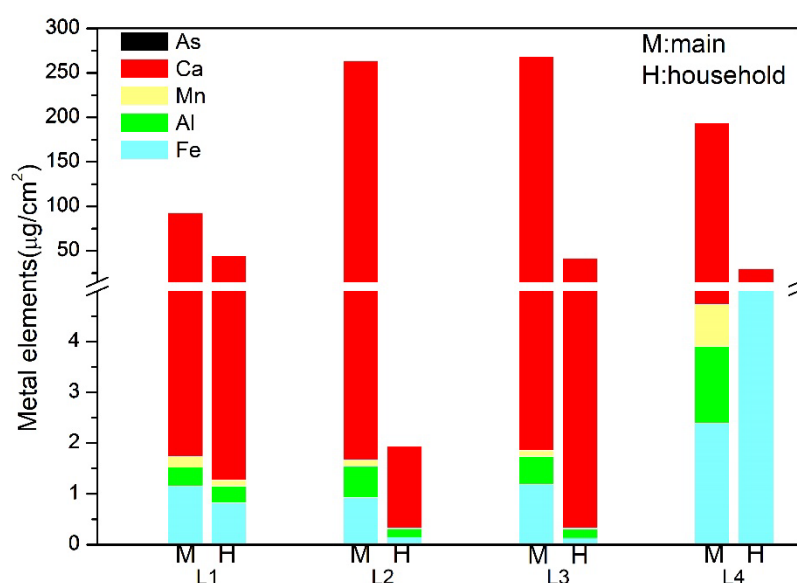


Figure 3.10 Biofilm metal elements concentration for 1st batch of pipes in June, 2017

Table 3.1 Biofilm metal elements concentration for 1st batch of pipes in June, 2017

Content(µg/cm ²)	L1		L2		L3		L4	
	Main	House	Main	House	Main	House	Main	House
Fe	1.15	0.83	0.93	0.14	1.18	0.13	2.39	11.24
Mn	0.21	0.11	0.12	0.02	0.12	0.02	0.83	1.77
Ca	90.59	43.09	261.81	1.60	266.74	41.36	188.84	15.75
Al	0.37	0.33	0.62	0.17	0.55	0.18	1.51	1.22
As	3.32E-03	2.06E-03	6.33E-03	1.18E-03	6.92E-03	1.11E-03	6.72E-03	3.78E-03

Generally, there were 2 tendencies shared among all samples, one was that biofilms in distribution pipes generally had higher metal content than household connection while the other one was that Ca was the predominate metal element in all samples irrespective of hydraulic condition and spatial location. To be more specific, Ca, Fe, Mn were the most abundant metal elements in biofilm observed in a descending order while the content of As were extremely low, of 3~4 magnitude lower than Fe. Apart from similarities, household pipes

at L2 was observed a total metal concentration smaller than $1\mu\text{g}/\text{cm}^2$, resulting from quite low contents of all elements, especially for Ca and Fe. Moreover, L4 manifested an obvious distinct metal composition structure comparing to other samples. The content of iron and manganese surged, but the total metal concentration didn't rise significantly, and even suffered a slight decrease. In terms of different pipes, main pipes possessed higher content in Ca, Al, As than household connection pipes.

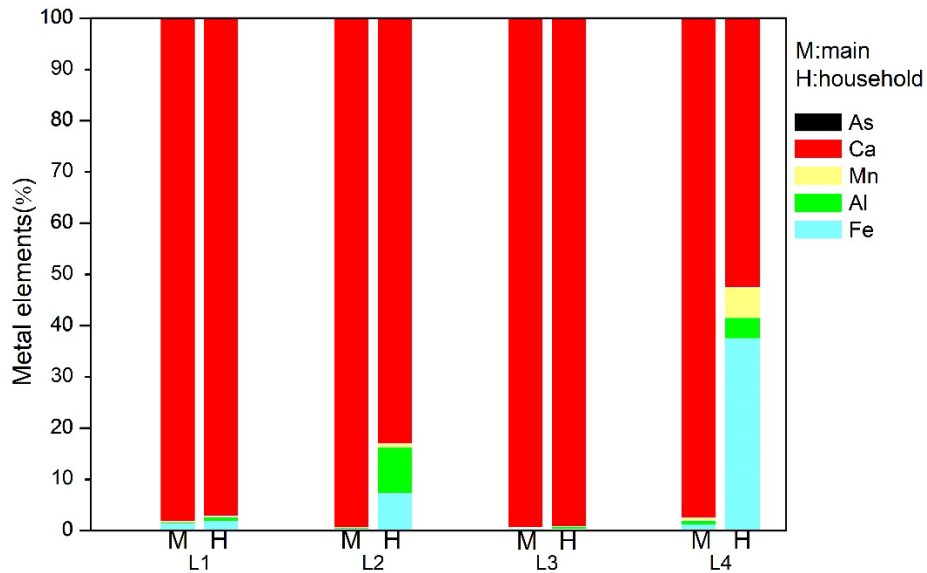


Figure 3.11 Biofilm metal elements content proportion for 1st batch of pipes in June, 2017

The observation of high Ca content in biofilm was in constituent with a finding that Ca performs a crucial role in biofilm formation under low substrates concentration (Hijnen et al., 2016). Accordingly, another investigation conducted in a Dutch unchlorinated drinking water distribution system also suggested that Ca was more often observed in biofilm rather than loose deposits (Gang Liu, Tao, et al., 2017). What also worth mentioning was that a related study in the same research area found out the total inorganic compounds (the same 5 metal elements), elevated towards the distal part of DWDS in bulk water phase. However, this tendency was not reflected in biofilm niche.

2nd batch

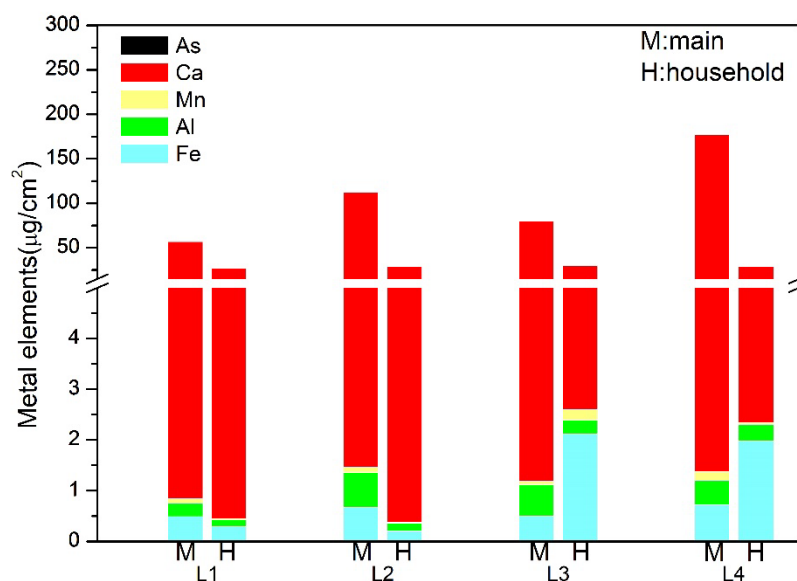


Figure 3.12 Biofilm metal elements concentration for 2nd batch of pipes in September, 2017

Table 3.2 Biofilm metal elements concentration for 2nd batch of pipes in September, 2017

Content(μ g/cm ²)	L1		L2		L3		L4	
	Main	House	Main	House	Main	House	Main	House
Fe	0.49	0.29	0.67	0.20	0.50	2.11	0.73	1.97
Mn	0.09	0.03	0.07	0.03	0.07	0.20	0.17	0.04
Ca	55.88	26.63	97.76	28.78	78.29	27.38	175.73	26.63
Al	0.27	0.13	0.68	0.15	0.62	0.28	0.48	0.33
As	2.65E-03	1.55E-03	4.81E-03	1.40E-03	3.12E-03	4.77E-03	7.50E-03	8.31E-03

Based on the columns depicted in the metal elements figure, total inorganic contents of main pipes fell in the range of 50~160 μ g/cm² while that of the household connection pipes stabilized around 45 μ g/cm². From comparison of the first two batch samples (see), the total inorganic metal elements content reduced on an average level and the constitute of metal compounds discriminated with the indigenous structure. Although calcium still possessed the predomination, contents such as iron, aluminum and manganese were witnessed to slightly account for higher proportion (but still low in proportion as compared to Ca) on an average level (L4 household pipe in not within this range). However, it is noteworthy that though the proportion of Al, Fe, Mn apparently increased, the content of each element decreased as total elements reduced. In other words, the content structure variation was rather attributed to those metals' lower release rates from biofilm comparing to calcium than their accumulation or adsorption onto pipe-wall biofilm. Higher the content was, faster the release ratio would like to be might be a reason why Ca was witnessed to have the most cut down.

Since new water submitted into pipeline system was characterized with less physical load and nutrient load, it was reasonable to say that the accumulated metal compounds on biofilm niche were likely to be released to the bulk water phase characterized as super oligotrophic

environment, driven by the disturbed dynamic equilibrium between different niches.

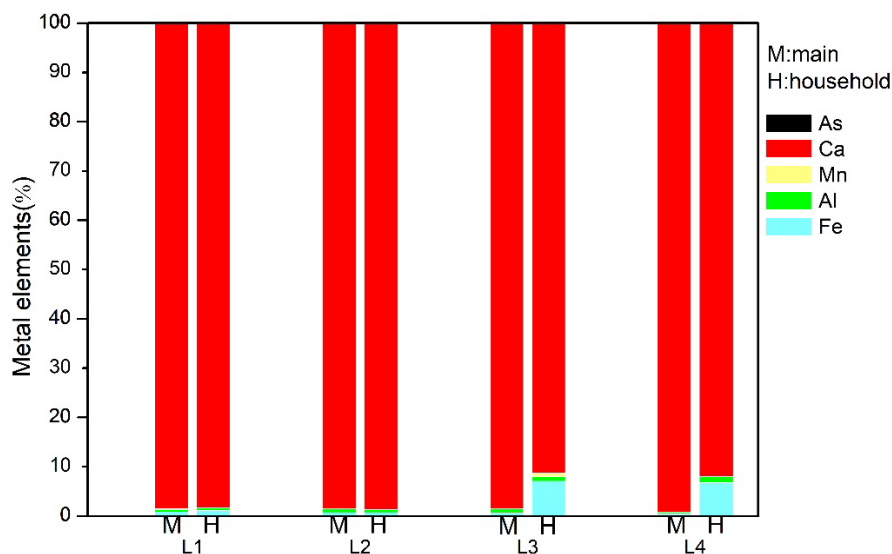


Figure 3.13 Biofilm metal elements content proportion for 2nd batch of pipes in September, 2017

Moreover, it was also reported that a decreased biofilm activity could lead to the release of accumulated Fe and Mn while with increased biofilm activity came an increase in Fe and Mn accumulation in an lab scale reactor in Australia (Ginige, Wylie, & Plumb, 2011). The ATP of the 2nd batch indicated that the biofilm activity remained the same level on main pipes but went up a little bit on household pipes while elements contents were only observed decrease comparing to previous batch. The discrimination could probably have resulted from that the amount of Fe and Mn increase boosted by the little biofilm activity increase could not overcome the release caused by the disturbed balance outweighed and hence, the final consequence turned out to be decreased.

3rd batch

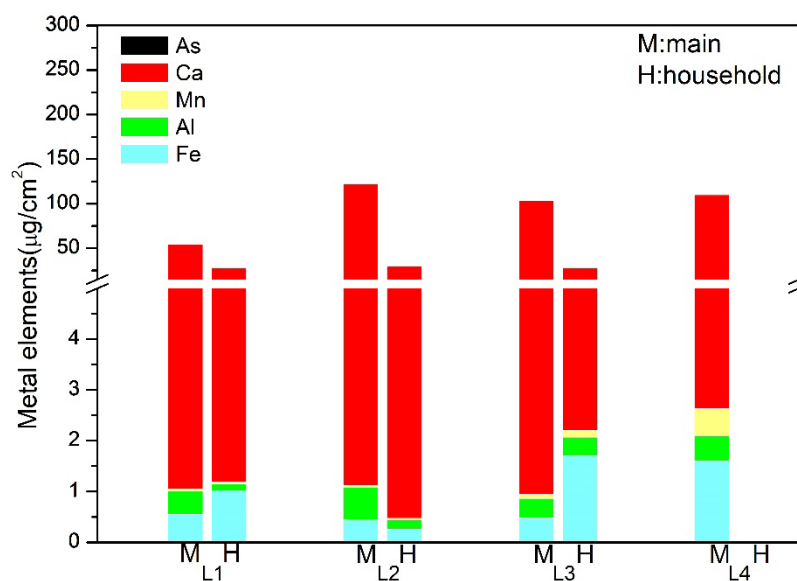


Figure 3.14 Biofilm metal elements concentration for 3rd batch pipe in December, 2017

Table 3.3 Biofilm metal elements concentration for 3rd batch pipe in December, 2017

Content(μ g/cm ²)	L1		L2		L3		L4	
	Main	House	Main	House	Main	House	Main	House
Fe	0.55	1.02	0.44	0.26	0.48	1.71	1.60	/
Mn	0.05	0.03	0.02	0.03	0.08	0.13	0.53	/
Ca	53.24	26.66	121.09	29.28	102.88	25.45	107.22	/
Al	0.46	0.13	0.65	0.19	0.37	0.36	0.50	/
As	4.40E-03	2.09E-03	4.39E-03	1.89E-03	8.53E-03	7.35E-03	8.16E-03	/

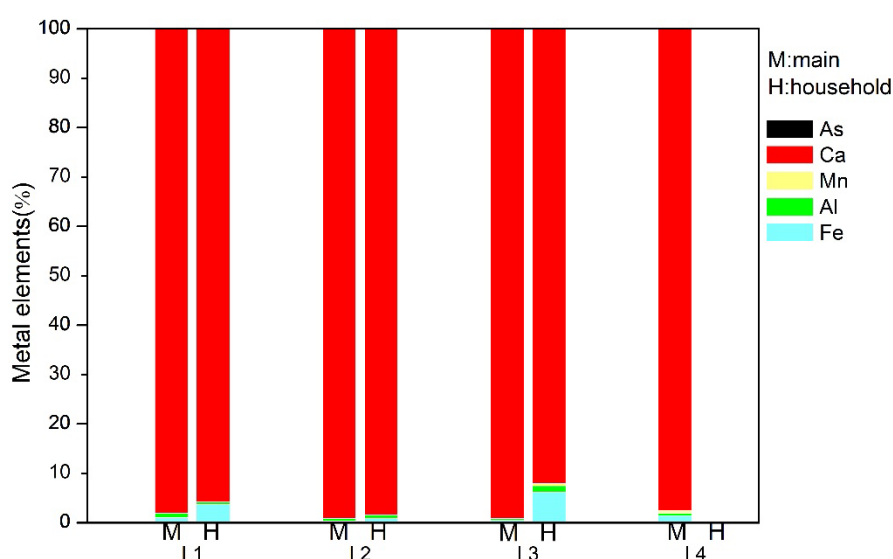


Figure 3.15 Biofilm metal elements content proportion for 3rd batch pipe in December, 2017

According to the shown columns and values, no significant changes were observed for elements contents as well as compounds structure comparing to the previous batch. For main pipes, total metal element contents were slightly dropped to 50~125 μ g/cm² with elements presenting in an descending order of Ca, Fe, Al, Mn, As. For household pipes, the contents were almost the same as before, stabilized at 45 μ g/cm², with a slight increase in Fe proportion. The insignificant variation in both contents and structure implied a new equilibrium was likely to be achieved after supply-water quality upgradation.

3.2 Filter bags

On one hand, due to the concern of not discouraging consumers' water usage experience, sufficient water pressure at taps was supposed to be guaranteed. On the other hand, if the pressure drop built up too quick on the filter media, the short running period and frequent replacement would also unfavored for customers' and water utilities. Based on the combined concerns, filter bags with a pore size of 50 micron was proposed for application in order to take advantages of its high surface, large flow and long operation cycle. The purpose of the

filter bags are to prevent appeared large particulate matters from reaching consumers' taps when potential transition effect happened after supply-water switch while allow water as well as small particles flush through under normal supply conditions. Due to safety concerns, filter bags adopted here were certificated to be utilized for food industry and the material harmless for human health. 放进 methodology

3.2.1 Visual observation

The 1st batch of filter bags were applied from 25th July for L2~L4 and 4th August for L1 until 27th September for all locations while the 2nd batch ran through 27th September to 13th December. For each running period, only one filter bag was applied in the ambient at each location so no duplicate available for filter bag samples.



Figure 3.16 Visual observation of 1st and 2nd batch filter bags sorting in distance order from L1 to L4.

The filter bags collected from 4 locations in 2 batches were demonstrated and compared in Figure 3.13. In terms of the 1st batch samples, there were macroscopic solids entrapped on all filter bags with colors of gradually turned darker from proximal to the distal part of the pipeline. This indicated that large particulate materials appeared in the presence of external disturbances such as supply-water quality change can be well captured by filter bags. And based on the shade of the color, further the site located from the pumping station, more particles were captured. This finding complied well with On-line Particle Sampling System (OPSS) research conducted in the same area (X. Li, 2017). On one hand, the long transportation routine for the end-points in DWDS increased the chance of involving more planktonic materials originated from pipe-wall biofilms or loose deposits that had potential to convert into suspended solids. On the other hand, the potentially happened biochemical

reaction such as coagulation or flocculation under Fe presence as well as the low flow rate also made the higher accumulation of particles at the distal reasonable. Colors of the trapped material were more yellowish at the first location while darker at the last two. It was also noteworthy that the shapes of the captured material were distinct for different locations. At L1 and L4, particles were characterized as dot-like particles in different size whereas for L2 and L3, solids were prone to attach to the surface in a sheet-like form.

When it came to the visual inspection of the 2nd batch, the colors of the filter bags turned lighter, especially for L3 and L4, compared to 1st batch, implying less presence of particulate materials in DWDS after new equilibrium was reached. L1 and L2 were inspected with yellowish particles both on top and bottom of the filter bags while L3 and L4 were even cleaner with a few particles distributed mainly at the bottom.

Since these batch of filter bags ran for a comparable period before replacement, less filtered solids confirmed the elevation of water quality at consumers' sides in terms of particle load.

3.2.2 Biological analysis

Discriminated from the pipe samples, biological and elemental contents on filter bags highly dependent on the amount of water consumption at each household. In order to make the results can be compared, results for biological and elemental analysis were normalized by their corresponding water consumption and the results were presented in the unit of content per liter.

3.2.2.1 ATP

1st batch

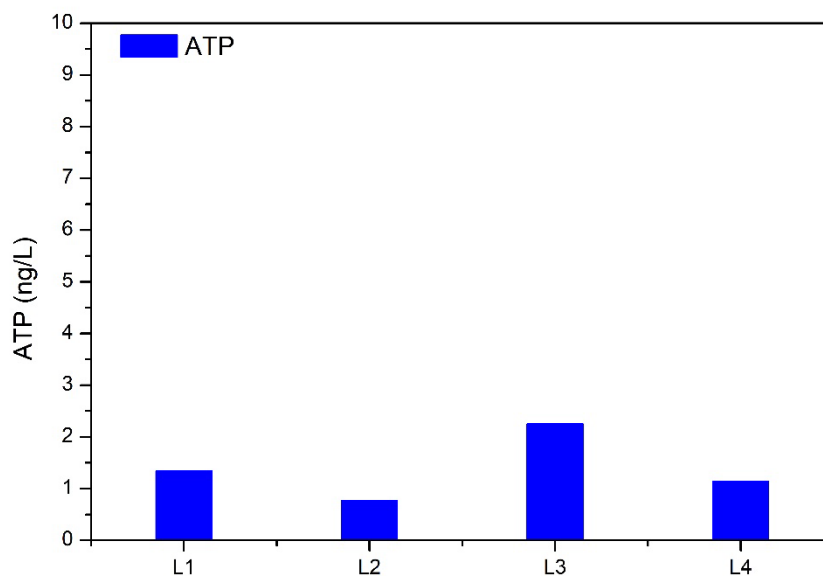


Figure 3.17 ATP concentration for 1st batch filter bags in September, 2017

In the first period, ATP was detected below 3 ng/L. The highest microbiological activity peaked out at L3 with a value of 2.25 ng/L while the rest in the descending order was 1.34 ng/L, 1.14 ng/L, 0.77 ng/L for L1, L4 and L3, respectively.

2nd batch

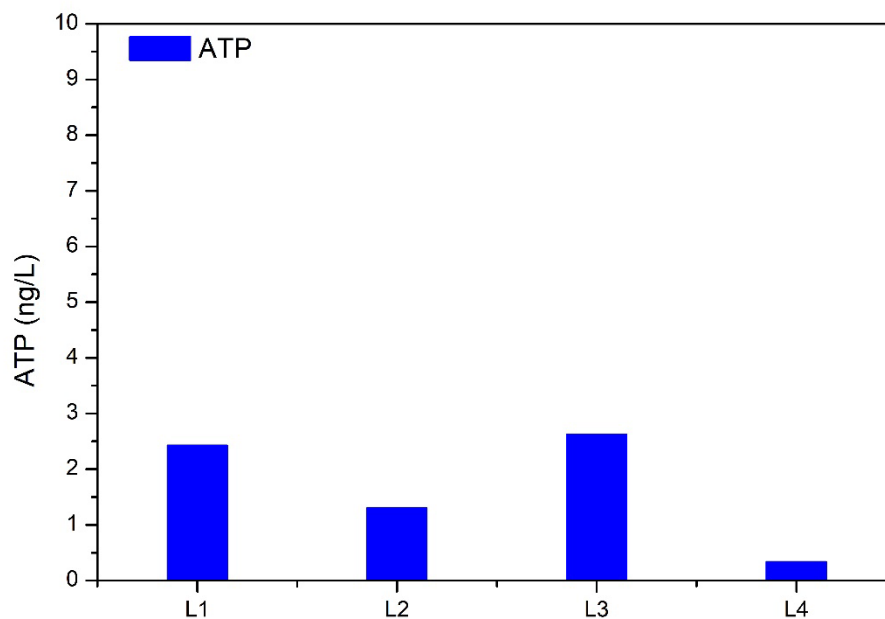


Figure 3.18 ATP concentration for 2nd batch of filter bags in November, 2017

For the second batch flushed with water that transition effect was supposed to be gradually settle down, ATP concentration on filter bags at each location was quite comparable with the previous with insignificant fluctuation. Synonymously, L3 still possessed the highest ATP content of 2.63 ng/L followed by 2.43 ng/L at L1, 1.30 ng/L at L2 and 0.34 ng/L at L4. The first 3 locations were observed a more or less increase while the last location had a decrease. But all variations were presented in a quite small range which can be regarded as comparable to 1st batch.

Since the results were normalized with consumed volume, it was supposed to be comparable or no larger than the ATP concentration on particulate materials delivered by water. However, upgraded water injected into the DWDS at the pumping station was detected with a ATP concentration around 1.2 µg/L. Besides, ATP contents on the particles was reported to account for 1~2% of that in water hence the supposed ATP in filtrates would be 0.05~0.5 ng/L. It was also worthy to point out that, according to a related research applying filter disks with a pore size of 1.2 micron filtering water from the main pipes in DWDS, the obtained ATP from the filtrates fall in the range of 0 to 0.2 ng/L in Lekkerkerk area which is much lower than that of this study (X. Li, 2017). One hypothesis for this high ATP concentration on filtrates was that the large surface of the filter bags and the episodically occurred stagnation provided favorable condition for biomass cultivation. The actual cause of this phenomenon still remained to be found. Although this was suppressed under an acceptable level and the filter

bags worked as final barrier hindering the active biomass from reaching the consumers, this contentious aspect should be pay more attention to and eventually eliminated in further improvement.

3.2.2.2 HPC

1st batch

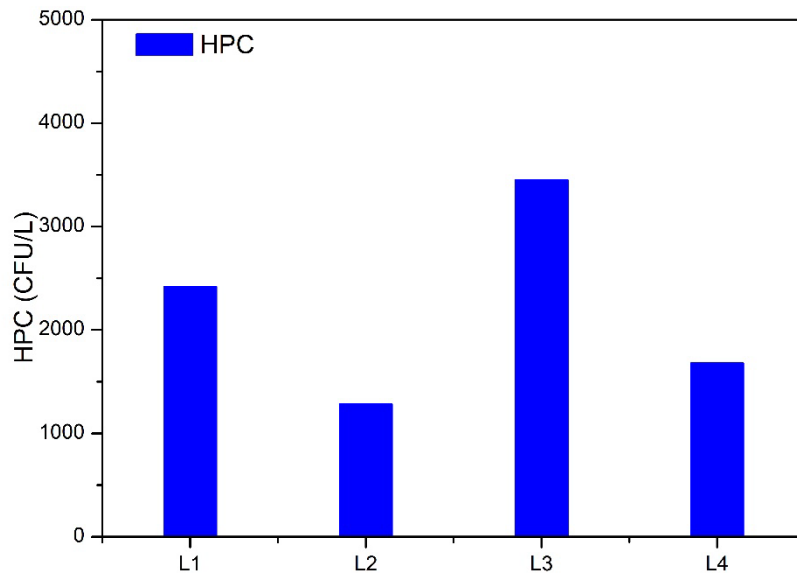


Figure 3.19 HPC concentration for 1st batch filter bags in September, 2017

HPC value varied a lot at different sampling locations. From the proximal to the distal in DWDS, the detected value was 2417 CFU/L, 1282 CFU/L, 3449 CFU/L and 1680 CFU/L, respectively. The reported value was quite high compared to the normal content in bulk water which can be attributed to the enrichment effect of the filter bag as well as the stagnation occurrence. Additionally, the relative high temperature in the ambient made it a favor for high HPC.

2nd batch

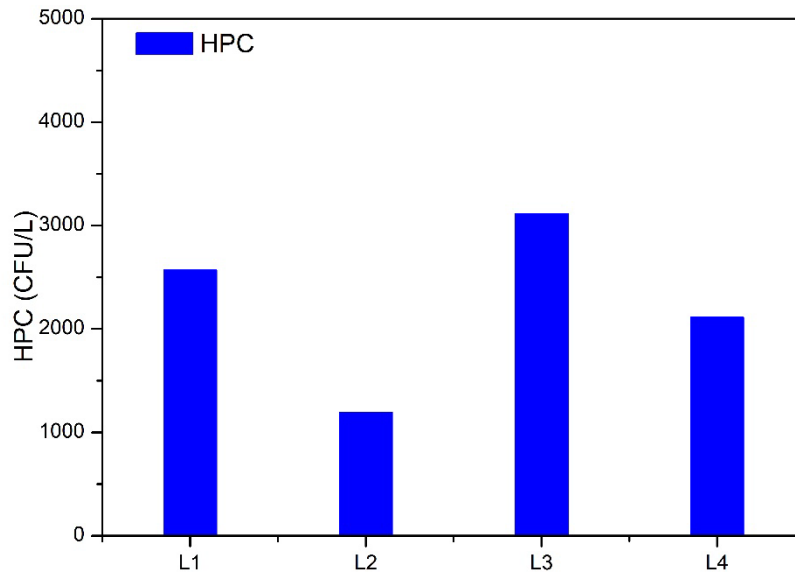


Figure 3.20 HPC concentration for 2nd batch of filter bags in November, 2017

Similar as ATP, the obtained HPC value for the 2nd batch filter bag was comparable with the previous with small fluctuation. HPC raised to 2568 CFU/L and 2111 CFU/L at L1 and L4 while went slightly down to 1192 CFU/L at L2 and 3113 CFU/L at L3. This fluctuation didn't lead any change to the locations' order of abundance.

3.2.2.3 Aeromonas

1st batch

No *Aeromonas* was detected on the filter bag of L1 after 7 weeks flowing with new water while the rest three locations were analyzed with 25 CFU/L, 103 CFU/L and 50 CFU/L, respectively. The purpose of the first batch of filter bags was to seize the potentially occurred physiochemical and microbiological water quality problems after supply-water quality change due to the conversion and release of DNHM in the form of suspended solids (Gang Liu, Zhang, et al., 2017). It was reported that loose deposits were the only accumulation site for *Aeromonas* indicating that one of the origins of the filtrates might be the loose deposits.

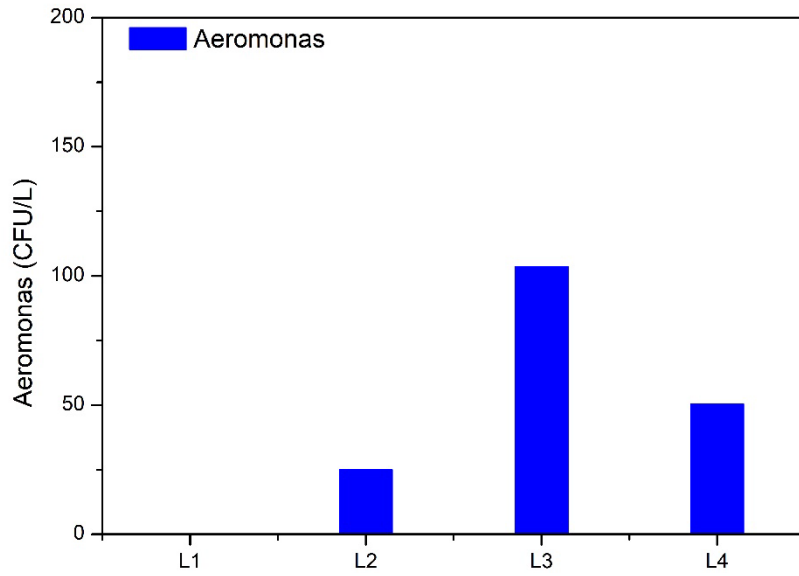


Figure 3.21 Aeromonas concentration for 1st batch filter bags in September, 2017

2nd batch

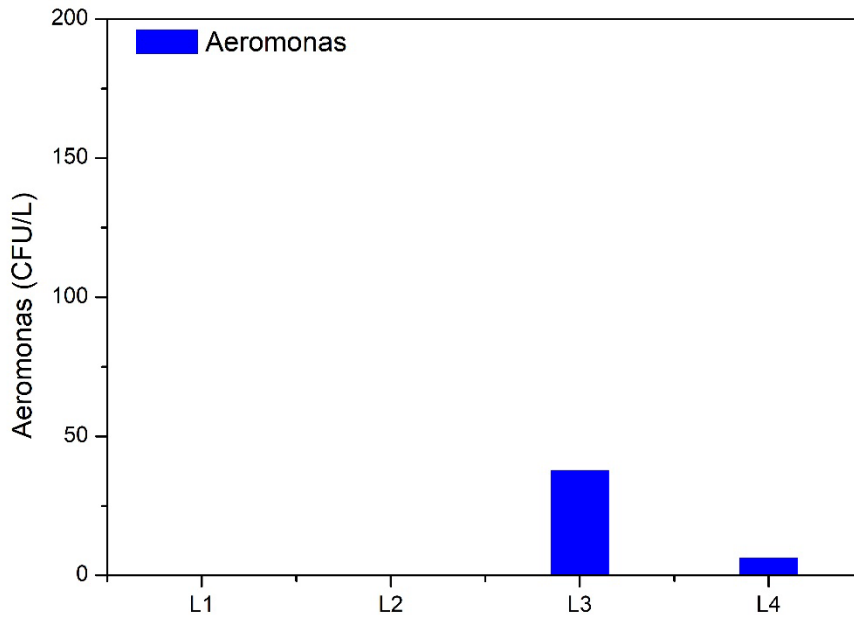


Figure 3.22 Aeromonas concentration for 2nd batch of filter bags in November, 2017

Compared with earlier results, half of the samples were detected with no Aeromonas while the other half was found with decreased contents which were 50 CFU/L at L3 and 6 CFU/L at L4. With the temporal extension after new water supplied, Aeromonas performed a downward trend at all sampling sites on an average level, implying less destabilized loose deposits were flushed to the consumers' taps which could probably be owing to the settle down of the transition effect.

3.2.3 Elemental analysis

1st batch

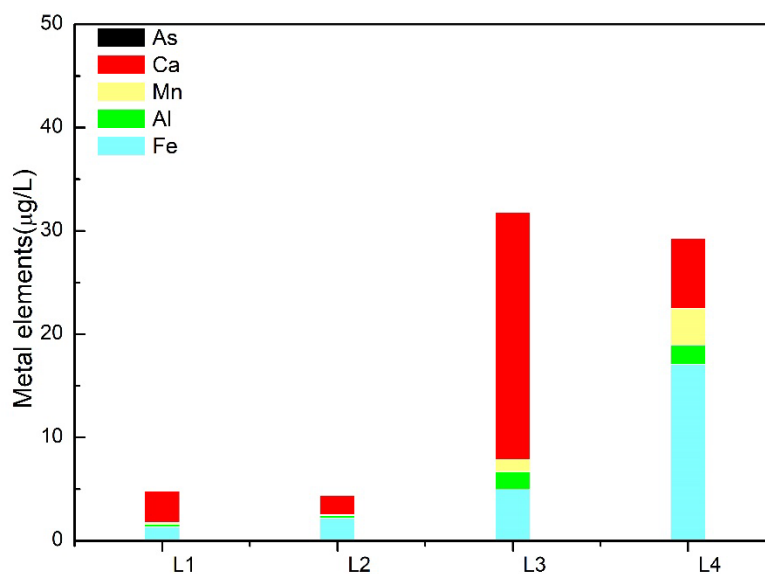


Figure 3.23 Metal elements concentration for 1st batch of filter bags in September, 2017

Table 3.4 Metal elements concentration for 1st batch of filter bags in September, 2017

Content(µg/L)	L1	L2	L3	L4
Fe	1.33	2.20	4.94	17.05
Mn	0.18	0.10	1.19	3.57
Ca	3.03	1.81	23.89	6.77
Al	0.24	0.24	1.76	1.89
As	1.53E-03	2.55E-03	8.93E-03	1.25E-02

Based on the provided elements information, total metal elements content on filter bags varied significant at different household. For sites located at the proximal part of the pipeline system, the detected total metal contents were as low as 4.78 µg/L, 4.35 µg/L for the first two locations. The other two at the distal possessed relative rich abundance with the highest 31.79 µg/L detected at L3 while L4 was 29.29 µg/L. Although the total contents varied, almost all samples shared the elements content structure in descending order of Ca, Fe, Al, Mn, As in terms of their relative abundance except for L4. At L4, Fe replaced Ca to become the most abundant elements and Mn outweighed Al in contents which was not observed in the others. When combining with its according biological analysis, the captured filtrates at L3 was characterized as both microbial active as well as metal abundant because of its high ATP concentration and high metal contents on filter bag. Moreover, even though the abundance order of elements in pipe-wall biofilm and filter bag filtrates was the same, relative abundance of individual metal still characterized this

structure different from the one on the biofilm if we compare the element contents of the 1st batch filter bag in Figure 3.23 and that on biofilm illustrated in Figure 3.12. Since, Fe was mainly accumulated in loose deposits niche, the raised Fe proportion in filtrates provided a clue that the captured filtrate was more likely to be a mixer of the resuspended loose deposits and detached biofilm rather than a single origin. This hypothesis could also be confirmed by the observed *Aeromonas* on filter bags since loose deposits were hotspots for *Aeromonas*.

2nd batch

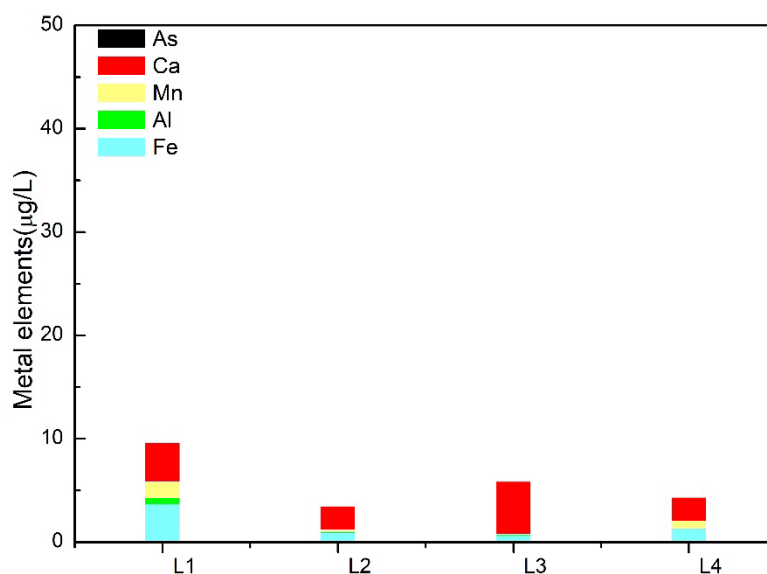


Figure 3.24 Metal elements concentration for 2nd batch of filter bags in November, 2017

Table 3.5 Metal elements concentration for 2nd batch of filter bags in November, 2017

Content(µg/L)	L1	L2	L3	L4
Fe	3.68	0.88	0.63	1.22
Mn	1.57	0.13	0.03	0.68
Ca	3.78	2.33	5.12	2.28
Al	0.59	0.15	0.08	0.14
As	4.67E-03	9.58E-04	1.05E-03	1.43E-03

After flowing with the same supply-water quality for the same 7 weeks, even fewer inorganic compounds were detected on the 2nd batch of filter bags. All samples were distributed under 10 µg/L. Compared with the previous batch, L1 was seen an increase almost doubled to 9.62 µg/L which complied with the visual observation that substantial yellowish and dark materials attached on the surface whereas L2 slightly dropped to 3.49 µg/L considered as comparable to before. Distinct from L1 and L2, metal contents at L3 and L4 collapsed to 5.86 µg/L and 4.33 µg/L respectively, due to the downturn of calcium and iron. The low element contents on filter bags at L3 and L4 reached a good agreement with the corresponding visual observation that the samples were quite clean. For the content

structure, the predominate elements was still Ca followed by Fe, Al, Mn and As. But for L1 and L4, Mn was observed higher than Al.

Much fewer particles and elements were detected in 2nd batch operation comparing to the previous cycle, indicated that less destabilized DNHM were converted and released in the form of suspended solids and delivered to the system end. In other words, the decreased captured filtrates implied that, with time moved on, the influence caused by transition effect during this supply-water switch gradually settled down and a new equilibrium consequently established among different niches in DWDS.

3.2.4 ESEM

For the sake of gaining a complement insight of the morphology of the captured particles and the elements distribution on the filtrates, an Environmental Scanning Electron Microscope test together with EDS was performed on 2 batch of filter bag pieces from sampling sites. Considering about the pore size and the large particle scale, the magnification was selected as 125 x .Due to the limited space, only results from EDS was presented in this section, further information can be found in Appendix B. ESEM and EDS results.

1st batch

Wires in the Figure 3.22 were the filter bag fibers and the EDS revealed that these fibers mainly comprised of carbon.

For L1, the entrapped particle was of irregular shape cross-wounded by the filter. The upper bright part was supposed to have good conductivity that mainly consisted of metal elements such as Fe, Mn and also non-metallic element O suggesting the particle existed in the form of iron and manganese oxides. The main body of the particle laid underneath in a greyscale was detected with high C and O content as well as sub-peaks belonging to Mn, Fe and Ca, which could probably be a mixer of organic material and metal oxides. Similarly, an identical phenomenon was found for L4 either for the morphology or compounds distribution but with a lower signal strength.

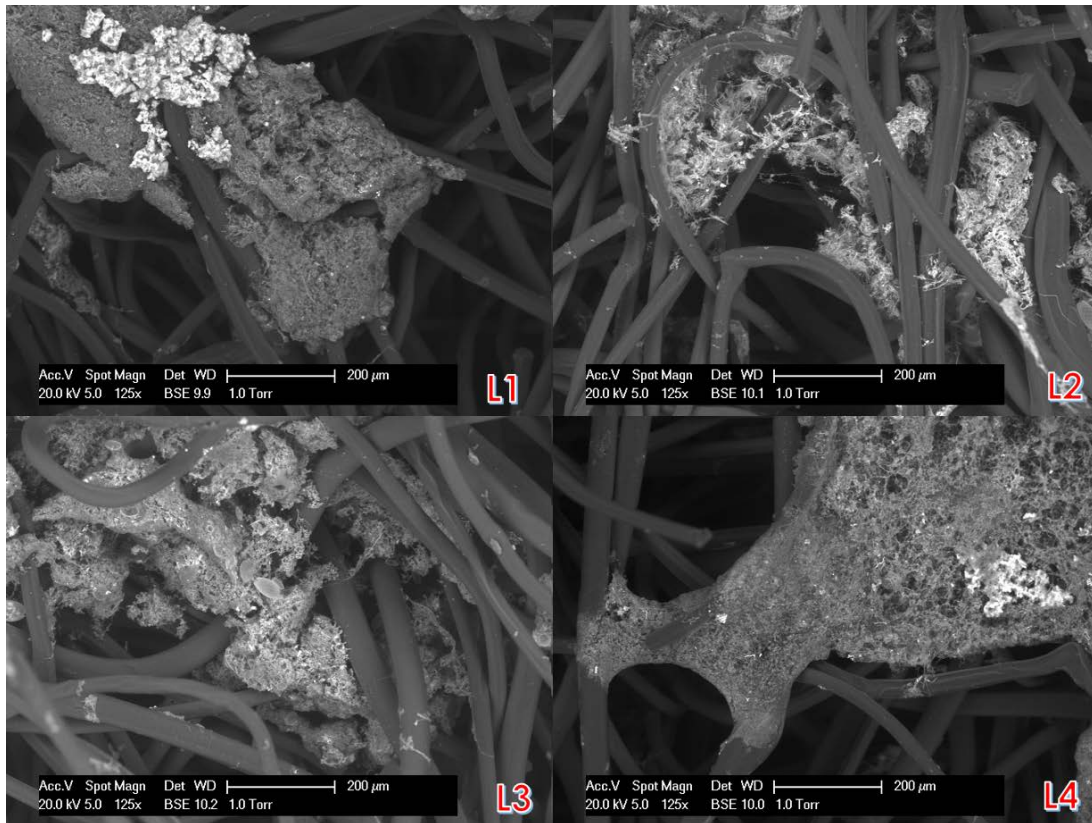


Figure 3.25 Environmental Scanning Electron Microscope (ESEM) image for the 1st batch filter bags from 4 sampling locations.

For L2 and L3, where quite amount of flat-sheet like yellowish particles were witnessed, the morphology of these particles was rather feathery and flocculent than the compact form at L1 and L4. Additionally, unlike the conglomerated form, metal contents in L2 and L3 were more evenly distributed in the particle in terms of oxides of iron, manganese and calcium. Because of the high signal strength of carbon detected, organic compounds were supposed to be one of the dominate contents. Apart from the similarity, some small rugby-shaped particles (lengthened 20~40 micron) abundant in C, Si, O with a rhombus cross arranged with dots pattern and a serrated opening on one side (also could be described as tulip-bud like) attached on the filter surface at L2 and L3. Its obvious artificial morphology suggested that it might originated from some man-made products instead of from the pumping station. Unfortunately, subjected to the limited information, the identification of this unique shaped particles required for further research.

The detected abundant metal content reached a good agreement with the filtrates lab analysis.

2nd batch

After flowing under the new water for a comparable period, captured particles by filter bags demonstrated different morphology but the abundant elements and their distribution remained the same comparing to the previous batch. It was noteworthy that the particle density on the filter bag pieces obvious reduced no matter where the pieces were cut from.

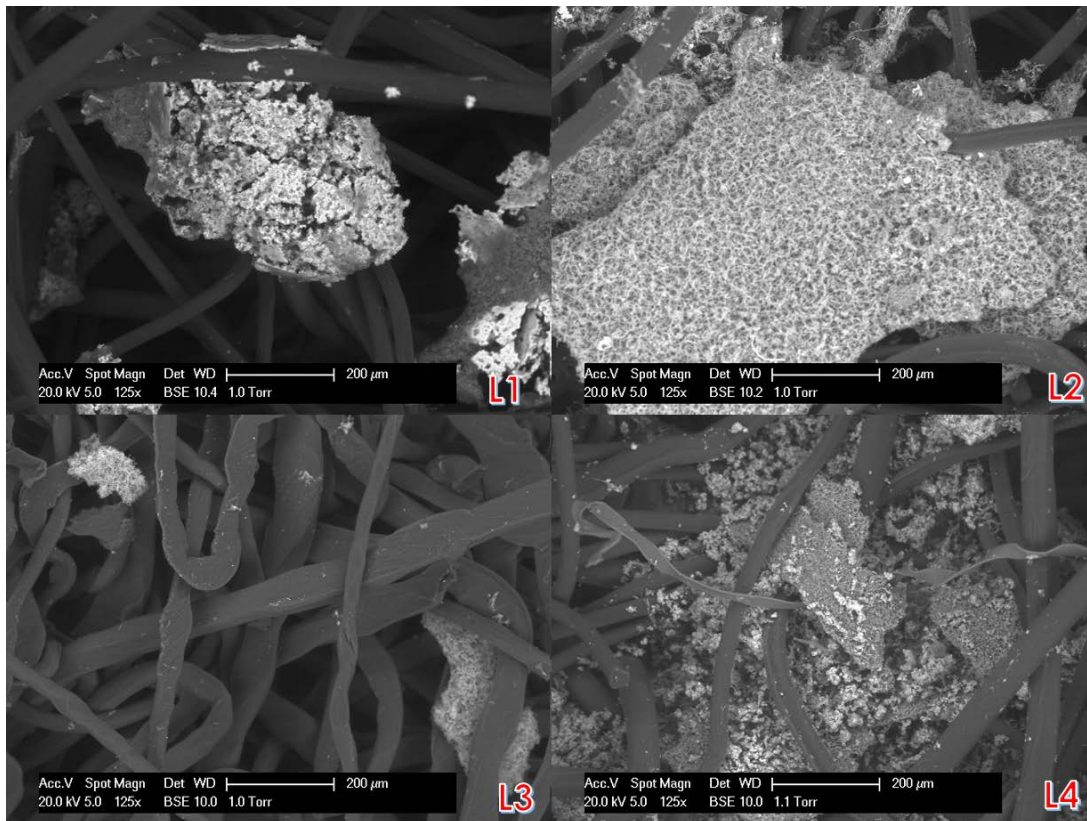


Figure 3.26 Environmental Scanning Electron Microscope (ESEM) image for the 2nd batch filter bags from 4 sampling locations.

For L1, the particles trapped by filter bag fibers were of compact texture like varied in irregular shapes with cracks on the surface. The surface of the particles were brighter which mainly consisted of manganese and iron oxides while the inner parts were more likely to be dominated by organic compounds where strong carbon signal strength were detected. Synonymously, sub-peaks of manganese, calcium and iron were also observed at the inner part. When it came to location 2, a unique morphology of large flat with uneven porous structure located on surface was witnessed which complied well with the flat-sheet like description obtained in visual observation. The elemental contents were rich in manganese, iron and oxygen followed by carbon, phosphorus and calcium indicating coexistence of metal oxides and nutrients containing carbon and phosphorus. Only few particles were found on filter bag pieces from sampling point 3 and the scale of the observed particles also smaller than the others. The observed particles in this figure were abundant in organic elements such as carbon, oxygen, phosphorus as well as inorganic elements like calcium. Besides, for that large particle lied in lower right corner, a small peak of Al was also observed. The low content of Fe and Mn indicated by EDS was consistent with lab elemental analysis in section 3.2.3. Comparing to the others, sample from L4 also performed a quite unique morphology where massive particles covered with evenly distributed metal-riched dots were trapped in fibers with a seaweed-like belt interspersed among. According to EDS results, carbon and calcium were the most abundant two elements in the main body with a comparable content while the bright dots on surface were characterized as metal abundant with Mn, Fe, Ca sorted in a descending order. For the belt, only peaks of C, O, Fe, Mn were observed. Additionally, carbon

and oxygen were not the only found inorganic elements performed, phosphorus also accounted for an inevitable proportion, indicating that part of the organic compounds were also P-enriched.

3.3 On-line monitoring

3.3.1 Pressure difference

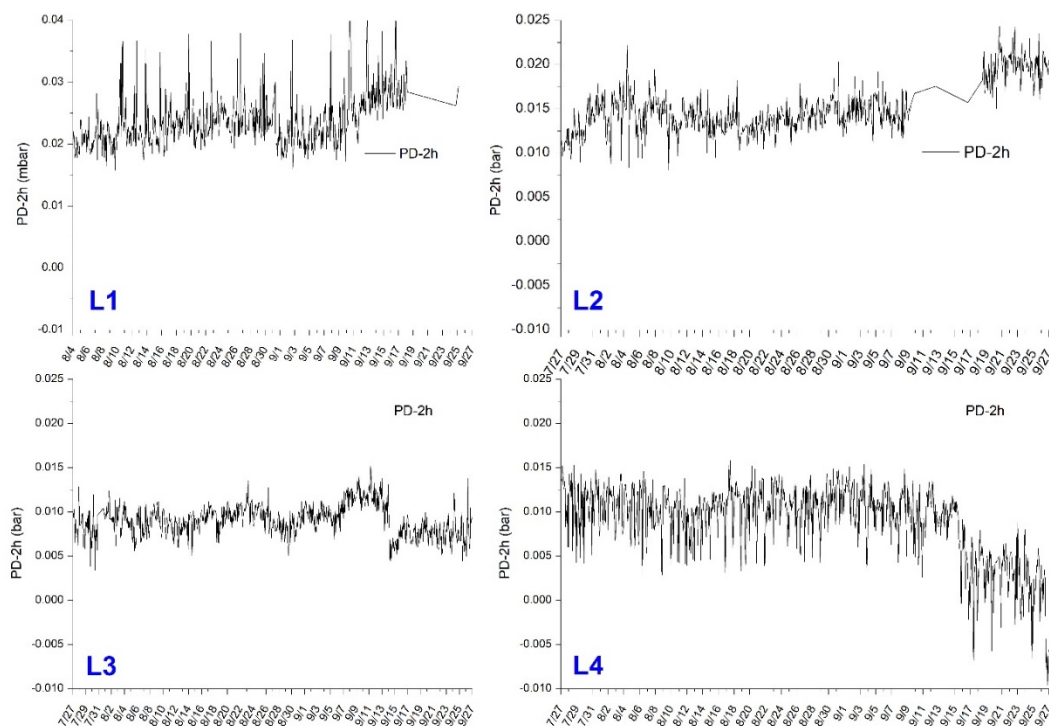


Figure 3.27 Comparison of pressure drop cross the filter bags during the operation of the 1st filter bag.

Generally speaking, pressure differences caused by filter bag were very low and quite stable (under 0.05 bar or 50 mbar) for all sampling points during 2 batches' operation, and most of which were even below 0.02bar referring to Figure 3.24 and Figure 3.25. In most cases no clear tendency could be drawn about the pressure drop variation especially for those filters running under totally different conditions such as flow rate, locations, particle load in inlet, etc. No obvious pressure difference build-up as initially supposed were witnessed. This, to a large extent, could be attributed to the huge capacity characterized by the large pore size and surface area. There was another possibility that the detached biofilms were smaller than 50 micron that can pass through the filter bag. Results from On-line Particle Sampling System (OPSS) study revealed that more suspended solids were entrapped after supply-water switch and the filtrates analysis suggested that these particles were more inorganic characterized than biomass characterized which confirmed the hypothesis that the destabilization indeed occurred with water quality shift. The small pressure drop could also probably be attributed to the ultra-low particle load in the new water supplied in the research area.

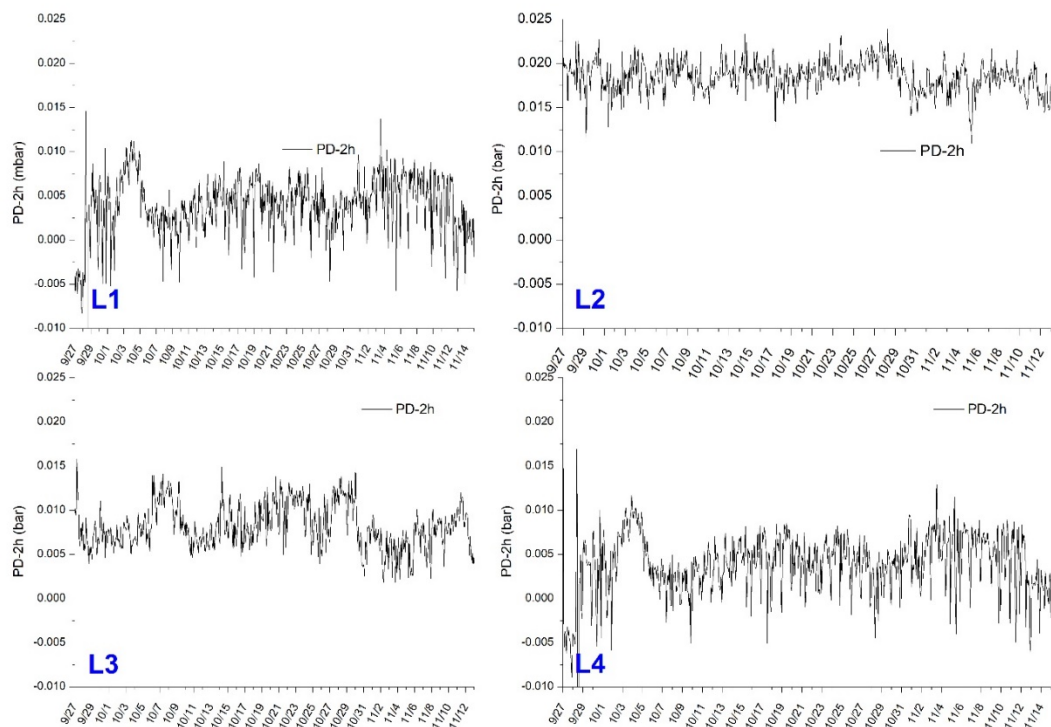


Figure 3.28 Comparison of drop cross the filter bags during the operation of the 2nd filter bag.

Temperature

Comparison of real time temperature variation at customers' within one (randomly picked) day (2017/08/01 00:00~ 2017/08/02 00:00) and the average temperature within the chosen period (2017/07.27~2017/08/31):

On one hand, the temperature is highly influenced by the inlet water temperature, atmospheric temperature, ambient temperature, water consumption habit (frequency) at each household. From a long temporal view, temperature fluctuated around the mean value while the averaged temperature within a certain period had little difference for our 4 sampling points. However, although the fluctuations of 4 points were not related and without regularity, they shared a common trend, that is subject to the environmental temperature. This impact might have different contributions for temperature variation at different location but when the external temperature raised or dropped, immediate accompanying respond were observed for all with similar tendency referring to the tendency shown in Figure 3.26.

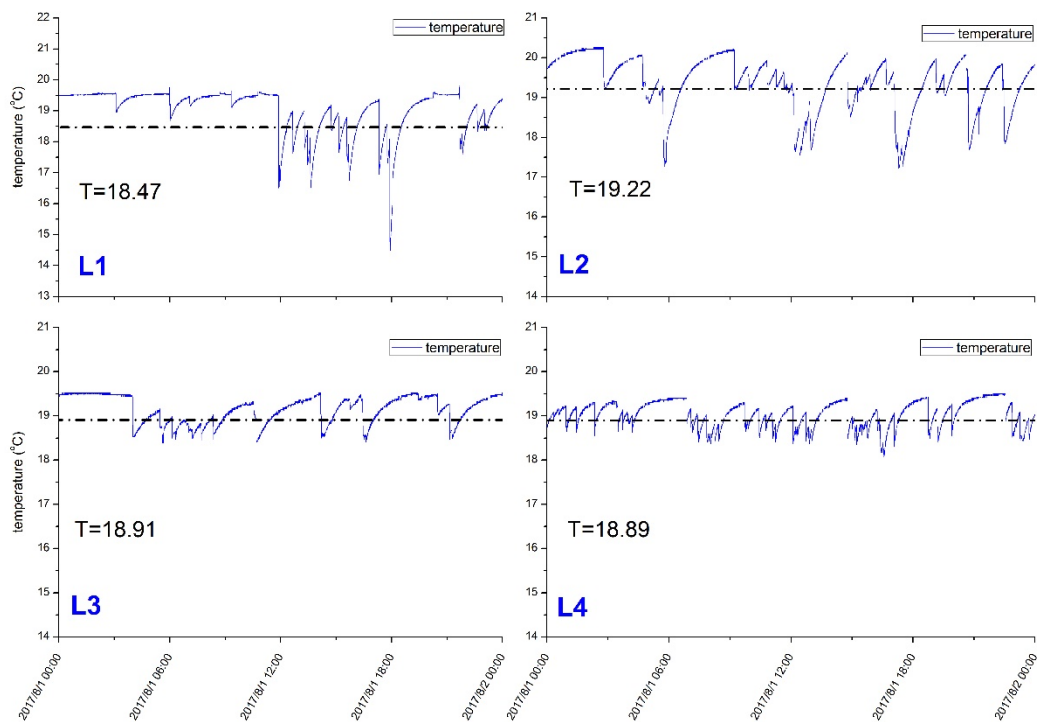


Figure 3.29 Comparison of temperature variation monitored by SWM within one day (2017/08/01) and the average temperature during a period (2017/07/27~2017/08/31).

On the other hand, stagnation overnight led to obvious rise on water temperature. Although for a long-term view, temperature didn't have violent change, when it came to discuss variation with a high temporal resolution, the situations were distinguished. Specially, water temperature was usually higher than the average temperature which could be attributed to reduced water consumption and the accumulated heat exchange with external environment during overnight stagnation. This finding was in consistent with a modelling study on domestic drinking water supply systems(Zlatanovic, Moerman, van der Hoek, Vreeburg, & Blokker, 2017). Since temperature is considered as a rate-controlling factor involved for many chemical and microbial processes and previous study also confirmed that when water temperature increased by 10°C, biological activity can be doubled, it is reasonable to hypothesize the microbial communities (structure) in the household connection pipes can be distinguished to those in the same DWDS systems.

4. Discussion

So far, all results either from the lab analysis or from the on-line monitoring were manifested in Section 3 to depict a complete picture of the physical, chemical and microbial characteristics for both the pipes flowing with new supply-water and the filter bags placed at the end-points of DWDS. In this chapter, comparison between two batch of filter bags were investigated to figure out whether transition effect occurred or not after supply-water quality switch; Further discussion focusing on temporal variation of pipe samples for different sampling points was proposed in section 4.2 to reveal how distribution network harbored material behaved during the occurrence of transition effect period; Furthermore, elemental comparison between variation in DWDS and at the end-points discussed the possible origination of the trapped destabilized DNHM in section 4.3.

4.1 Comparison between filter bags

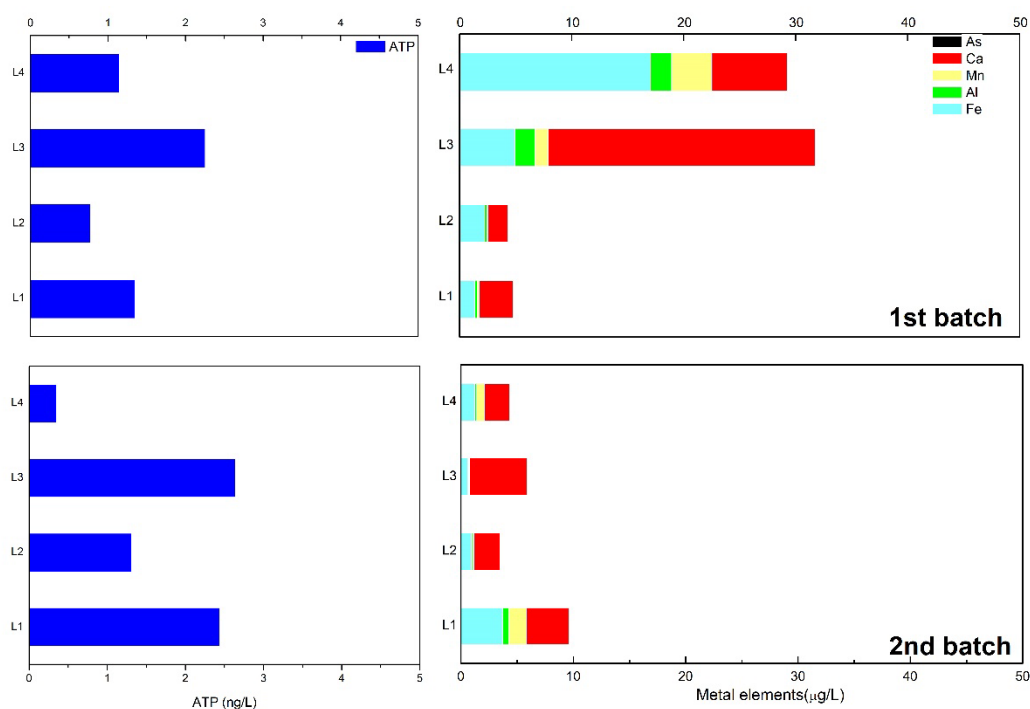


Figure 4.1 Comparison of different batch of filter bag samples.

Since the foremost target of Smart Water Meter study was tell whether the potentially occurred water quality deterioration caused by DNHM destabilization and detachment happened or not and prevent these released particulate matters from reaching the consumers' side. Because the ultimate form of transition effect was supposed to be large suspended solids, hence the trapped filtrates in filter bags would be the most direct and efficient approach to confirm the occurrence of transition effect and their amount and content could also indicate the severity and biochemical characteristics.

Directly from the visual observation mentioned in section 3.2.1, all samples in 2 batches of

filter bags were witnessed with yellowish or dark particulate materials in large scale that could be seen by naked eyes. This suggested that some big particles (at least larger than 50 micron) that usually would not be observed under normal operation condition were generated during water delivery and finally flushed to the end-points and consequently, identified the occurrence of transition effect soon after the supply-water quality change.

Besides, these captured particles were of high biological active and metal abundant. From the perspective of temporal variation (see Figure 4.1), ATP level were quite comparable of the 2 batch samples with a very slight increase on an average level. The obtained value here were larger than a related research conducted in the same area implying possible (re)growth on the filter bag (X. Li, 2017).

No obvious trend could be concluded from the biological activity of the filtrates based on ATP analysis. This was because the operational condition for filter bags was quite unique that the stagnation occurred episodically, and the water temperature was promoted by the indoor temperature especially in winter time when heat-supply was on. The stagnated hydraulic condition and the elevated temperature would favor the (re)growth of microorganism on the surface and hence, the obtained ATP would rather be an indication of the indigenous plus the regrowth rather than the released DNHM itself. The slightly increased ATP value might be resulted from higher temperature.

Discriminated from ATP value, obvious downward trend was observed between 2 batch samples with the main decrease occurred on most two abundant metals, Ca and Fe. It was believed that this collapse was, to a large extent, led by the significant decreased amount of filtrates observed from the second batch since no obvious signal strength reduction of the certain metals was indicated by EDS. In other words, fewer undesired large particles were generated, either from the detached biofilm or from the resuspension of loose deposits. New physiochemical and microbiological equilibriums seemed to be gradually reached among the four niches in DWDS with transition effect settled down over time.

In summary, the biological active (relative high ATP value) and metal abundant particulate matters corroborated the occurrence of water quality deterioration in the form of large suspended particles after the purification technology upgraded in Lekkerkerk area, but the disturbance seemed to be settled down as the destabilized system gradually get used to the new condition over time.

4.2 Comparison between pipe samples

Although the detection of transition effect was achieved at the end-points of the pipeline system, since the generation of the suspended solid converting from biofilm or loose deposits actually carried out in pipelines, how transition effect behaved and developed throughout the period was mainly demonstrated by the 3 batch of pipe samples.

4.2.1 Microbial

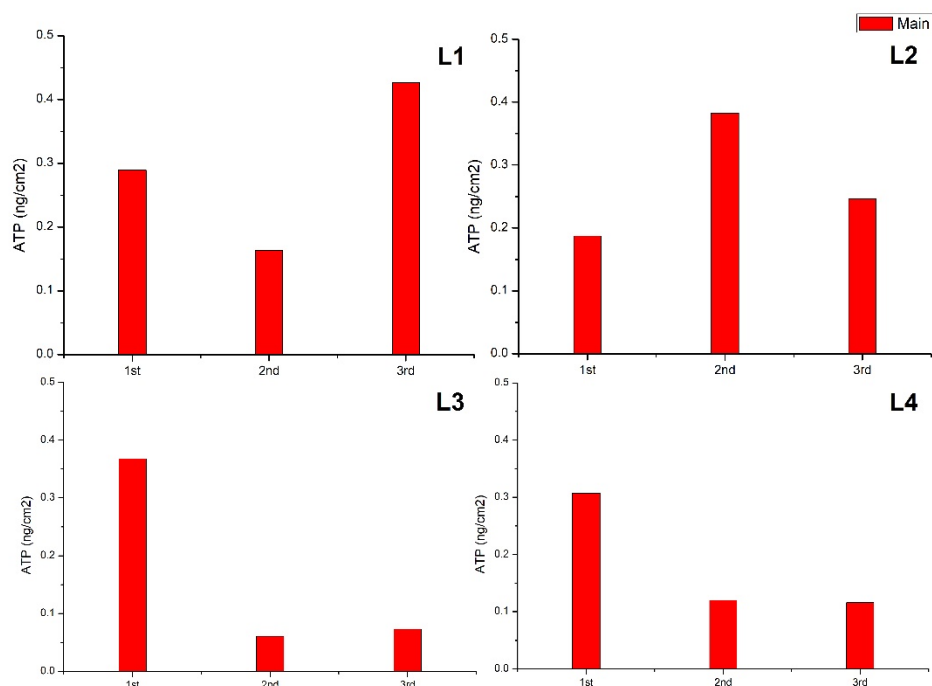


Figure 4.2 Comparison of temporal ATP variation on main pipes from 4 sampling locations.

From the temporal point of view, the 1st batch represented the indigenous characteristics of the historically balanced biofilm niche before external perturbation introduced, while 2nd batch was taken 3 months after to perform the influence of transition effect on biofilm. The 3rd sampled another 3 months afterwards was supposed to provide clues for the post-stage. In order to make the data comparable, analysis for each location was manifested over time and cross compared among locations. The results shown in Figure 4.2 suggested that expect for L2, an obvious reduction on biological activity was observed after new water was introduced into DWDS. It was reasonable since RO effluent would make the supply water characterized with both low nutrient loads and particle loads. The super oligotrophic water environment was likely to starve the microorganisms on biofilm and the microorganisms with low food supply turned out to lose activity and finally detached from biofilm in a planktonic mode. The contrary situation occurred at L2 might result from the unevenly distribution of biofilm on specimens or the contamination of loose deposits in filling-in water from tap at that location. Then, ATP either stable or decreased except for L1 who was observed more particles on filter bag. This unexpected increase at L1 could be probably attributed to maintenance (or construction) activity such as filter back-wash in treatment plant since L1 almost located next to the treatment as well as the date was coincident. The comparison of the 2nd and the 3rd suggested a rebalanced bacteriology on main pipe biofilm was gradually achieved.

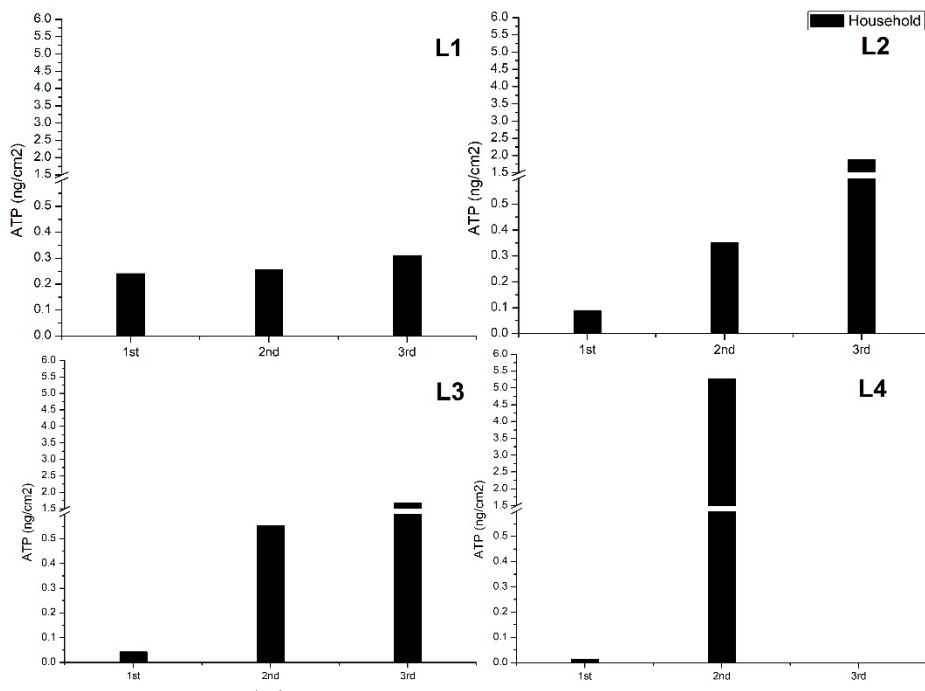


Figure 4.3 Comparison of temporal ATP variation on household connection pipes from 4 sampling locations.

Different from the district distribution pipes, household connections pipes shared the same increasing trend along time in terms of ATP (see Figure 4.3). Between the first two batches, an obvious raise was captured among household connection pipes even flowing with improved water quality, when bacteria were detaching from main pipes at the meantime. A reasonable postulation was that the released DNMHs from the main pipes were distributed and delivered to the downstream of DWDS. Meanwhile, the relative low flow velocity in household inlet tubes would like to sediment the detached biofilm or/and resuspended loose deposit who might in turn act as nutrients to favor microorganism development. When it came to the post-stage of transition effect, ATP value continuously went up implied the transition effect still lasted at the end of DWDS. Comparing with the same period in main pipes where transition effect gradually faded out, there seemed to be a time difference for transition effect flowing from the main DWDS to the dead-end. This delay was also reasonable since water required time for distribution in field pipeline works, especially in large scale DWDS. DWDS is a sealed system, and the transition effect was concluded to gradually moved from main pipes to the household connection pipes downstream. Since the new equilibrium has accomplished in main pipes, based on the above analysis, the influence brought by transition effect on household pipes would settled down soon.

4.2.2 Elemental

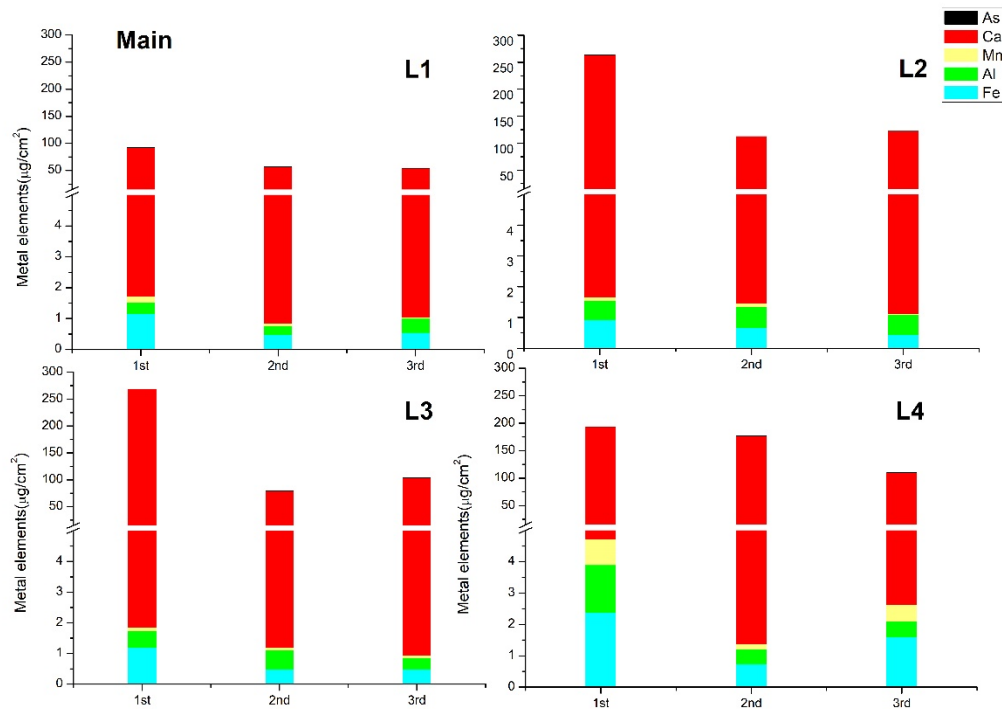


Figure 4.4 Comparison of temporal elements contents and structure variation on main pipes from 4 sampling locations.

Total elements on main pipes possessed a similar decrease trend among all locations with the main reduction from calcium and iron (see Figure 4.4). Afterwards, the elements contents became steady with comparable value detected between the last 2 batch. In terms of contents, a possible speculation of the decrease was that the reduced part was corresponding to the elements contained in the potentially detached biofilm and was flushed away when they transferred into suspended solids under disturbance. This could be also indicated by the pipes' biological analysis as well as the elements abundant particles found at downstream filter bags. Apart from this, metal elements drop could also be a consequence of equilibrium destabilization between bulk water and biofilm niches. The ultra-low elements concentration in new bulk water made the already established elements balance tilted towards the water phase, so elements on biofilm with relative high contents tended to dissolve into bulk water to neutralize unbalance. Even though not in the form of suspended solids, this would lead to a chemical deterioration of water quality comparing to injected water and still fell under the rubric of transition effect. The identical phenomenon also seen on household connection pipes referring to Figure 4.5.

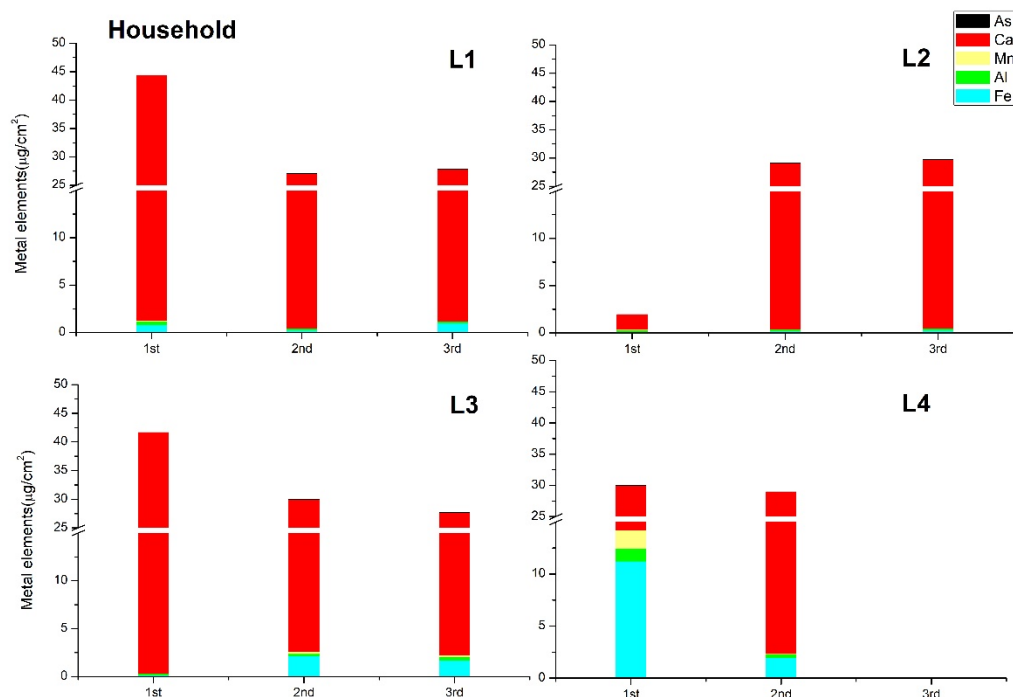


Figure 4.5 Comparison of temporal elements contents and structure variation on household connection pipes from 4 sampling locations.

Comparing to the content variation, the compounds structure change was more smooth. Ca maintained its predominance in biofilm throughout the period since calcium is of significant importance for biofilm formation especially, under low substrate condition (Hijnen et al., 2016). This was confirmed by another research that Ca was more observed in biofilm niche rather than loose deposits on PVC-U pipes in an unchlorinated DWDS (Gang Liu, Tao, et al., 2017). The order of the rest metal elements was Fe, Al, Mn, As sorted in a descending order. Higher Fe contents were observed at L1 in the first batch either for main pipe or household connection pipe while the cause remained to be found.

4.3 Elemental comparison between pipe samples and filter bags

Since the variation on pipe samples highly indicated the generation and behavior of transition effect in DWDS while filtrates analysis provided information of the destabilized DNHM arrived at the system end, a cross comparison on elements was supposed to help us gain an insight into the relation between the released and the trapped. Comparison was performed between the 1st batch of pipe samples and the 1st batch of filter bags because they represent the features of the indigenous biofilm before external perturbation and the destabilized DNHM during transition effect, respectively. Due to the enrichment function of the filter bags, though the absolute content of the elements was of little comparability, the relative proportion of each elements could reveal the dissimilarity on composition structure.

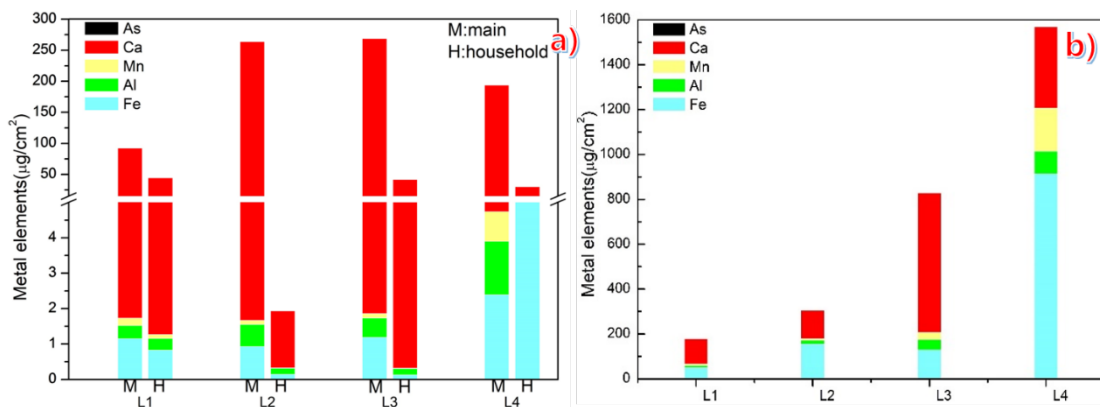


Figure 4.6 Cross comparison on elements contents and structure between a) pipe samples and b) filter bags.

According to Figure 4.6, calcium had the overwhelming abundance in both main and household pipes, consistent with its critical role in biofilm formation. However, when it came to the destabilized particles captured at end-points, though the filtrates still rich in calcium, the dramatically elevated iron proportion even replaced calcium to be the predominate elements at some of the sampling points. The high iron proportion different from the biofilm strongly indicated that the detached biofilms no matter from main or household connection pipes were not the only origin of the destabilized DNHM. It was supposed to be a mix of destabilized material from different niches. Since loose deposits were reported as the iron abundant material rather than biofilm (Gang Liu, Tao, et al., 2017), it was speculated that loose deposits in DWDS were resuspended as a consequence of hydraulic condition change such as flow velocity surge or biochemical equilibrium break-up, and finally settled or captured by filter bags at downstream. The detected *Aeromonas* on filter bags could also be a confirmation of the occurrence of transition effect since it was expected to detached from the hotspots loose deposits and carried to the filter bags. However, it should be noteworthy that the iron itself could function as flocculant that tended to conglomerate particles into larger scale. In other words, particulate matters containing iron were more likely to appear in big size and entrapped by the filter bags. Therefore, it cannot be concluded that the destabilized DNHMs were derived from loose deposits than biofilm. Further monitoring and analysis are required to figure out the exact attribution ratio for the destabilized DNHM.

5. Conclusions and recommendations

5.1 Conclusions

Smart Water Meter is an emerging on-line approach to detect and monitor potentially occurred physiochemical and microbiological water quality deterioration when external disturbances such as hydraulic turbulence and supply-water quality switch were introduced in DWDS. Meanwhile, sampling and lab test of pipes, filter bags were carried out to analysis and confirm the development and behavior of transition effect from a multiple perspectives. Overall, the transition effect occurred in the study area can be well captured and sampled by the Smart Water Meter together accompanied with pipe and filter bag samples. Here are the conclusions we have come with:

1. The improved Smart Water Meter equipped with filter bags, sensors and on-line data uploading system can well capture transition effect occurred in DWDS and prevent undesirable large particulate matter from reaching the consumers'
The Smart Water Meter was improved to equipped with pressure sensors, temperature sensor, a 50micron pore size filter bag and a real-time data updating monitor box to realize on-line monitoring and sampling. 50 microns was a suitable pore size to seize destabilized DNHM during transition effect while allow most particles pass through under normal condition. Under this circumstance, Smart Water Meter can well capture the destabilized DNHM without compensate consumers' consumption experience or reduce the running cycle.
2. Transition effect occurred after supply-water quality upgradation in Lekkerkerk area.
After RO was inaugurated in Lekkerkerk system, the reduced microorganism activity and element contents on pipes as well as the metal abundant filtrates on filter bags surface were observed. The new water with super low nutrient load and particle load broke the indigenous equilibrium among different niches and triggered the transition effect as a consequence.
3. Transition effect triggered in this case was not violate and gradually settled down with temporal extension.
Although both pipe and filter bags indicated the occurrence of transition effect, the corresponding physiochemical and microbiological water quality deterioration were not as serious as experienced from previous studies. The triggered large particles were even filtered before reaching the customers'. Moreover, the steady microbial and element contents and the fewer captured particles in filter bags implied the transition effect gradually settled down along time. New equilibrium has been established in main pipes in DWDS but not yet reached in household connection pipes at the downstream. But since the transition effect moved from upstream to downstream, restablization on household connection pipe is predicted to be reached soon.

4. Ca and Fe are the dominate compounds in filtrates which could probably originated from detached biofilm and resuspended loose deposits.

Calcium possessed the predominance in both pipe-wall biofilm and destabilized DNHM, especially overwhelming in biofilm because of its critical role for biofilm formation. Iron was the second abundant metal elements but accounted for much higher proportion in filtrates than biofilm. The different metal contents structure showed that the destabilized DNHM was not only originated from detached biofilm but also might attributed to loose deposits.

5.2 Recommendations

The recommendations provided here mainly focusing on set-up improvement and experimental design to help the further research to gain an even better understanding of the system.

1. Improving pressure sensors with higher accuracy and sensitivity to even make the on-line monitoring of pressure-drop as an indicator for system early warning.
2. Optimizing pore size selection for filter bags such as smaller pore size in further study to depict a clearer correlation among pressure-drop build-up, filtrates amount and the run time.
3. Water samples from consumers' taps and treatment plants are also highly suggested to be included in further research during application of filter bags to make sure the disturbance from set-up won't pose any threats to human health and to figure out the change in water quality along the transportation pipelines.
4. Application of DNA extraction and pyrosequencing technology will make the trace-back for the destabilized DNHM more feasible and accurate.

Bibliography

- Boe-Hansen, R., Albrechtsen, H.-J., Arvin, E., & Jørgensen, C. (2002). Bulk water phase and biofilm growth in drinking water at low nutrient conditions. *Water Research*, *36*(18), 4477–4486. [http://doi.org/10.1016/S0043-1354\(02\)00191-4](http://doi.org/10.1016/S0043-1354(02)00191-4)
- Dietrich, A. M. (2006). Aesthetic issues for drinking water. *Journal of Water and Health*, *4*(SUPPL. 1), 11–16. <http://doi.org/10.2166/wh.2005.034>
- Dusseldorp, J. (2013). The effect of pre-treatment with Reverse Osmosis on the biological stability in a drinking water treatment plant.
- Emtiazi, F., Schwartz, T., Marten, S. M., Krolla-Sidenstein, P., & Obst, U. (2004). Investigation of natural biofilms formed during the production of drinking water from surface water embankment filtration. *Water Research*, *38*(5), 1197–1206. <http://doi.org/10.1016/J.WATRES.2003.10.056>
- Falkinham, J., Pruden, A., & Edwards, M. (2015). Opportunistic Premise Plumbing Pathogens: Increasingly Important Pathogens in Drinking Water. *Pathogens*, *4*(2), 373–386. <http://doi.org/10.3390/pathogens4020373>
- Feazel, L. M., Baumgartner, L. K., Peterson, K. L., Frank, D. N., Harris, J. K., & Pace, N. R. (2009). Opportunistic pathogens enriched in showerhead biofilms. *Proceedings of the National Academy of Sciences of the United States of America*, *106*(38), 16393–9. <http://doi.org/10.1073/pnas.0908446106>
- Gauthier, V., Barbeau, B., Millette, R., Block, J.-C., & Prévost, M. (2001). Suspended particles in the drinking water of two distribution systems. *Water Science and Technology: Water Supply*, *1*(4). Retrieved from <http://ws.iwaponline.com/content/1/4/237>
- Ginige, M. P., Wylie, J., & Plumb, J. (2011). Influence of biofilms on iron and manganese deposition in drinking water distribution systems. *Biofouling*, *27*(2), 151–163. <http://doi.org/10.1080/08927014.2010.547576>
- Hijnen, W. A. M., Schultz, F., Harmsen, D. J. H., Brouwer-Hanzens, A. H., van der Wielen, P. W. J., & Cornelissen, E. R. (2016). Calcium removal by softening of water affects biofilm formation on PVC, glass and membrane surfaces. *Water Science and Technology: Water Supply*, *16*(4), 888–895. <http://doi.org/10.2166/ws.2016.021>
- Inkinen, J., Kaunisto, T., Pursiainen, A., Miettinen, I. T., Kusnetsov, J., Riihinen, K., & Keinänen-Toivola, M. M. (2014). Drinking water quality and formation of biofilms in an office building during its first year of operation, a full scale study. *Water Research*, *49*, 83–91. <http://doi.org/10.1016/j.watres.2013.11.013>
- Li, D., Li, Z., Yu, J., Cao, N., Liu, R., & Yang, M. (2010). Characterization of Bacterial Community Structure in a Drinking Water Distribution System during an Occurrence of Red Water. *Applied and Environmental Microbiology*, *76*(21), 7171–7180. <http://doi.org/10.1128/AEM.00832-10>
- Li, X. (2017). Assessing particle characteristics and water quality changes in distribution systems by online particle sampling system (OPSS).
- Liu, G., Tao, Y., Zhang, Y., Lut, M., Knibbe, W.-J., van der Wielen, P., ... van der Meer, W. (2017). Hotspots for selected metal elements and microbes accumulation and the corresponding water quality deterioration potential in an unchlorinated drinking water distribution system.

- Water Research*, 124, 435–445. <http://doi.org/10.1016/j.watres.2017.08.002>
- Liu, G., Van der Mark, E. J., Verberk, J. Q. J. C., & Van Dijk, J. C. (2013). Flow cytometry total cell counts: a field study assessing microbiological water quality and growth in unchlorinated drinking water distribution systems. *BioMed Research International*, 2013, 595872. <http://doi.org/10.1155/2013/595872>
- Liu, G., Verberk, J. Q. J. C., & Van Dijk, J. C. (2013a). Bacteriology of drinking water distribution systems: an integral and multidimensional review. *Applied Microbiology and Biotechnology*, 97(21), 9265–9276. <http://doi.org/10.1007/s00253-013-5217-y>
- Liu, G., Verberk, J. Q. J. C., & Van Dijk, J. C. (2013b). Bacteriology of drinking water distribution systems: an integral and multidimensional review. *Applied Microbiology and Biotechnology*, 97(21), 9265–9276. <http://doi.org/10.1007/s00253-013-5217-y>
- Liu, G., Zhang, Y., Knibbe, W.-J., Feng, C., Liu, W., Medema, G., & van der Meer, W. (2017). Potential impacts of changing supply-water quality on drinking water distribution: A review. *Water Research*, 116, 135–148. <http://doi.org/10.1016/J.WATRES.2017.03.031>
- Proctor, C. R., & Hammes, F. (2015). Drinking water microbiology — from measurement to management. *Current Opinion in Biotechnology*, 33, 87–94. <http://doi.org/10.1016/J.COPBIO.2014.12.014>
- Schwake, D. O., Garner, E., Strom, O. R., Pruden, A., & Edwards, M. A. (2016). *Legionella* DNA Markers in Tap Water Coincident with a Spike in Legionnaires' Disease in Flint, MI. *Environmental Science & Technology Letters*, 3(9), 311–315. <http://doi.org/10.1021/acs.estlett.6b00192>
- Tang, Z., Hong, S., Xiao, W., & Taylor, J. (2006). Characteristics of iron corrosion scales established under blending of ground, surface, and saline waters and their impacts on iron release in the pipe distribution system. *Corrosion Science*, 48(2), 322–342. <http://doi.org/10.1016/J.CORSCI.2005.02.005>
- Vreeburg, I. J. H. G., & Boxall, D. J. B. (2007). Discolouration in potable water distribution systems: A review. *Water Research*, 41(3), 519–529. <http://doi.org/10.1016/j.watres.2006.09.028>
- Vreeburg, J. H. G., Schippers, D., Verberk, J. Q. J. C., & van Dijk, J. C. (2008). Impact of particles on sediment accumulation in a drinking water distribution system. *Water Research*, 42(16), 4233–4242. <http://doi.org/10.1016/j.watres.2008.05.024>
- Wang, H., Bédard, E., Prévost, M., Camper, A. K., Hill, V. R., & Pruden, A. (2017). Methodological approaches for monitoring opportunistic pathogens in premise plumbing: A review. *Water Research*, 117, 68–86. <http://doi.org/10.1016/J.WATRES.2017.03.046>
- Wang, H., Proctor, C. R., Edwards, M. A., Pryor, M., Santo Domingo, J. W., Ryu, H., ... Pruden, A. (2014). Microbial Community Response to Chlorine Conversion in a Chloraminated Drinking Water Distribution System. *Environmental Science & Technology*, 48(18), 10624–10633. <http://doi.org/10.1021/es502646d>
- Zhang, Q. (2009). The South-to-North Water Transfer Project of China: Environmental Implications and Monitoring Strategy. *JAWRA Journal of the American Water Resources Association*, 45(5), 1238–1247. <http://doi.org/10.1111/j.1752-1688.2009.00357.x>
- Zlatanovic, L., Moerman, A., van der Hoek, J. P., Vreeburg, J., & Blokker, M. (2017). Development and validation of a drinking water temperature model in domestic drinking water supply systems. *Urban Water Journal*, 1–7. <http://doi.org/10.1080/1573062X.2017.1325501>

Appendix A. Microbiological parameter data for pipes and filter bags

A.1 Pipe samples

- ATP

Table App. A- 1 Biofilm ATP concentration for 1st batch pipe samples in June, 2017

ATP(ng/cm ²)	L1	L2	L3	L4
Main	0.29	0.19	0.37	0.31
Household	0.24	0.09	0.04	0.01

Table App. A- 2 Biofilm ATP concentration for 2nd batch pipe samples in September, 2017

ATP(ng/cm ²)	L1	L2	L3	L4
Main	0.16	0.38	0.06	0.12
Household	0.17	0.21	0.55	5.29

Table App. A- 3 Biofilm ATP concentration for 3rd batch pipe samples in December, 2017

ATP(ng/cm ²)	L1	L2	L3	L4
Main	0.43	0.25	0.07	0.12
Household	0.31	1.889	1.687	/

- HPC

Table App. A- 4 Biofilm HPC concentration for 1st batch pipe samples in June, 2017

HPC(CFU/cm ²)	L1	L2	L3	L4
Main	0	0	0	4
Household	0	0	0	0

Table App. A- 5 Biofilm HPC concentration for 2nd batch pipe samples in September, 2017

HPC(CFU/cm ²)	L1	L2	L3	L4
Main	0	1	0	0
Household	0	0	1	0

Table App. A- 6 Biofilm HPC concentration for 3rd batch pipe samples in December, 2017

HPC(CFU/cm ²)	L1	L2	L3	L4
Main	0	0	0	0
Household	0	0	0	0

- Aeromonas

Table App. A- 7 Biofilm Aeromonas concentration for 1st batch pipe samples in June, 2017

Aeromonas (CFU/cm ²)	L1	L2	L3	L4
Main	0	0	0	1
Household	0	0	0	1

Table App. A- 8 Biofilm Aeromonas concentration for 2nd batch pipe samples in September, 2017

Aeromonas (CFU/cm ²)	L1	L2	L3	L4
Main	0	0	0	0
Household	0	0	0	0

Table App. A- 9 Biofilm Aeromonas concentration for 3rd batch pipe samples in December, 2017

Aeromonas (CFU/cm ²)	L1	L2	L3	L4
Main	0	0	0	0
Household	0	0	1	/

A.2 Filter samples

- ATP

Table App. A- 10 ATP concentration for 1st batch filter bags in September, 2017

ATP(ng/L)	L1	L2	L3	L4
Filter bag	1.34	0.77	2.25	1.14

Table App. A- 11 ATP concentration for 2nd batch of filter bags in November, 2017

ATP(ng/L)	L1	L2	L3	L4
Main	2.43	1.30	2.63	0.34

- HPC

Table App. A- 12 HPC concentration for 1st batch filter bags in September, 2017

HPC(CFU/L)	L1	L2	L3	L4
Filter bag	2417	1282	3449	1680

Table App. A- 13 HPC concentration for 2nd batch of filter bags in November, 2017

HPC(CFU/L)	L1	L2	L3	L4
Filter bag	2568	1192	3113	2111

- **Aeromonas**

Table App. A- 14 Aeromonas concentration for 1st batch filter bags in September, 2017

Aeromonas (CFU/L)	L1	L2	L3	L4
Filter bag	0	25	103	50

Table App. A- 15 Aeromonas concentration for 2nd batch of filter bags in November, 2017

Aeromonas (CFU/L)	L1	L2	L3	L4
Filter bag	0	0	38	6

Appendix B. Pressure drop resolution

Since the data logged every 8s, there were hundreds of thousands raw data collected. In order to make the data visualized and the results clearer, 2 different temporal resolution were compared to see which means would be better to describe the results. For all locations, the comparison for pressure and pressure difference were demonstrated below.

2h average was finally selected because it is capable to visualize data and describe the characteristics of the results in a comprise way where either the data amount or the resolution were acceptable. It is also especially suitable to manifest the pressure difference result. Because the (raw data) monitor has a very high temporal resolution, pressure fluctuation caused by hydraulic conditions (such as small sudden pressure change) in DWDS itself can be well captured by our monitor. However, as a consequence, instead of representing the pressure loss of the filter bag, the pressure difference obtained by the raw data calculation was an overlay of the pressure fluctuation in DWDS itself and the pressure drop caused by filter entrapment. As the pressure fluctuation is deliverable, an average of an appropriate resolution was able to eliminate the DWDS influence to a large extent. After average the data for 2h, pressure differences were all laying above zero.

Location 1:

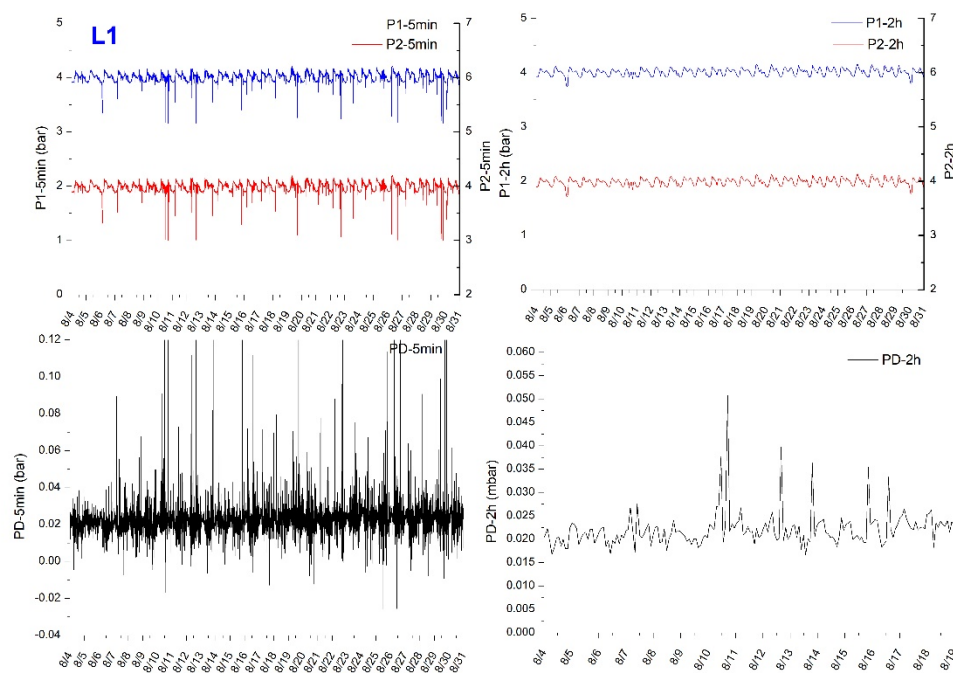


Figure App. B- 1 Comparison of 5min averaged pressure drop and 2h averaged pressure drop at L1.

Location 2:

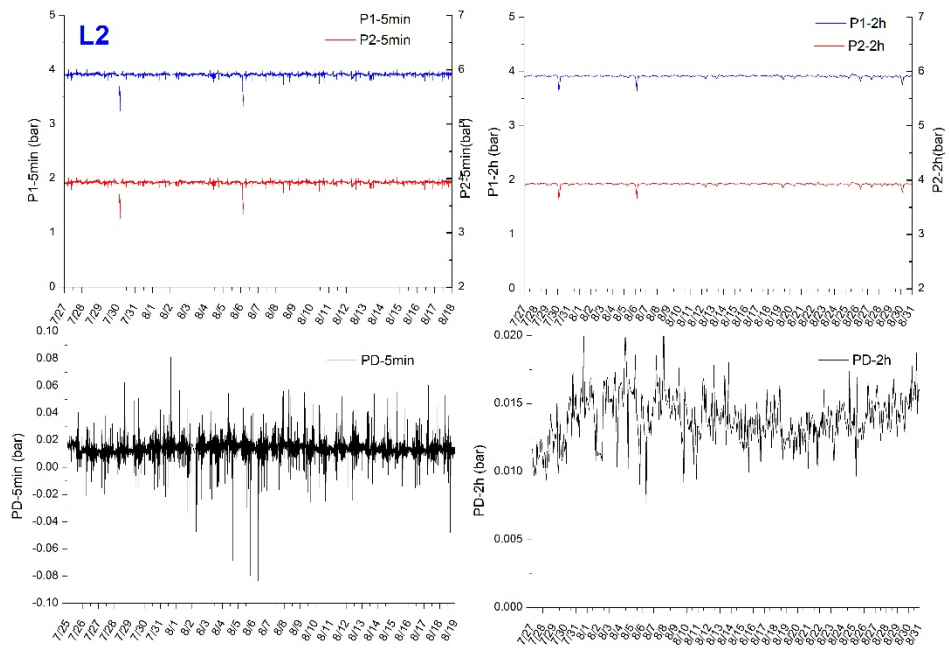


Figure App. B- 2 Comparison of 5min averaged pressure drop and 2h averaged pressure drop at L2.

Location 3:

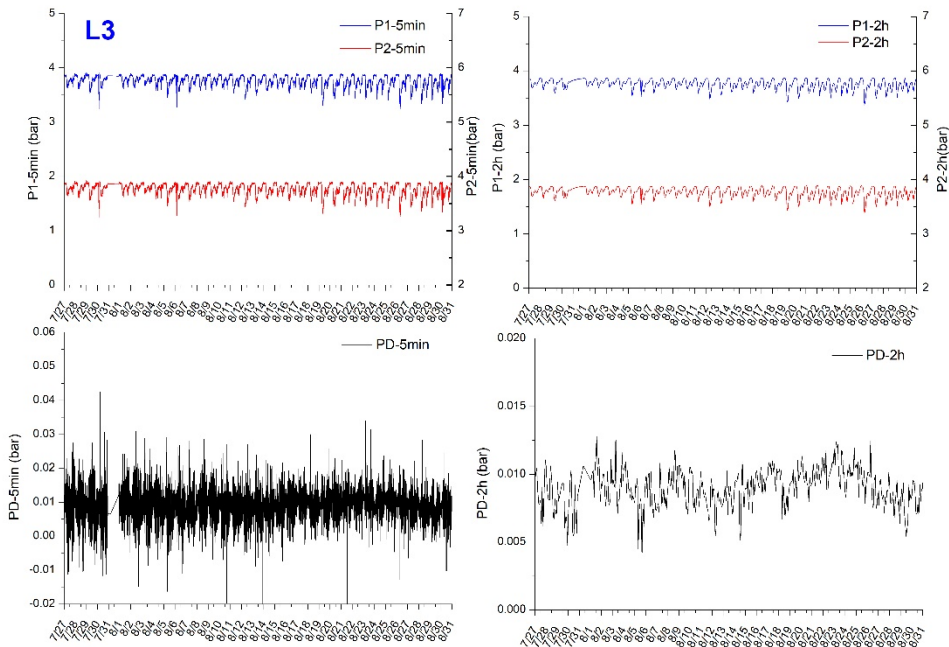


Figure App. B- 3 Comparison of 5min averaged pressure drop and 2h averaged pressure drop at L3.

Location 4:

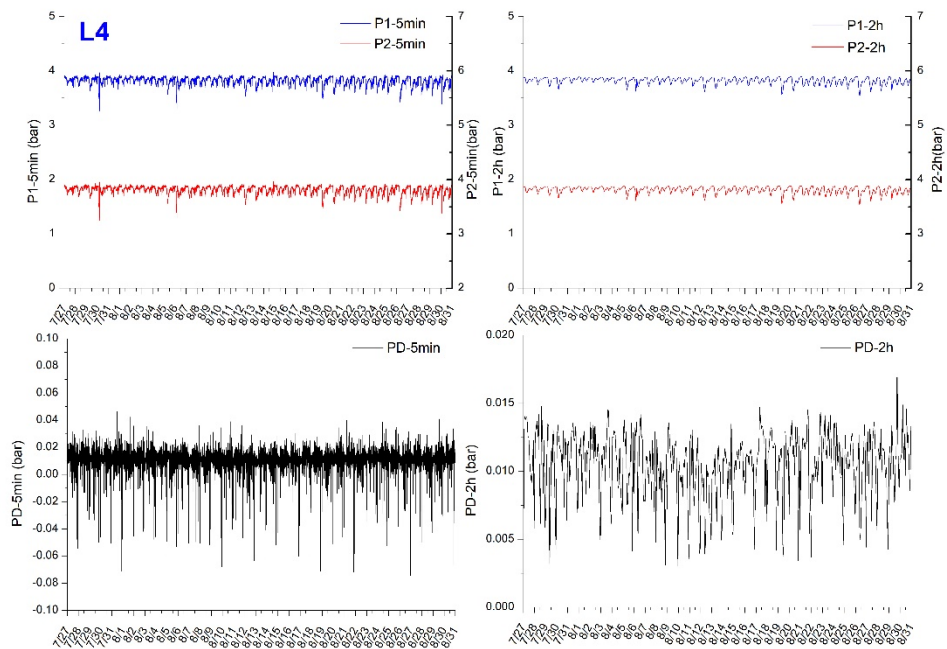


Figure App. B- 4 Comparison of 5min averaged pressure drop and 2h averaged pressure drop at L4.

The 2h averaged pressure drop can well describe the characteristics of pressure drop variation and was therefore selected as the resolution for data processing in this research.

Appendix C. ESEM and EDS results

B1-L1:

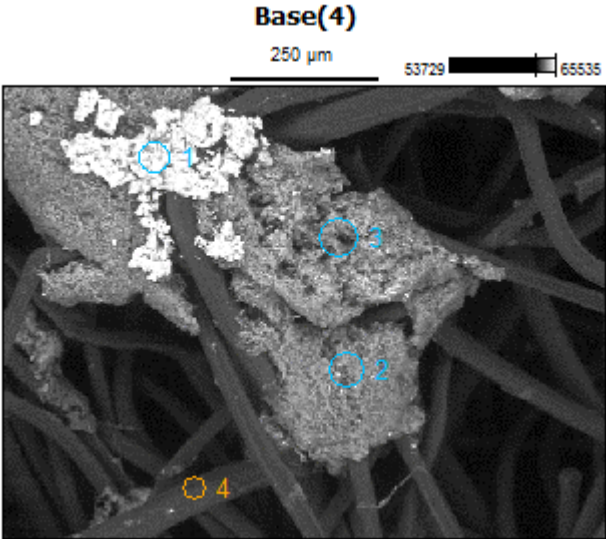
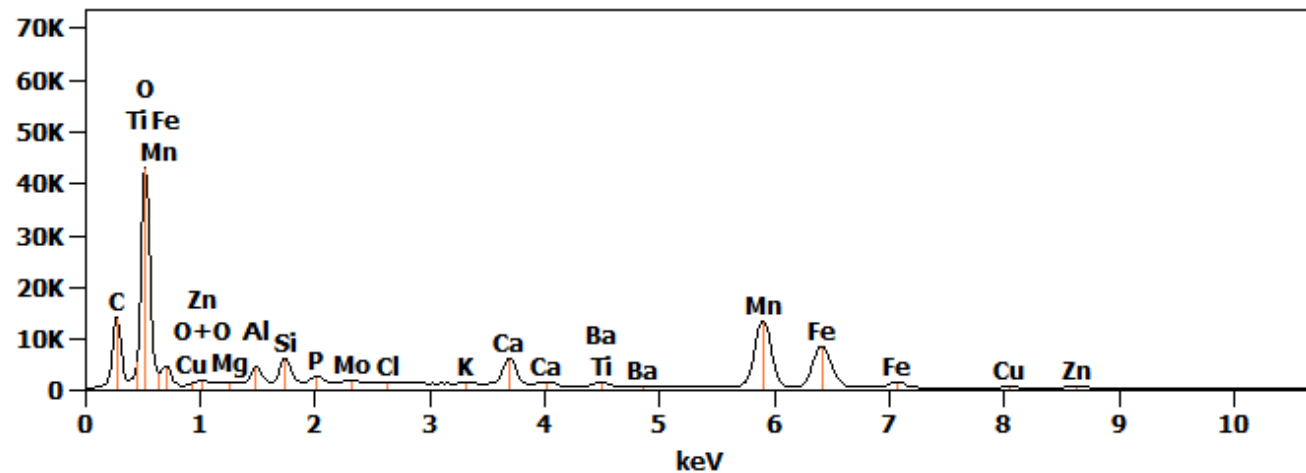


Image Name:	Base(4)
Image Resolution:	512 by 384
Image Pixel Size:	1.97 µm
Acc. Voltage:	20.0 kV
Magnification:	125

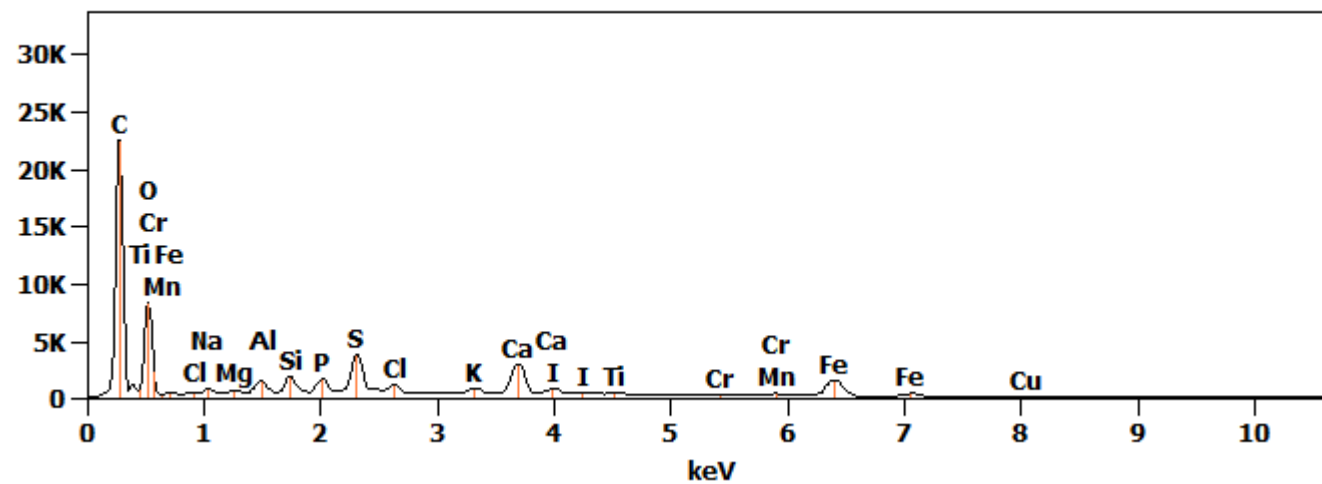
Full scale counts: 42956

Base(4)_pt1



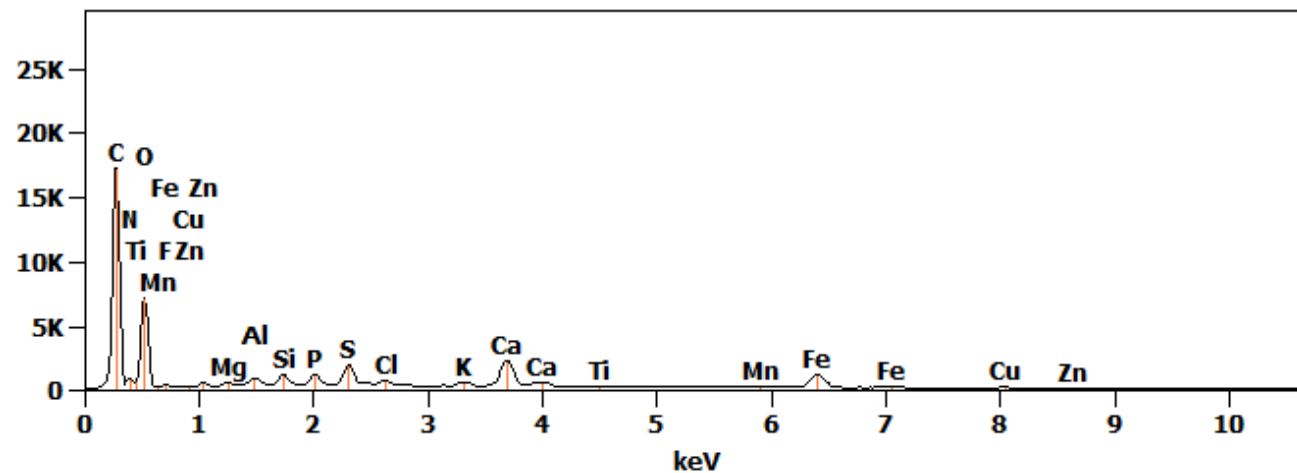
Full scale counts: 22462

Base(4)_pt2



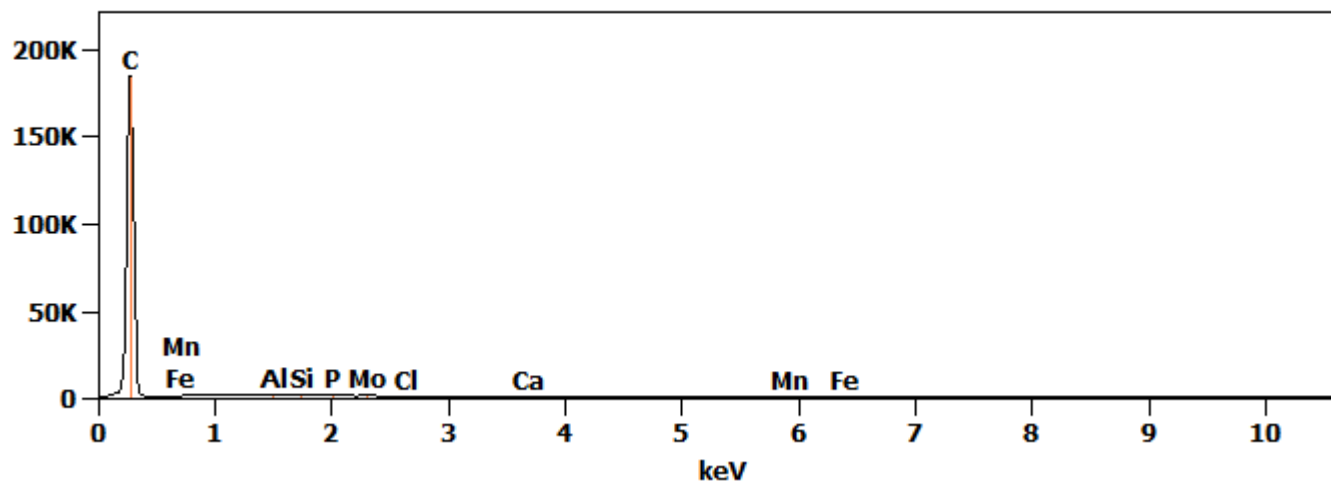
Full scale counts: 17239

Base(4)_pt3



Full scale counts: 184191

Base(4)_pt4



Net Counts

	<i>C-K</i>	<i>N-K</i>	<i>O-K</i>	<i>F-K</i>	<i>Na-K</i>	<i>Mg-K</i>	<i>Al-K</i>	<i>Si-K</i>	<i>P-K</i>	<i>S-K</i>	<i>Cl-K</i>	<i>K-K</i>	<i>Ca-K</i>	<i>Ti-K</i>	<i>Cr-K</i>	<i>Mn-K</i>	<i>Fe-K</i>	<i>Cu-K</i>	<i>Zn-K</i>	<i>Mo-L</i>	<i>I-L</i>	<i>Ba-L</i>	
<i>Base(</i>																							
<i>4)_pt1</i>	907		275			144	282	476	169		452	240	697	334		211	128	255	576	128		638	
	53		781			4	23	91	35		7	4	55	7		634	108	9	7	03		7	
<i>Base(</i>																							
<i>4)_pt2</i>	128		404		270	151	804	111	123	384	661	510	343	152	420	182	223	121			380		
	754		20		6	8	7	05	54	74	5	0	07	4		9	99	3			6		
<i>Base(</i>																							
<i>4)_pt3</i>	976	675	429	0		613	532	712	815	186	377	281	240	941		136	153	999	665				
	29	0	47				6	3	3	08	5	1	33			6	66						
<i>Base(</i>																							
<i>4)_pt4</i>	879						106	134	923		564		184			768	156				213		
	398						7	3					7				8				0		

Weight %

	<i>C-K</i>	<i>N-K</i>	<i>O-K</i>	<i>F-K</i>	<i>Na-K</i>	<i>Mg-K</i>	<i>Al-K</i>	<i>Si-K</i>	<i>P-K</i>	<i>S-K</i>	<i>Cl-K</i>	<i>K-K</i>	<i>Ca-K</i>	<i>Ti-K</i>	<i>Cr-K</i>	<i>Mn-K</i>	<i>Fe-K</i>	<i>Cu-K</i>	<i>Zn-K</i>	<i>Mo-L</i>	<i>I-L</i>	<i>Ba-L</i>	
<i>Base(4)</i>																							
<i>)_pt1</i>	20.9		43.3			0.08	1.09	1.56	0.48		0.13	0.08	2.42	0.16		16.6	10.7	0.37	1.02	0.55		0.46	
	0		5													4	1						
<i>Base(4)</i>																							
<i>)_pt2</i>	54.7		30.3		0.39	0.14	0.59	0.73	0.73	2.19	0.46	0.40	2.95	0.19	0.06	0.36	4.69	0.44				0.63	
	3		3																				
<i>Base(4)</i>																							
<i>)_pt3</i>	35.6	20.8	34.5	0.00		0.06	0.38	0.45	0.47	1.03	0.25	0.21	2.00	0.11		0.26	3.12	0.35	0.28				
	4	7	2																				
<i>Base(4)</i>																							
<i>)_pt4</i>	99.2						0.04	0.05	0.03		0.02		0.11			0.10	0.23			0.13			
	8																						

Atom %

	<i>C-K</i>	<i>N-K</i>	<i>O-K</i>	<i>F-K</i>	<i>Na-K</i>	<i>Mg-K</i>	<i>Al-K</i>	<i>Si-K</i>	<i>P-K</i>	<i>S-K</i>	<i>Cl-K</i>	<i>K-K</i>	<i>Ca-K</i>	<i>Ti-K</i>	<i>Cr-K</i>	<i>Mn-K</i>	<i>Fe-K</i>	<i>Cu-K</i>	<i>Zn-K</i>	<i>Mo-L</i>	<i>I-L</i>	<i>Ba-L</i>	
Base(4)																							
<i>)_pt1</i>	33.7		52.5			0.06	0.78	1.08	0.30		0.07	0.04	1.17	0.06		5.87	3.72	0.11	0.30	0.11		0.07	
	4		2																				
Base(4)																							
<i>)_pt2</i>	66.8		27.8		0.25	0.09	0.32	0.38	0.35	1.00	0.19	0.15	1.08	0.06	0.02	0.10	1.23	0.10				0.07	
	3		0																				
Base(4)																							
<i>)_pt3</i>	43.4	21.8	31.5	0.00		0.03	0.21	0.24	0.22	0.47	0.10	0.08	0.73	0.03		0.07	0.82	0.08	0.06				
	5	2	9																				
Base(4)																							
<i>)_pt4</i>	99.8						0.02	0.02	0.01		0.01		0.03			0.02	0.05				0.02		
	2																						

Formula

	<i>C-K</i>	<i>N-K</i>	<i>O-K</i>	<i>F-K</i>	<i>Na-K</i>	<i>Mg-K</i>	<i>Al-K</i>	<i>Si-K</i>	<i>P-K</i>	<i>S-K</i>	<i>Cl-K</i>	<i>K-K</i>	<i>Ca-K</i>	<i>Ti-K</i>	<i>Cr-K</i>	<i>Mn-K</i>	<i>Fe-K</i>	<i>Cu-K</i>	<i>Zn-K</i>	<i>Mo-L</i>	<i>I-L</i>	<i>Ba-L</i>
<i>Base(4)_pt1</i>	C		O			Mg	Al	Si	P		Cl	K	Ca	Ti		Mn	Fe	Cu	Zn	Mo		Ba
<i>Base(4)_pt2</i>	C		O		Na	Mg	Al	Si	P	S	Cl	K	Ca	Ti	Cr	Mn	Fe	Cu			I	
<i>Base(4)_pt3</i>	C	N	O	F		Mg	Al	Si	P	S	Cl	K	Ca	Ti		Mn	Fe	Cu	Zn			
<i>Base(4)_pt4</i>	C						Al	Si	P		Cl		Ca			Mn	Fe				Mo	

Compound %

	<i>C</i>	<i>N</i>	<i>O</i>	<i>F</i>	<i>Na</i>	<i>Mg</i>	<i>Al</i>	<i>Si</i>	<i>P</i>	<i>S</i>	<i>Cl</i>	<i>K</i>	<i>Ca</i>	<i>Ti</i>	<i>Cr</i>	<i>Mn</i>	<i>Fe</i>	<i>Cu</i>	<i>Zn</i>	<i>Mo</i>	<i>I</i>	<i>Ba</i>	
<i>Base(4)</i>																							
<i>)_pt1</i>	20.9		43.3			0.08	1.09	1.56	0.48		0.13	0.08	2.42	0.16		16.6	10.7	0.37	1.02	0.55			0.46
	0		5													4	1						
<i>Base(4)</i>																							
<i>)_pt2</i>	54.7		30.3		0.39	0.14	0.59	0.73	0.73	2.19	0.46	0.40	2.95	0.19	0.06	0.36	4.69	0.44				0.63	
	3		3																				
<i>Base(4)</i>																							
<i>)_pt3</i>	35.6	20.8	34.5	0.00		0.06	0.38	0.45	0.47	1.03	0.25	0.21	2.00	0.11		0.26	3.12	0.35	0.28				
	4	7	2																				
<i>Base(4)</i>																							
<i>)_pt4</i>	99.2						0.04	0.05	0.03		0.02		0.11			0.10	0.23				0.13		
	8																						

B1-L2:

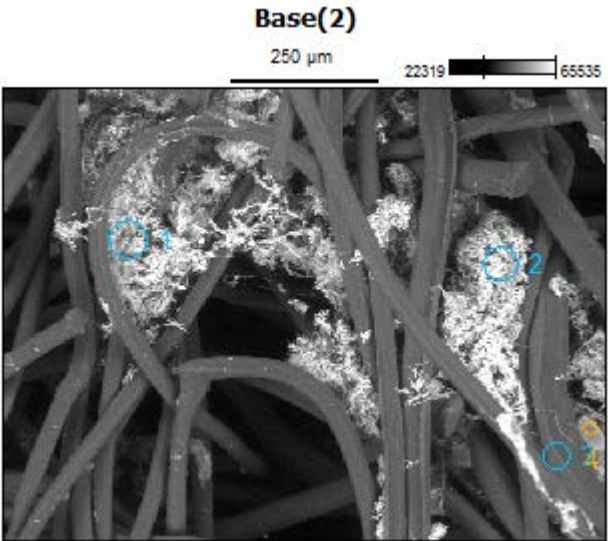
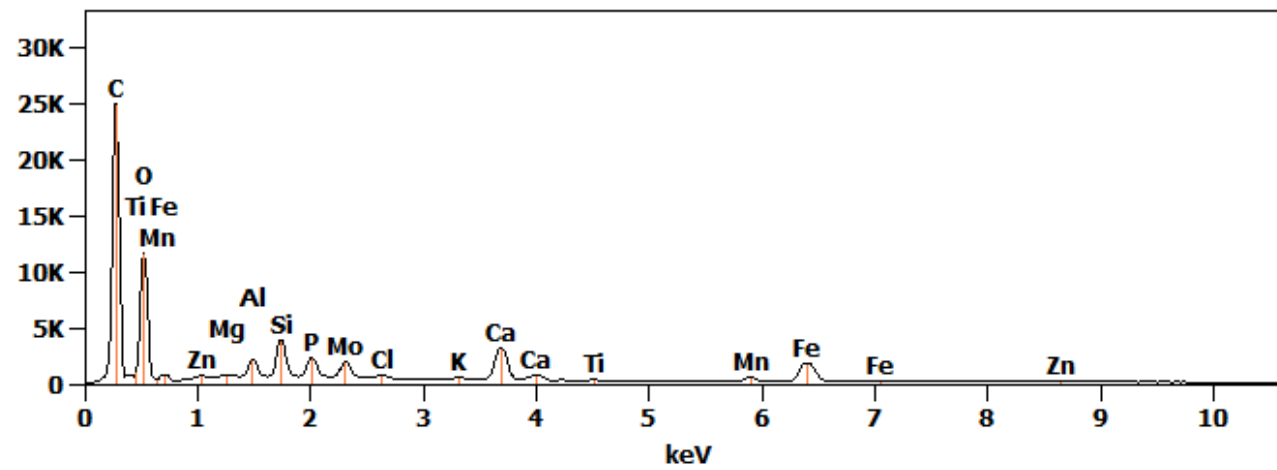


Image Name:	Base(2)
Image Resolution:	512 by 384
Image Pixel Size:	1.97 µm
Acc. Voltage:	20.0 kV
Magnification:	125

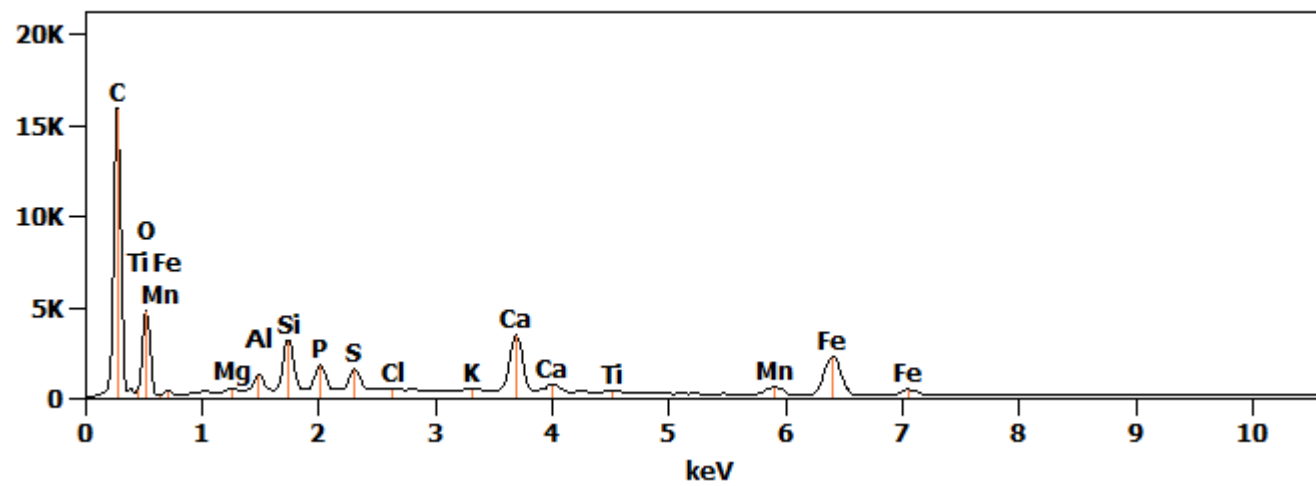
Full scale counts: 24916

Base(2)_pt1



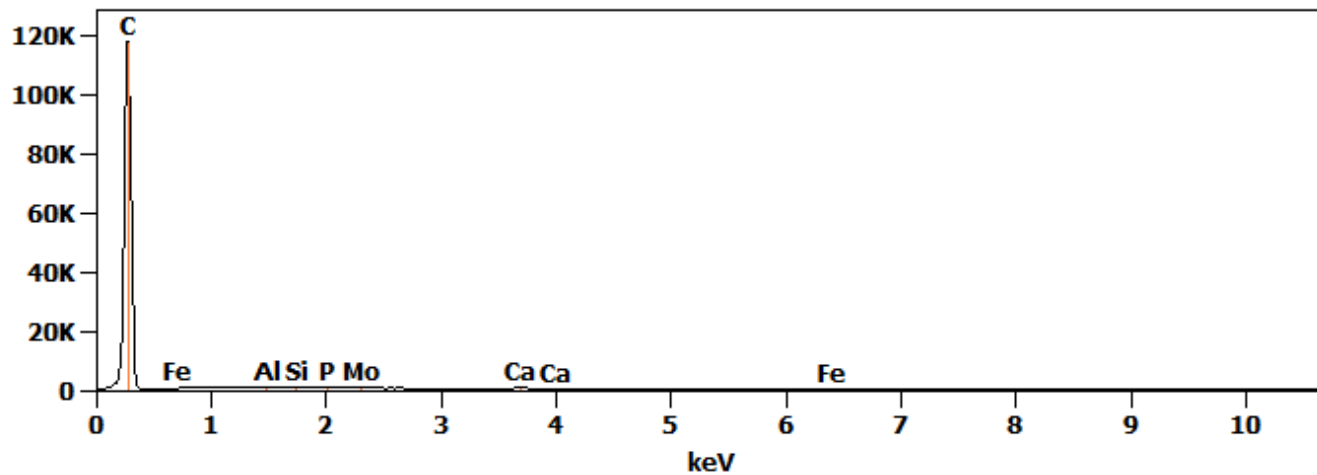
Full scale counts: 15930

Base(2)_pt2



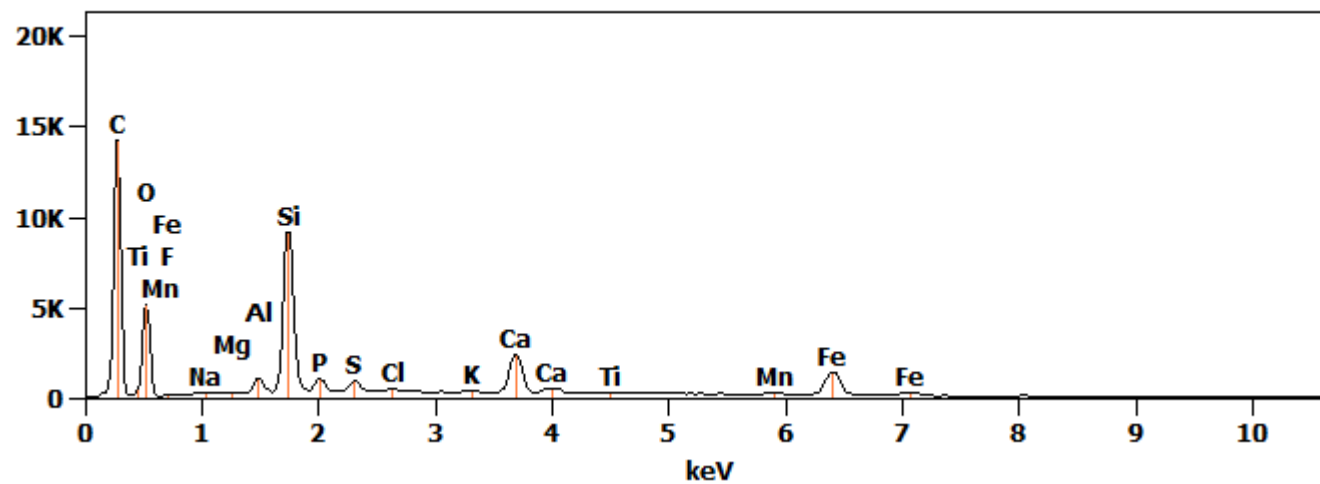
Full scale counts: 117451

Base(2)_pt3



Full scale counts: 14203

Base(2)_pt4



Net Counts

	<i>C-K</i>	<i>O-K</i>	<i>F-K</i>	<i>Na-K</i>	<i>Mg-K</i>	<i>Al-K</i>	<i>Si-K</i>	<i>P-K</i>	<i>S-K</i>	<i>Cl-K</i>	<i>K-K</i>	<i>Ca-K</i>	<i>Ti-K</i>	<i>Mn-K</i>	<i>Fe-K</i>	<i>Zn-K</i>	<i>Mo-L</i>
<i>Base(2)_pt1</i>	13729	65320			2345	13531	29914	18448		6444	1462	33649	1265	5109	27836	660	26023
<i>Base(2)_pt2</i>	89109	25834			992	7747	26072	14410	13660	2064	1614	36856	1544	6588	33708		
<i>Base(2)_pt3</i>	56422					1324	2480	1306				2926			1980		1629
<i>Base(2)_pt4</i>	79619	29598	0	361	516	6644	81004	7720	6670	1342	1177	26127	1335	2347	19131		

Weight %

	<i>C-K</i>	<i>O-K</i>	<i>F-K</i>	<i>Na-K</i>	<i>Mg-K</i>	<i>Al-K</i>	<i>Si-K</i>	<i>P-K</i>	<i>S-K</i>	<i>Cl-K</i>	<i>K-K</i>	<i>Ca-K</i>	<i>Ti-K</i>	<i>Mn-K</i>	<i>Fe-K</i>	<i>Zn-K</i>	<i>Mo-L</i>
<i>Base(2)_p t1</i>	48.41	36.82			0.19	0.84	1.67	0.94		0.38	0.10	2.44	0.13	0.84	4.88	0.24	2.13
<i>Base(2)_p t2</i>	53.28	25.61			0.13	0.76	2.29	1.16	1.06	0.19	0.17	4.15	0.25	1.70	9.26		
<i>Base(2)_p t3</i>	98.86					0.08	0.14	0.07				0.26			0.44		0.15
<i>Base(2)_p t4</i>	53.05	28.87	0.00	0.07	0.06	0.62	6.84	0.64	0.53	0.12	0.12	2.97	0.22	0.61	5.28		

Atom %

	<i>C-K</i>	<i>O-K</i>	<i>F-K</i>	<i>Na-K</i>	<i>Mg-K</i>	<i>Al-K</i>	<i>Si-K</i>	<i>P-K</i>	<i>S-K</i>	<i>Cl-K</i>	<i>K-K</i>	<i>Ca-K</i>	<i>Ti-K</i>	<i>Mn-K</i>	<i>Fe-K</i>	<i>Zn-K</i>	<i>Mo-L</i>
<i>Base(2)_p</i>																	
<i>t1</i>	60.46	34.53			0.12	0.47	0.89	0.45		0.16	0.04	0.91	0.04	0.23	1.31	0.06	0.33
<i>Base(2)_p</i>																	
<i>t2</i>	67.85	24.49			0.08	0.43	1.25	0.57	0.50	0.08	0.06	1.58	0.08	0.47	2.54		
<i>Base(2)_p</i>																	
<i>t3</i>	99.68					0.04	0.06	0.03				0.08			0.09		0.02
<i>Base(2)_p</i>																	
<i>t4</i>	65.72	26.85	0.00	0.04	0.04	0.34	3.62	0.31	0.24	0.05	0.05	1.10	0.07	0.16	1.41		

Formula

	<i>C-K</i>	<i>O-K</i>	<i>F-K</i>	<i>Na-K</i>	<i>Mg-K</i>	<i>Al-K</i>	<i>Si-K</i>	<i>P-K</i>	<i>S-K</i>	<i>Cl-K</i>	<i>K-K</i>	<i>Ca-K</i>	<i>Ti-K</i>	<i>Mn-K</i>	<i>Fe-K</i>	<i>Zn-K</i>	<i>Mo-L</i>
<i>Base(2)_pt1</i>	C	O			Mg	Al	Si	P		Cl	K	Ca	Ti	Mn	Fe	Zn	Mo
<i>Base(2)_pt2</i>	C	O			Mg	Al	Si	P	S	Cl	K	Ca	Ti	Mn	Fe		
<i>Base(2)_pt3</i>	C					Al	Si	P				Ca			Fe		Mo
<i>Base(2)_pt4</i>	C	O	F	Na	Mg	Al	Si	P	S	Cl	K	Ca	Ti	Mn	Fe		

Compound %

	<i>C</i>	<i>O</i>	<i>F</i>	<i>Na</i>	<i>Mg</i>	<i>Al</i>	<i>Si</i>	<i>P</i>	<i>S</i>	<i>Cl</i>	<i>K</i>	<i>Ca</i>	<i>Ti</i>	<i>Mn</i>	<i>Fe</i>	<i>Zn</i>	<i>Mo</i>
<i>Base(2)_p</i>																	
<i>t1</i>	48.41	36.82			0.19	0.84	1.67	0.94		0.38	0.10	2.44	0.13	0.84	4.88	0.24	2.13
<i>Base(2)_p</i>																	
<i>t2</i>	53.28	25.61			0.13	0.76	2.29	1.16	1.06	0.19	0.17	4.15	0.25	1.70	9.26		
<i>Base(2)_p</i>																	
<i>t3</i>	98.86					0.08	0.14	0.07				0.26			0.44		0.15
<i>Base(2)_p</i>																	
<i>t4</i>	53.05	28.87	0.00	0.07	0.06	0.62	6.84	0.64	0.53	0.12	0.12	2.97	0.22	0.61	5.28		

B1-L3:

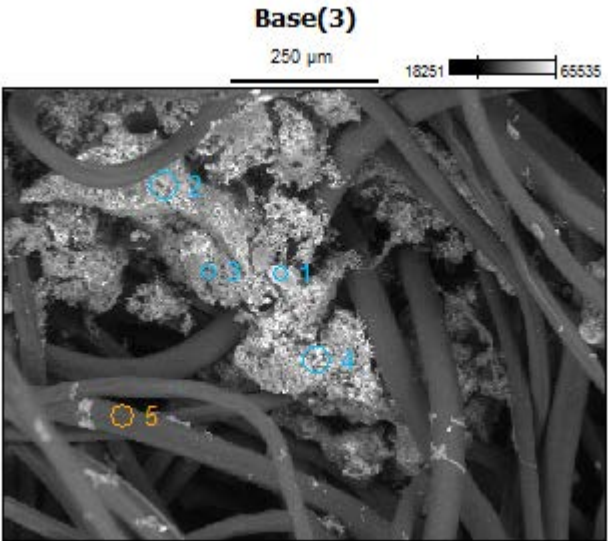
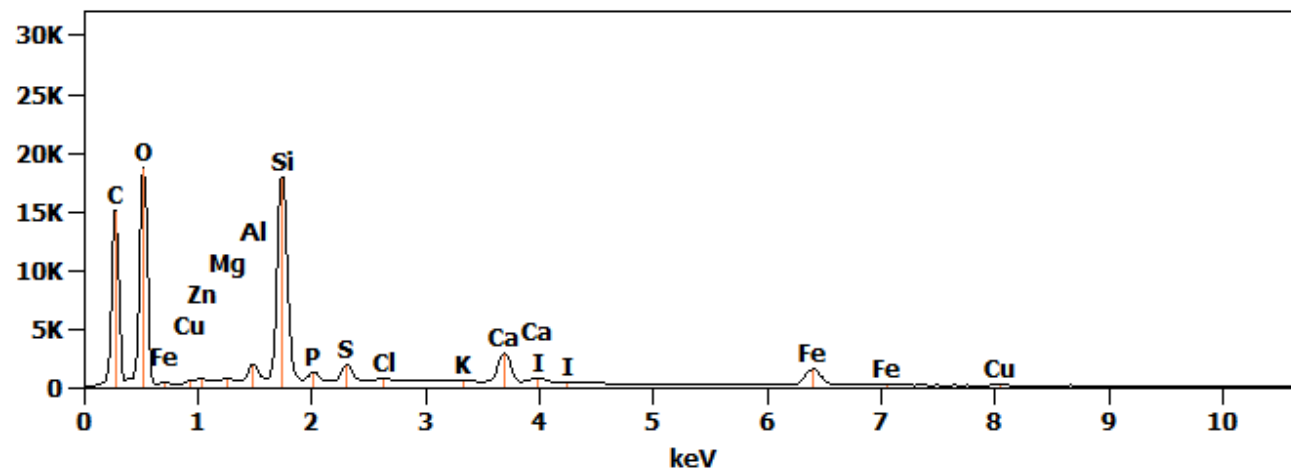


Image Name:	Base(3)
Image Resolution:	512 by 384
Image Pixel Size:	1.97 μm
Acc. Voltage:	20.0 kV
Magnification:	125

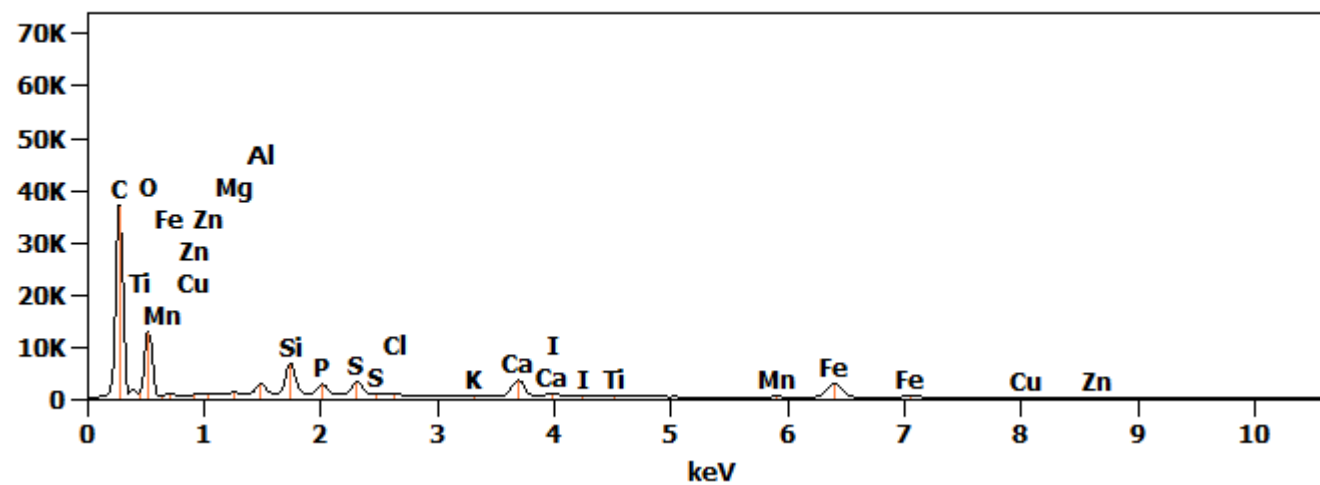
Full scale counts: 18727

Base(3)_pt1



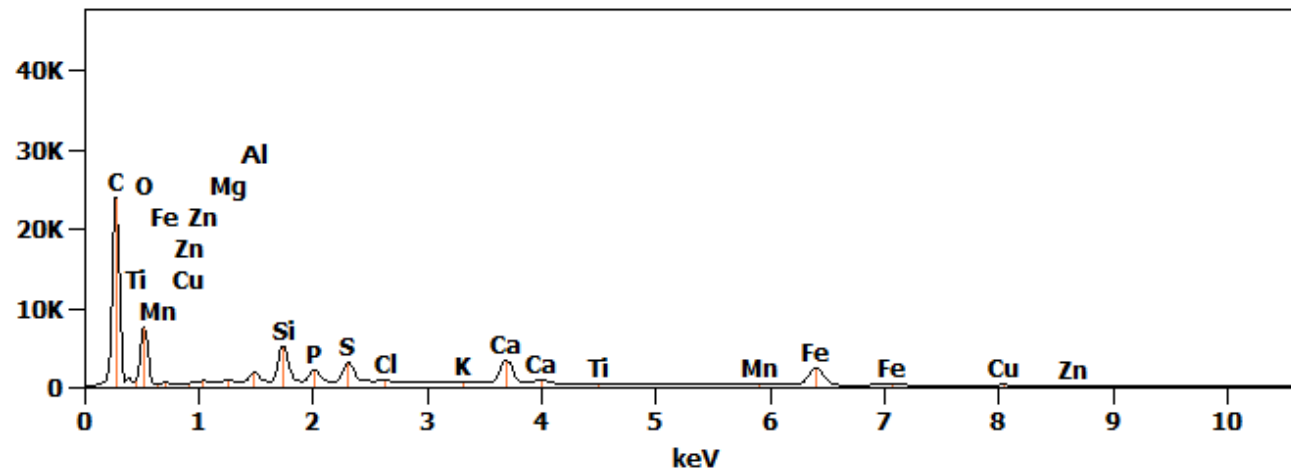
Full scale counts: 37059

Base(3)_pt2



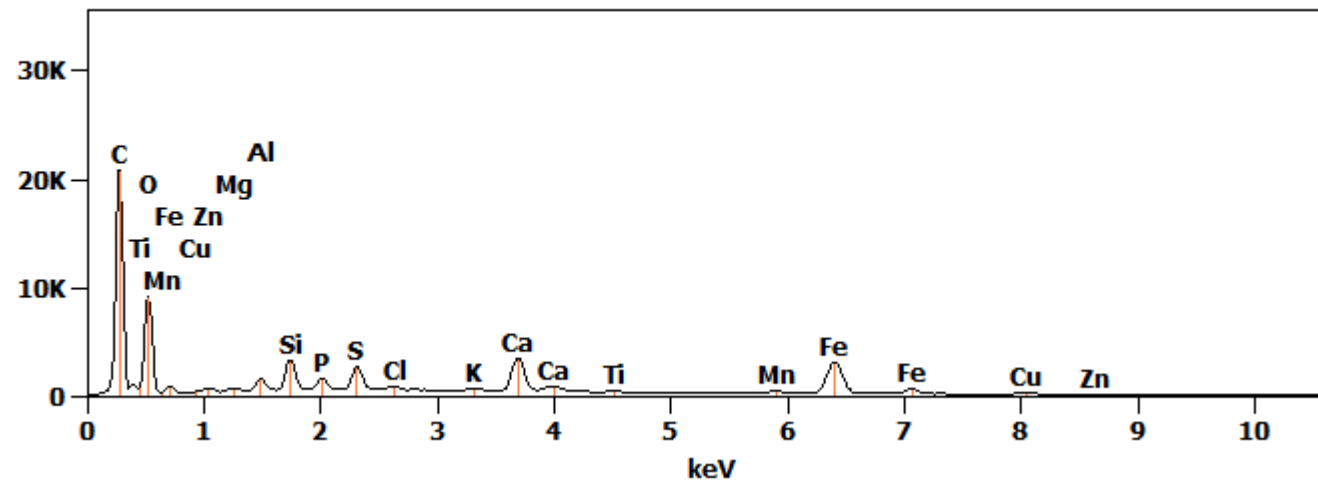
Full scale counts: 23895

Base(3)_pt3



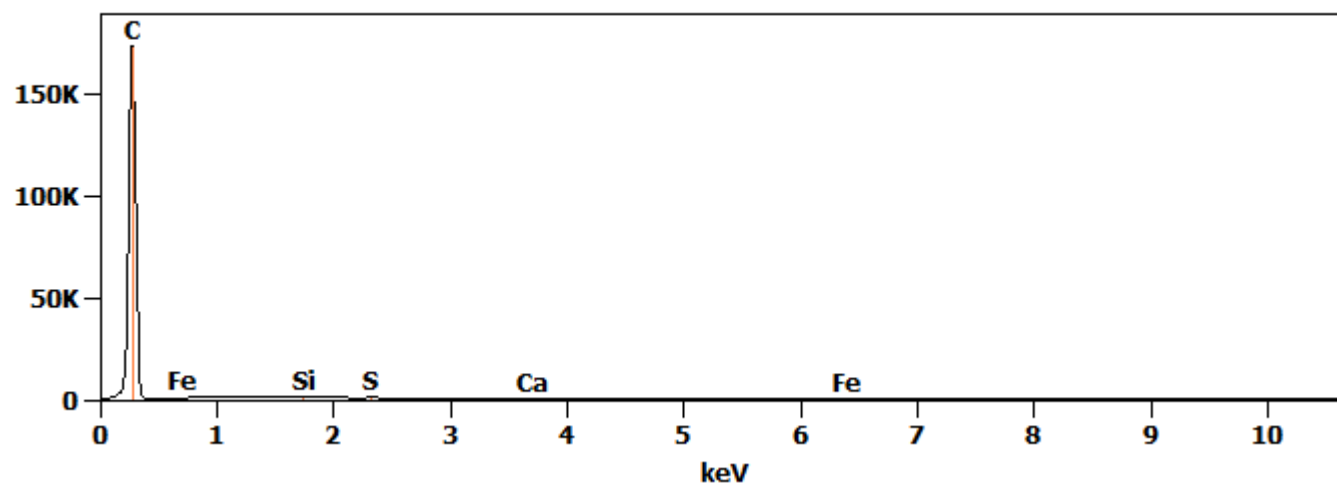
Full scale counts: 20772

Base(3)_pt4



Full scale counts: 172755

Base(3)_pt5



Net Counts

	<i>C-K</i>	<i>O-K</i>	<i>Mg-K</i>	<i>Al-K</i>	<i>Si-K</i>	<i>P-K</i>	<i>S-K</i>	<i>Cl-K</i>	<i>K-K</i>	<i>Ca-K</i>	<i>Ti-K</i>	<i>Mn-K</i>	<i>Fe-K</i>	<i>Cu-K</i>	<i>Zn-K</i>	<i>I-L</i>
<i>Base(3)_p</i>																
<i>t1</i>	80712	110480	1794	11980	161149	8493	15844	3753	1237	30434			22620	1445	889	3724
<i>Base(3)_p</i>																
<i>t2</i>	213145	82804	3071	17149	52935	21824	28435	2905	1332	37037	1729	1618	40767	1820	714	4278
<i>Base(3)_p</i>																
<i>t3</i>	136878	47654	1992	9778	41722	15688	27766	3490	1911	34255	1161	1130	33239	1673	719	
<i>Base(3)_p</i>																
<i>t4</i>	109765	57475	1756	10074	25974	11794	23076	4136	1618	36062	1566	3906	45423	1645	945	
<i>Base(3)_p</i>																
<i>t5</i>	943340				1210		1222			1506			1320			

Weight %

	<i>C-K</i>	<i>O-K</i>	<i>Mg-K</i>	<i>Al-K</i>	<i>Si-K</i>	<i>P-K</i>	<i>S-K</i>	<i>Cl-K</i>	<i>K-K</i>	<i>Ca-K</i>	<i>Ti-K</i>	<i>Mn-K</i>	<i>Fe-K</i>	<i>Cu-K</i>	<i>Zn-K</i>	<i>I-L</i>
<i>Base(3)_pt</i>																
<i>1</i>	36.58	46.02	0.13	0.68	8.25	0.43	0.75	0.21	0.08	2.05			3.64	0.40	0.30	0.48
<i>Base(3)_pt</i>																
<i>2</i>	52.83	33.96	0.17	0.75	2.07	0.78	0.98	0.12	0.06	1.89	0.13	0.19	5.07	0.39	0.19	0.42
<i>Base(3)_pt</i>																
<i>3</i>	53.79	30.52	0.17	0.63	2.42	0.84	1.43	0.21	0.13	2.60	0.13	0.20	6.13	0.53	0.28	
<i>Base(3)_pt</i>																
<i>4</i>	46.81	34.77	0.17	0.73	1.66	0.68	1.27	0.27	0.12	2.89	0.18	0.71	8.82	0.55	0.38	
<i>Base(3)_pt</i>																
<i>5</i>	99.65				0.04		0.04			0.08			0.18			

Atom %

	<i>C-K</i>	<i>O-K</i>	<i>Mg-K</i>	<i>Al-K</i>	<i>Si-K</i>	<i>P-K</i>	<i>S-K</i>	<i>Cl-K</i>	<i>K-K</i>	<i>Ca-K</i>	<i>Ti-K</i>	<i>Mn-K</i>	<i>Fe-K</i>	<i>Cu-K</i>	<i>Zn-K</i>	<i>I-L</i>
<i>Base(3)_pt1</i>	47.42	44.79	0.09	0.39	4.57	0.22	0.36	0.09	0.03	0.80			1.01	0.10	0.07	0.06
<i>Base(3)_pt2</i>	64.24	31.00	0.10	0.40	1.08	0.37	0.45	0.05	0.02	0.69	0.04	0.05	1.33	0.09	0.04	0.05
<i>Base(3)_pt3</i>	66.09	28.15	0.10	0.35	1.27	0.40	0.66	0.09	0.05	0.96	0.04	0.05	1.62	0.12	0.06	
<i>Base(3)_pt4</i>	59.99	33.45	0.11	0.41	0.91	0.34	0.61	0.12	0.05	1.11	0.06	0.20	2.43	0.13	0.09	
<i>Base(3)_pt5</i>	99.90				0.02		0.02			0.03			0.04			

Formula

	<i>C-K</i>	<i>O-K</i>	<i>Mg-K</i>	<i>Al-K</i>	<i>Si-K</i>	<i>P-K</i>	<i>S-K</i>	<i>Cl-K</i>	<i>K-K</i>	<i>Ca-K</i>	<i>Ti-K</i>	<i>Mn-K</i>	<i>Fe-K</i>	<i>Cu-K</i>	<i>Zn-K</i>	<i>I-L</i>
<i>Base(3)_pt1</i>	C	O	Mg	Al	Si	P	S	Cl	K	Ca			Fe	Cu	Zn	I
<i>Base(3)_pt2</i>	C	O	Mg	Al	Si	P	S	Cl	K	Ca	Ti	Mn	Fe	Cu	Zn	I
<i>Base(3)_pt3</i>	C	O	Mg	Al	Si	P	S	Cl	K	Ca	Ti	Mn	Fe	Cu	Zn	
<i>Base(3)_pt4</i>	C	O	Mg	Al	Si	P	S	Cl	K	Ca	Ti	Mn	Fe	Cu	Zn	
<i>Base(3)_pt5</i>	C				Si		S			Ca			Fe			

Compound %

	<i>C</i>	<i>O</i>	<i>Mg</i>	<i>Al</i>	<i>Si</i>	<i>P</i>	<i>S</i>	<i>Cl</i>	<i>K</i>	<i>Ca</i>	<i>Ti</i>	<i>Mn</i>	<i>Fe</i>	<i>Cu</i>	<i>Zn</i>	<i>I</i>
<i>Base(3)_pt</i>																
<i>1</i>	36.58	46.02	0.13	0.68	8.25	0.43	0.75	0.21	0.08	2.05			3.64	0.40	0.30	0.48
<i>Base(3)_pt</i>																
<i>2</i>	52.83	33.96	0.17	0.75	2.07	0.78	0.98	0.12	0.06	1.89	0.13	0.19	5.07	0.39	0.19	0.42
<i>Base(3)_pt</i>																
<i>3</i>	53.79	30.52	0.17	0.63	2.42	0.84	1.43	0.21	0.13	2.60	0.13	0.20	6.13	0.53	0.28	
<i>Base(3)_pt</i>																
<i>4</i>	46.81	34.77	0.17	0.73	1.66	0.68	1.27	0.27	0.12	2.89	0.18	0.71	8.82	0.55	0.38	
<i>Base(3)_pt</i>																
<i>5</i>	99.65				0.04		0.04			0.08			0.18			

B1-L4:

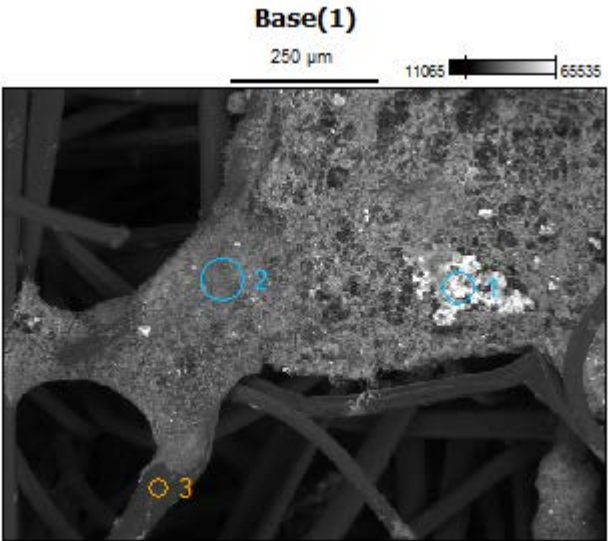
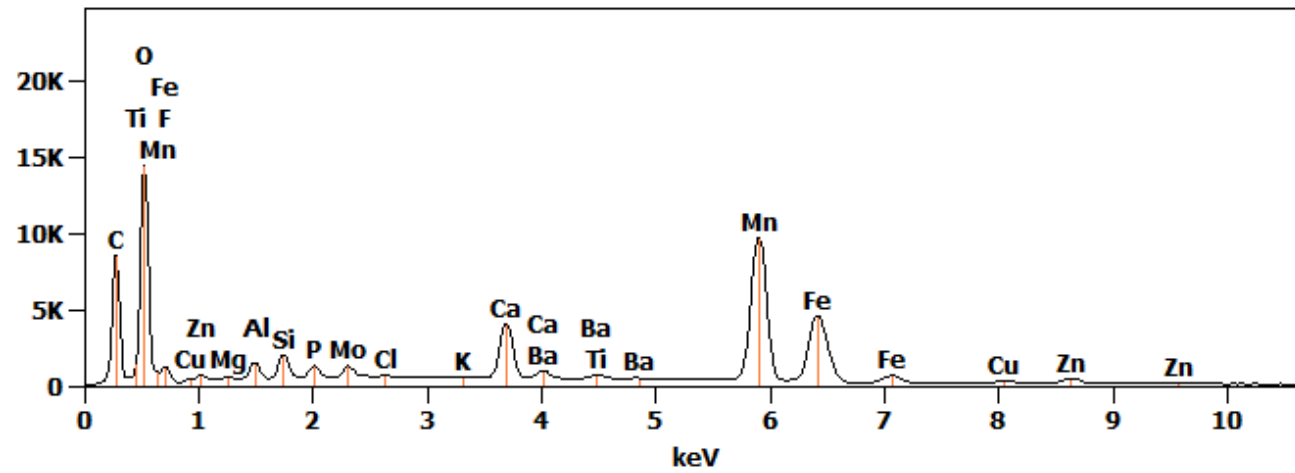


Image Name:	Base(1)
Image Resolution:	512 by 384
Image Pixel Size:	1.97 μm
Acc. Voltage:	20.0 kV
Magnification:	125

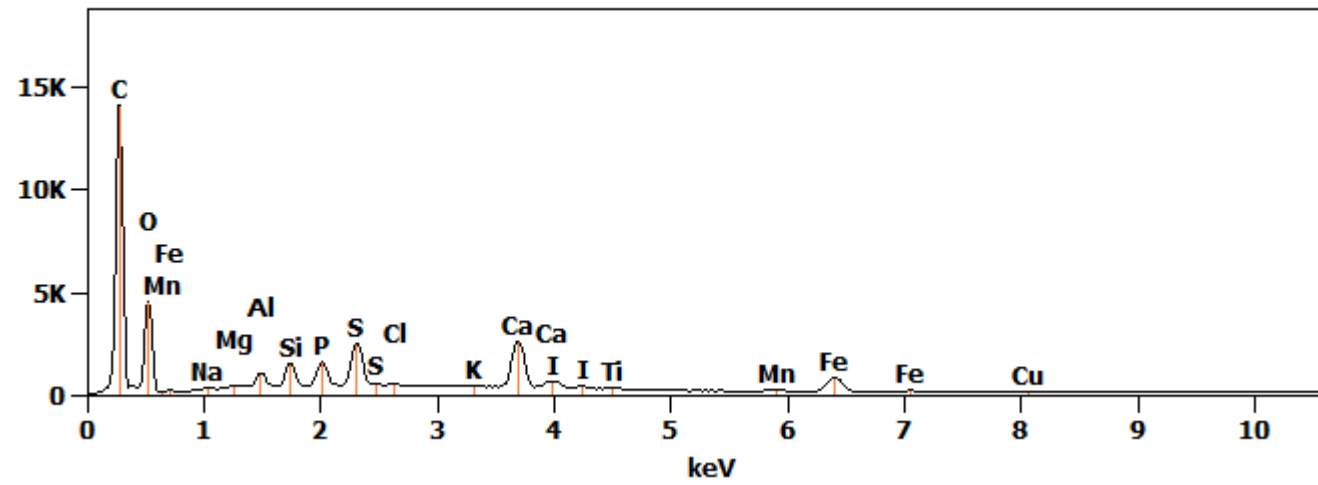
Full scale counts: 14430

Base(1)_pt1



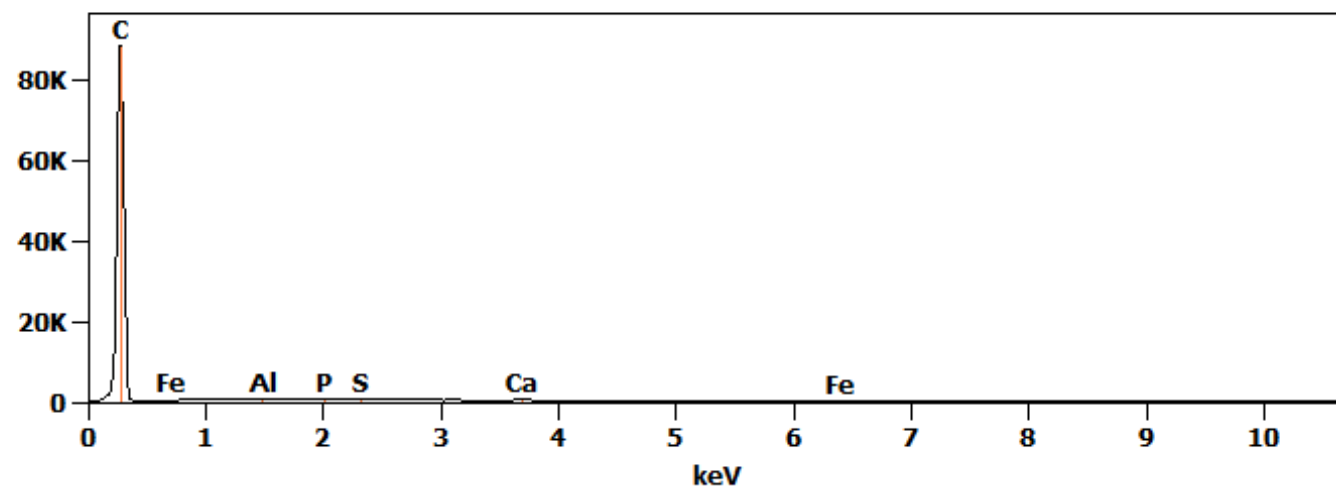
Full scale counts: 14074

Base(1)_pt2



Full scale counts: 88461

Base(1)_pt3



Net Counts

	C- K	O- K	F- K	Na- K	Mg- K	Al- K	Si- K	P- K	S- K	Cl- K	K- K	Ca- K	Ti- K	Mn- K	Fe- K	Cu- K	Zn- K	Mo- L	I- L	Ba- L
Base(1)																				
_pt1	5007	8730	0		1032	9604	1478	7758		2716	622	4644	2976	1500	6537	3565	6038	1278		3249
	9	6					5					1		11	1			2		
Base(1)																				
_pt2	7890	2440		740	1113	5326	9848	1196	2490	1789	1019	2934	835	1472	1101	733				4345
	3	4						4	0			1			7					
Base(1)																				
_pt3	4761					1199		1117	1384			1535			842					
	57																			

Weight %

	C- K	O- K	F- K	Na- K	Mg- K	Al- K	Si- K	P- K	S- K	Cl- K	K- K	Ca- K	Ti- K	Mn- K	Fe- K	Cu- K	Zn- K	Mo- L	I- L	Ba- L
Base(1)																				
_pt1	23.6	31.3	0.00		0.12	0.77	0.99	0.44		0.16	0.04	3.21	0.28	23.4	10.8	1.04	2.12	1.12		0.47
	9	2												0	2					
Base(1)																				
_pt2	54.4	29.8		0.17	0.17	0.62	1.03	1.13	2.29	0.20	0.13	4.06	0.17	0.47	3.71	0.42			1.15	
	4	5																		
Base(1)																				
_pt3	99.3					0.09		0.07	0.09			0.16			0.23					
	5																			

Atom %

	C- K	O- K	F- K	Na- K	Mg- K	Al- K	Si- K	P- K	S- K	Cl- K	K- K	Ca- K	Ti- K	Mn- K	Fe- K	Cu- K	Zn- K	Mo- L	I- L	Ba- L
Base(1)																				
_pt1	41.1 9	40.8 9	0.00		0.10	0.60	0.74	0.30		0.10	0.02	1.67	0.12	8.90	4.05	0.34	0.68	0.24		0.07
Base(1)																				
_pt2	66.8 1	27.5 0		0.11	0.10	0.34	0.54	0.54	1.05	0.08	0.05	1.49	0.05	0.12	0.98	0.10			0.13	
Base(1)																				
_pt3	99.8 0					0.04		0.03	0.03			0.05			0.05					

Formula

	C- K	O- K	F- K	Na- K	Mg- K	Al- K	Si- K	P- K	S- K	Cl- K	K- K	Ca- K	Ti- K	Mn- K	Fe- K	Cu- K	Zn- K	Mo- L	I- L	Ba- L
Base(1)_ pt1	C	O	F		Mg	Al	Si	P		Cl	K	Ca	Ti	Mn	Fe	Cu	Zn	Mo		Ba
Base(1)_ pt2	C	O		Na	Mg	Al	Si	P	S	Cl	K	Ca	Ti	Mn	Fe	Cu			I	
Base(1)_ pt3	C					Al		P	S			Ca			Fe					

Compound %

	<i>C</i>	<i>O</i>	<i>F</i>	<i>Na</i>	<i>Mg</i>	<i>Al</i>	<i>Si</i>	<i>P</i>	<i>S</i>	<i>Cl</i>	<i>K</i>	<i>Ca</i>	<i>Ti</i>	<i>Mn</i>	<i>Fe</i>	<i>Cu</i>	<i>Zn</i>	<i>Mo</i>	<i>I</i>	<i>Ba</i>
<i>Base(1)</i>																				
<i>_pt1</i>	23.6	31.3	0.00		0.12	0.77	0.99	0.44		0.16	0.04	3.21	0.28	23.4	10.8	1.04	2.12	1.12		0.47
	9	2												0	2					
<i>Base(1)</i>																				
<i>_pt2</i>	54.4	29.8		0.17	0.17	0.62	1.03	1.13	2.29	0.20	0.13	4.06	0.17	0.47	3.71	0.42			1.15	
	4	5																		
<i>Base(1)</i>																				
<i>_pt3</i>	99.3					0.09		0.07	0.09			0.16			0.23					
	5																			

B2-L1:

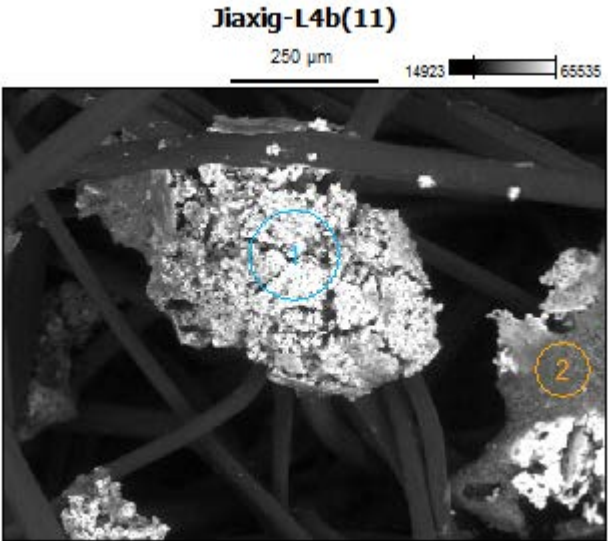
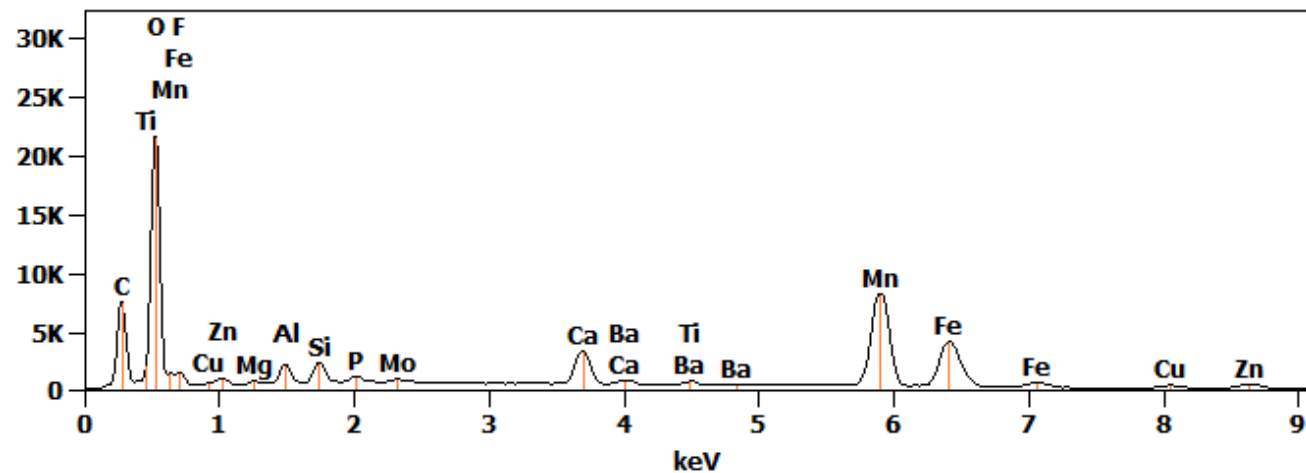


Image Name: Jiaxig-L4b(11)
Image Resolution: 512 by 384
Image Pixel Size: 1.97 μm
Acc. Voltage: 20.0 kV
Magnification: 125

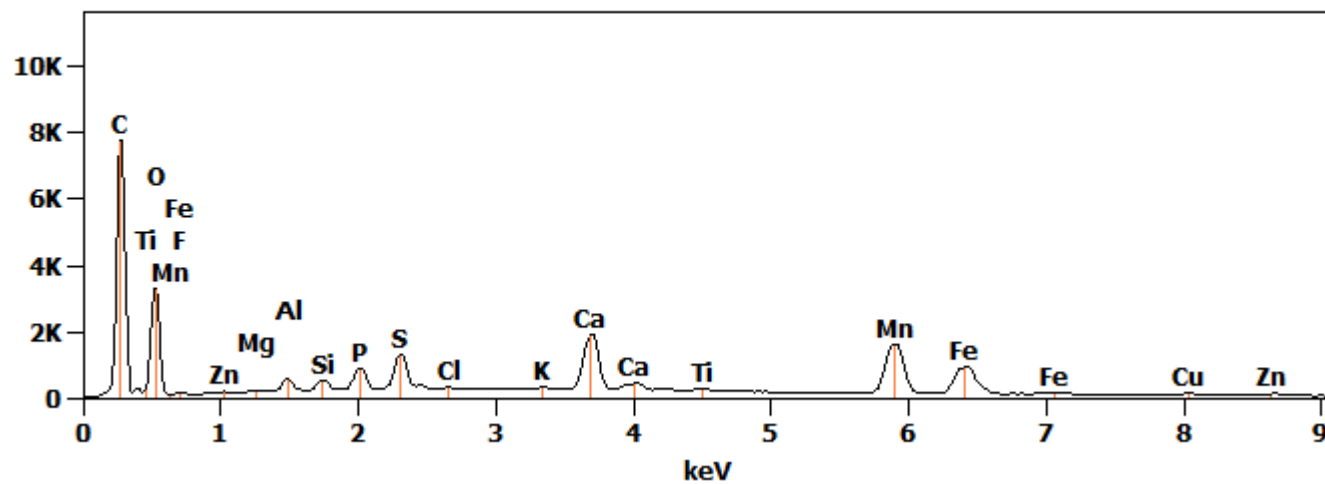
Full scale counts: 21567

Jiaxig-L4b(11)_pt1



Full scale counts: 7725

Jiaxig-L4b(11)_pt2



Net Counts

	C- K	O- K	F- K	Mg- K	Al- K	Si-K	P- K	S- K	Cl-K	K- K	Ca- K	Ti-K	Mn- K	Fe- K	Cu- K	Zn- K	Mo-L	Ba- L
<i>Jiaxig- L4b(11)_pt1</i>	3973	1285	0	1196	1294	1621	6412				3683	1658	1264	5746	2803	4794	4768	4173
	9	14			8	3					6		18	1				
<i>Jiaxig- L4b(11)_pt2</i>	4352	2070	0	433	3108	3010	6943	1183	524	477	2023	785	2291	1248	607	693		
	7	8						4			5		0	4				

Weight %

	C- K	O- K	F- K	Mg- K	Al- K	Si-K	P- K	S- K	Cl- K	K- K	Ca- K	Ti-K	Mn- K	Fe- K	Cu- K	Zn- K	Mo- L	Ba- L
<i>Jiaxig- L4b(11)_pt1</i>	19.30	40.71	0.00	0.14	1.08	1.14	0.38				2.66	0.16	20.73	10.01	0.86	1.77	0.44	0.63
<i>Jiaxig- L4b(11)_pt2</i>	45.13	29.99	0.00	0.11	0.56	0.48	0.96	1.57	0.08	0.08	3.86	0.21	10.00	5.80	0.49	0.68		

Atom %

	C- K	O- K	F- K	Mg- K	Al- K	Si-K	P- K	S- K	Cl-K	K- K	Ca- K	Ti-K	Mn- K	Fe- K	Cu- K	Zn- K	Mo- L	Ba- L
<i>Jiaxig-L4b(11)_pt1</i>	32.62	51.65	0.00	0.12	0.81	0.82	0.25				1.35	0.07	7.66	3.64	0.27	0.55	0.09	0.09
<i>Jiaxig-L4b(11)_pt2</i>	60.97	30.41	0.00	0.07	0.34	0.27	0.51	0.79	0.04	0.03	1.56	0.07	2.95	1.69	0.12	0.17		

Formula

	C- K	O- K	F- K	Mg- K	Al- K	Si- K	P- K	S- K	Cl- K	K- K	Ca- K	Ti- K	Mn- K	Fe- K	Cu- K	Zn- K	Mo- L	Ba- L
<i>Jiaxig-L4b(11)_pt1</i>	C	O	F	Mg	Al	Si	P				Ca	Ti	Mn	Fe	Cu	Zn	Mo	Ba
<i>Jiaxig-L4b(11)_pt2</i>	C	O	F	Mg	Al	Si	P	S	Cl	K	Ca	Ti	Mn	Fe	Cu	Zn		

Compound %

	C	O	F	Mg	Al	Si	P	S	Cl	K	Ca	Ti	Mn	Fe	Cu	Zn	Mo	Ba
<i>Jiaxig-L4b(11)_pt1</i>	19.30	40.71	0.00	0.14	1.08	1.14	0.38				2.66	0.16	20.73	10.01	0.86	1.77	0.44	0.63
<i>Jiaxig-L4b(11)_pt2</i>	45.13	29.99	0.00	0.11	0.56	0.48	0.96	1.57	0.08	0.08	3.86	0.21	10.00	5.80	0.49	0.68		

B2-L2:

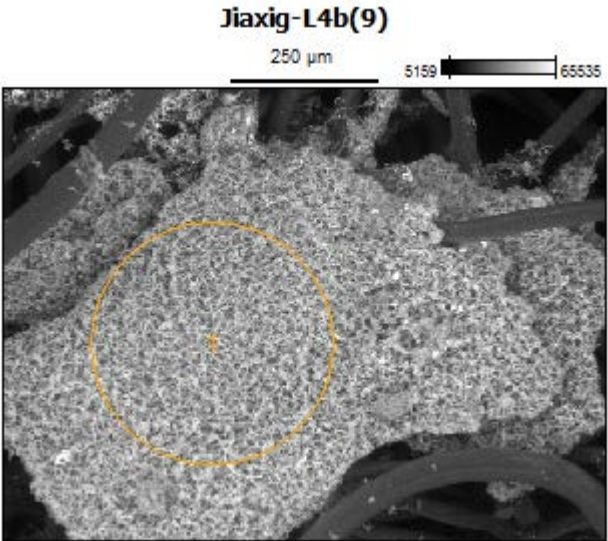
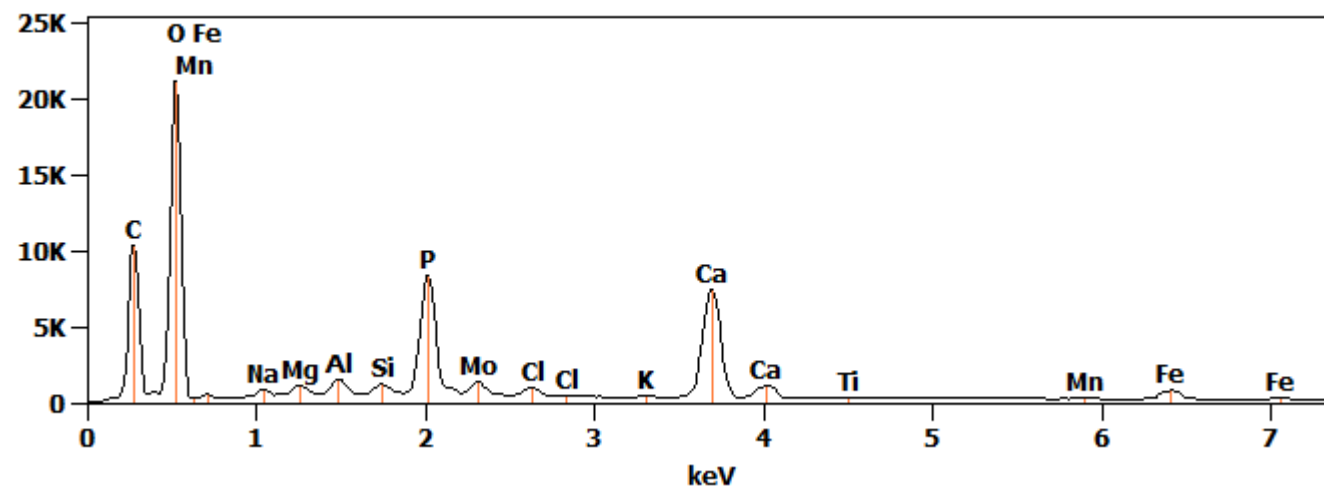


Image Name:	Jiaxig-L4b(9)
Image Resolution:	512 by 384
Image Pixel Size:	1.97 μm
Acc. Voltage:	20.0 kV
Magnification:	125

Full scale counts: 21184

Jiaxig-L4b(9)_pt1



Net Counts

	<i>C-K</i>	<i>O-K</i>	<i>Na-K</i>	<i>Mg-K</i>	<i>Al-K</i>	<i>Si-K</i>	<i>P-K</i>	<i>Cl-K</i>	<i>K-K</i>	<i>Ca-K</i>	<i>Ti-K</i>	<i>Mn-K</i>	<i>Fe-K</i>	<i>Mo-L</i>
<i>Jiaxig-L4b(9)_pt1</i>	55184	123276	2663	5003	6906	5477	82896	7462	864	90997	563	831	10249	13907

Weight %

	<i>C-K</i>	<i>O-K</i>	<i>Na-K</i>	<i>Mg-K</i>	<i>Al-K</i>	<i>Si-K</i>	<i>P-K</i>	<i>Cl-K</i>	<i>K-K</i>	<i>Ca-K</i>	<i>Ti-K</i>	<i>Mn-K</i>	<i>Fe-K</i>	<i>Mo-L</i>
<i>Jiaxig-L4b(9)_pt1</i>	25.87	56.86	0.38	0.46	0.48	0.34	4.51	0.48	0.06	7.15	0.06	0.15	1.94	1.26

Atom %

	<i>C-K</i>	<i>O-K</i>	<i>Na-K</i>	<i>Mg-K</i>	<i>Al-K</i>	<i>Si-K</i>	<i>P-K</i>	<i>Cl-K</i>	<i>K-K</i>	<i>Ca-K</i>	<i>Ti-K</i>	<i>Mn-K</i>	<i>Fe-K</i>	<i>Mo-L</i>
<i>Jiaxig-L4b(9)_pt1</i>	34.94	57.66	0.27	0.31	0.29	0.19	2.36	0.22	0.03	2.89	0.02	0.04	0.56	0.21

Formula

	<i>C-K</i>	<i>O-K</i>	<i>Na-K</i>	<i>Mg-K</i>	<i>Al-K</i>	<i>Si-K</i>	<i>P-K</i>	<i>Cl-K</i>	<i>K-K</i>	<i>Ca-K</i>	<i>Ti-K</i>	<i>Mn-K</i>	<i>Fe-K</i>	<i>Mo-L</i>
<i>Jiaxig-L4b(9)_pt1</i>	C	O	Na	Mg	Al	Si	P	Cl	K	Ca	Ti	Mn	Fe	Mo

Compound %

	<i>C</i>	<i>O</i>	<i>Na</i>	<i>Mg</i>	<i>Al</i>	<i>Si</i>	<i>P</i>	<i>Cl</i>	<i>K</i>	<i>Ca</i>	<i>Ti</i>	<i>Mn</i>	<i>Fe</i>	<i>Mo</i>
<i>Jiaxig-L4b(9)_pt1</i>	25.87	56.86	0.38	0.46	0.48	0.34	4.51	0.48	0.06	7.15	0.06	0.15	1.94	1.26

B2-L3:

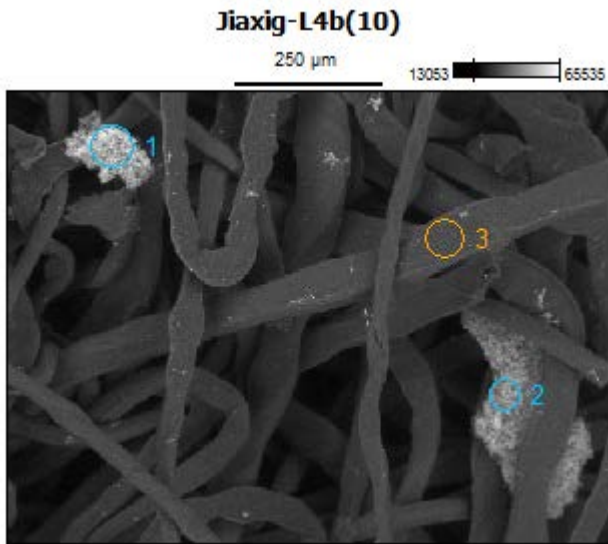
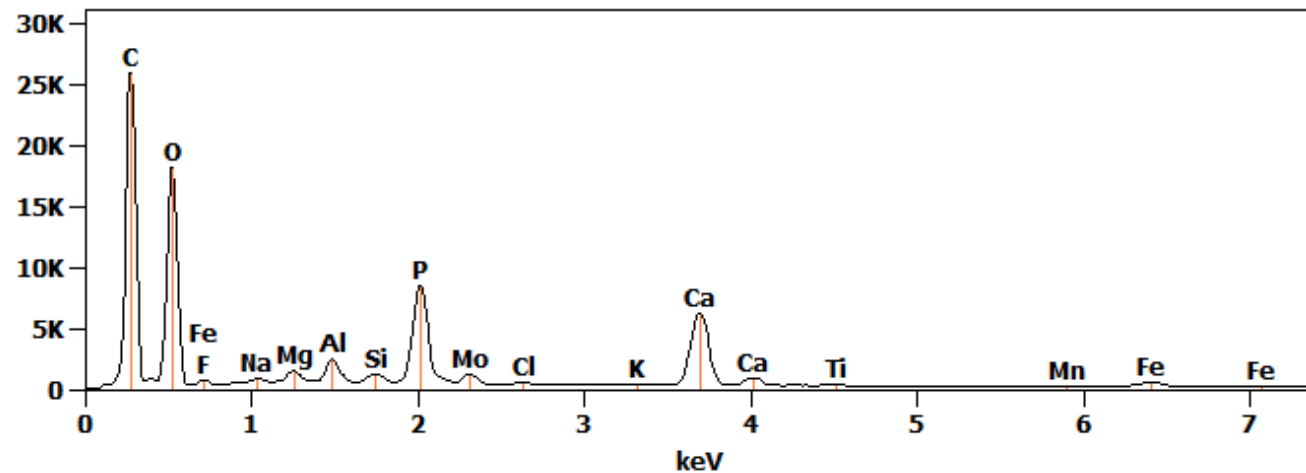


Image Name: Jiaxig-L4b(10)
Image Resolution: 512 by 384
Image Pixel Size: 1.97 μm
Acc. Voltage: 20.0 kV
Magnification: 125

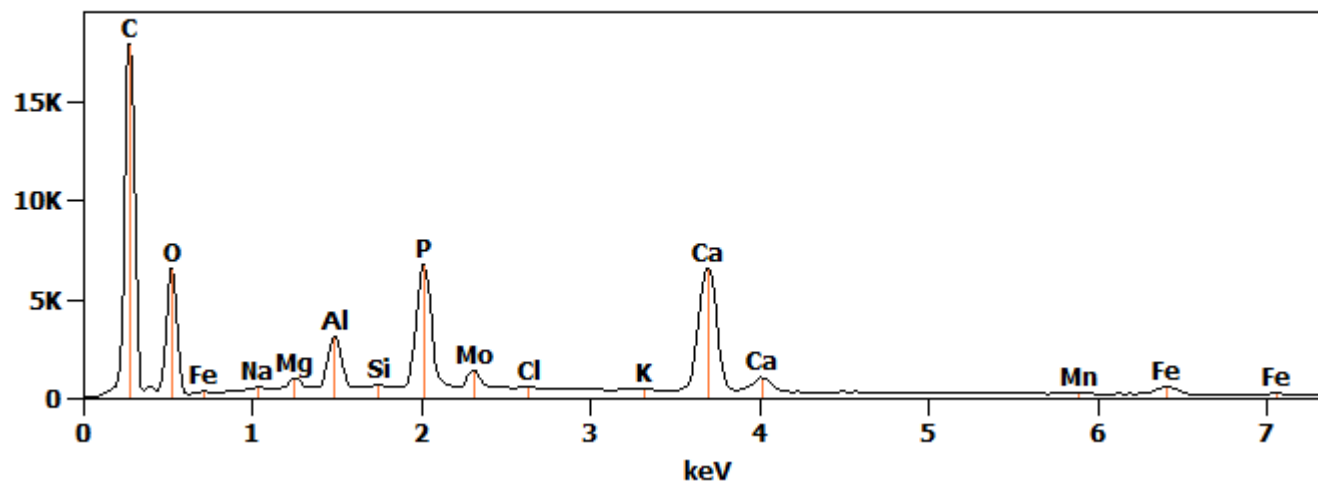
Full scale counts: 25855

Jiaxig-L4b(10)_pt1



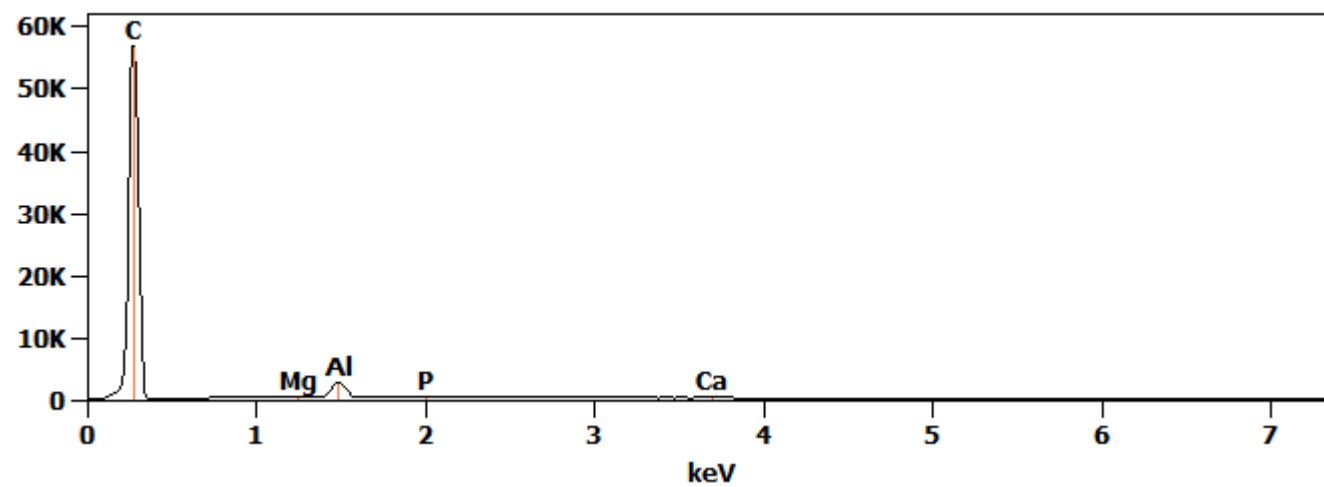
Full scale counts: 17857

Jiaxig-L4b(10)_pt2



Full scale counts: 56677

Jiaxig-L4b(10)_pt3



Net Counts

	<i>C-K</i>	<i>O-K</i>	<i>F-K</i>	<i>Na-K</i>	<i>Mg-K</i>	<i>Al-K</i>	<i>Si-K</i>	<i>P-K</i>	<i>Cl-K</i>	<i>K-K</i>	<i>Ca-K</i>	<i>Ti-K</i>	<i>Mn-K</i>	<i>Fe-K</i>	<i>Mo-L</i>
<i>Jiaxig-L4b(10)_pt1</i>	141314	102872	0	2217	6217	13435	5111	85374	4249	631	76378	543	736	7641	11425
<i>Jiaxig-L4b(10)_pt2</i>	95795	35873		1055	4200	21206	1775	65896	3713	702	80503		684	5329	14748
<i>Jiaxig-L4b(10)_pt3</i>	303230				956	20996		713			775				

Weight %

	<i>C-K</i>	<i>O-K</i>	<i>F-K</i>	<i>Na-K</i>	<i>Mg-K</i>	<i>Al-K</i>	<i>Si-K</i>	<i>P-K</i>	<i>Cl-K</i>	<i>K-K</i>	<i>Ca-K</i>	<i>Ti-K</i>	<i>Mn-K</i>	<i>Fe-K</i>	<i>Mo-L</i>
<i>Jiaxig-L4b(10)_pt1</i>	42.64	45.39	0.00	0.22	0.41	0.68	0.23	3.50	0.21	0.03	4.62	0.05	0.10	1.12	0.78
<i>Jiaxig-L4b(10)_pt2</i>	49.58	32.40		0.16	0.43	1.69	0.13	4.32	0.29	0.06	7.90		0.15	1.27	1.63
<i>Jiaxig-L4b(10)_pt3</i>	97.70				0.11	2.02		0.06			0.11				

Atom %

	<i>C-K</i>	<i>O-K</i>	<i>F-K</i>	<i>Na-K</i>	<i>Mg-K</i>	<i>Al-K</i>	<i>Si-K</i>	<i>P-K</i>	<i>Cl-K</i>	<i>K-K</i>	<i>Ca-K</i>	<i>Ti-K</i>	<i>Mn-K</i>	<i>Fe-K</i>	<i>Mo-L</i>
<i>Jiaxig-L4b(10)_pt1</i>	52.88	42.26	0.00	0.14	0.25	0.38	0.12	1.68	0.09	0.01	1.72	0.01	0.03	0.30	0.12
<i>Jiaxig-L4b(10)_pt2</i>	62.23	30.53		0.11	0.27	0.94	0.07	2.10	0.12	0.02	2.97		0.04	0.34	0.26
<i>Jiaxig-L4b(10)_pt3</i>	98.98				0.06	0.91		0.02			0.03				

Formula

	<i>C-K</i>	<i>O-K</i>	<i>F-K</i>	<i>Na-K</i>	<i>Mg-K</i>	<i>Al-K</i>	<i>Si-K</i>	<i>P-K</i>	<i>Cl-K</i>	<i>K-K</i>	<i>Ca-K</i>	<i>Ti-K</i>	<i>Mn-K</i>	<i>Fe-K</i>	<i>Mo-L</i>
<i>Jiaxig-L4b(10)_pt1</i>	C	O	F	Na	Mg	Al	Si	P	Cl	K	Ca	Ti	Mn	Fe	Mo
<i>Jiaxig-L4b(10)_pt2</i>	C	O		Na	Mg	Al	Si	P	Cl	K	Ca		Mn	Fe	Mo
<i>Jiaxig-L4b(10)_pt3</i>	C				Mg	Al		P			Ca				

Compound %

	<i>C</i>	<i>O</i>	<i>F</i>	<i>Na</i>	<i>Mg</i>	<i>Al</i>	<i>Si</i>	<i>P</i>	<i>Cl</i>	<i>K</i>	<i>Ca</i>	<i>Ti</i>	<i>Mn</i>	<i>Fe</i>	<i>Mo</i>
<i>Jiaxig-L4b(10)_pt1</i>	42.64	45.39	0.00	0.22	0.41	0.68	0.23	3.50	0.21	0.03	4.62	0.05	0.10	1.12	0.78
<i>Jiaxig-L4b(10)_pt2</i>	49.58	32.40		0.16	0.43	1.69	0.13	4.32	0.29	0.06	7.90		0.15	1.27	1.63
<i>Jiaxig-L4b(10)_pt3</i>	97.70				0.11	2.02		0.06			0.11				

B2-L4:

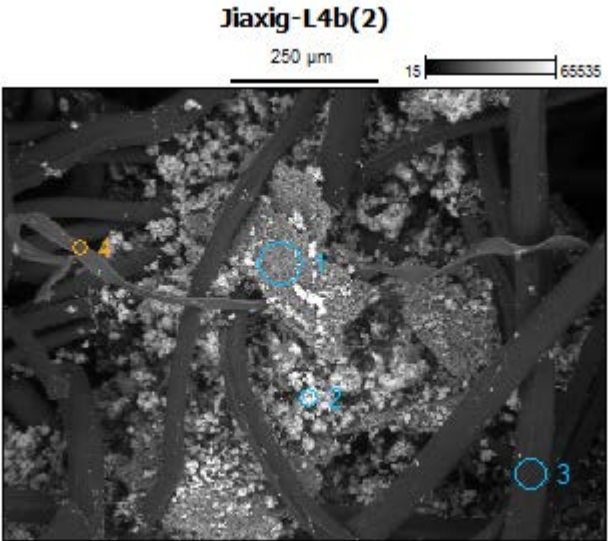
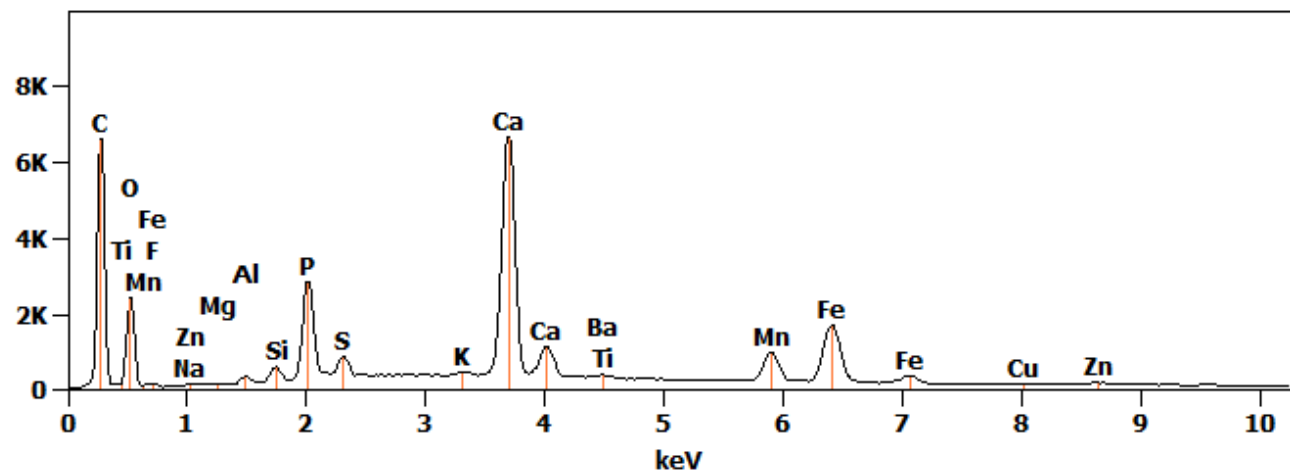


Image Name:	Jiaxig-L4b(2)
Image Resolution:	512 by 384
Image Pixel Size:	1.97 μm
Acc. Voltage:	20.0 kV
Magnification:	125

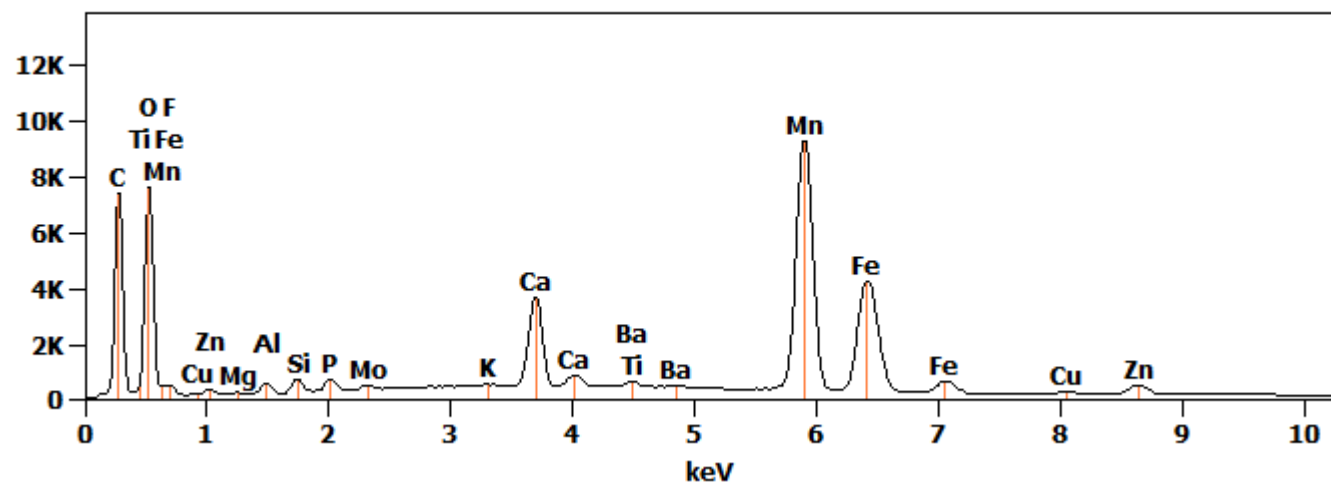
Full scale counts: 6657

Jiaxig-L4b(2)_pt1



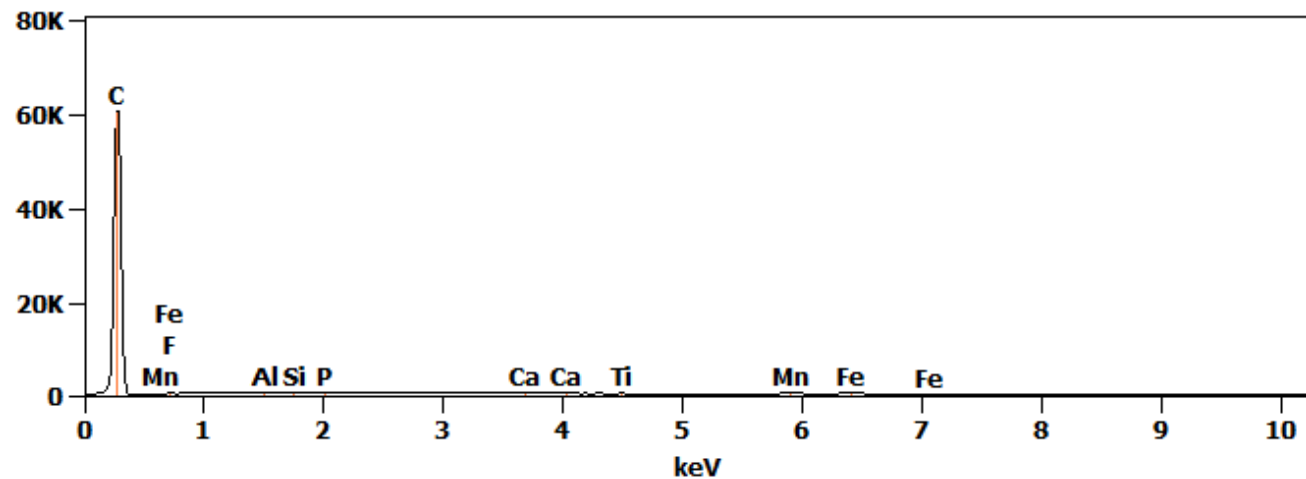
Full scale counts: 9234

Jiaxig-L4b(2)_pt2



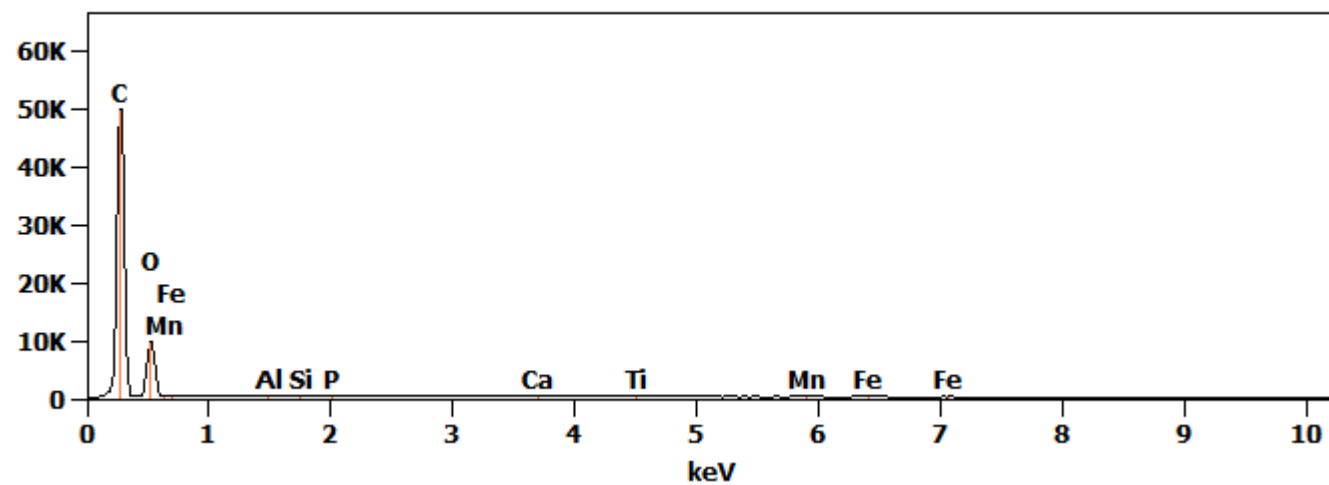
Full scale counts: 60602

Jiaxig-L4b(2)_pt3



Full scale counts: 49934

Jiaxig-L4b(2)_pt4



Net Counts

	C- K	O- K	F- K	Na- K	Mg- K	Al- K	Si-K	P- K	S- K	K- K	Ca- K	Ti-K	Mn- K	Fe- K	Cu- K	Zn- K	Mo- L	Ba- L	
<i>Jiaxig- L4b(2)_pt1</i>	3801 2	1537 8	0	147	290	1240	3428	2749 0	5543	867	8050 0	623	1112 4	2467 2	528	1765		1514	
<i>Jiaxig- L4b(2)_pt2</i>	3866 8	4541 9	0		348	3115	4635	4879		779	4181 1	731	1429 82	6151 0	1541	6116	2756	3733	
<i>Jiaxig- L4b(2)_pt3</i>	3299 89		0			404	960	817			2241	210	4169	4235					
<i>Jiaxig- L4b(2)_pt4</i>	2775 64	5336 4				909	1838	1122			3361	560	6065	7376					

Weight %

	C- K	O- K	F- K	Na- K	Mg- K	Al- K	Si-K	P- K	S- K	K- K	Ca- K	Ti-K	Mn- K	Fe- K	Cu- K	Zn- K	Mo-L	Ba- L
<i>Jiaxig- L4b(2)_pt1</i>	39.16	24.30	0.00	0.05	0.07	0.21	0.50	3.48	0.68	0.13	13.90	0.16	4.43	10.41	0.38	1.54		0.59
<i>Jiaxig- L4b(2)_pt2</i>	24.56	22.39	0.00		0.06	0.36	0.43	0.38		0.07	3.83	0.09	29.74	13.58	0.60	2.87	0.33	0.71
<i>Jiaxig- L4b(2)_pt3</i>	96.65		0.00			0.04	0.09	0.07			0.31	0.04	1.34	1.46				
<i>Jiaxig- L4b(2)_pt4</i>	62.99	34.11				0.06	0.10	0.06			0.25	0.06	1.04	1.35				

Atom %

	C- K	O- K	F- K	Na- K	Mg- K	Al- K	Si-K	P- K	S- K	K- K	Ca- K	Ti-K	Mn- K	Fe- K	Cu- K	Zn- K	Mo-L	Ba- L
<i>Jiaxig- L4b(2)_pt1</i>	58.24	27.14	0.00	0.04	0.05	0.14	0.32	2.01	0.38	0.06	6.20	0.06	1.44	3.33	0.11	0.42		0.08
<i>Jiaxig- L4b(2)_pt2</i>	46.13	31.56	0.00		0.05	0.30	0.35	0.28		0.04	2.16	0.04	12.21	5.48	0.21	0.99	0.08	0.12
<i>Jiaxig- L4b(2)_pt3</i>	99.19		0.00			0.02	0.04	0.03			0.09	0.01	0.30	0.32				
<i>Jiaxig- L4b(2)_pt4</i>	70.54	28.68				0.03	0.05	0.02			0.08	0.02	0.25	0.33				

Formula

	<i>C-</i>	<i>O-</i>	<i>F-</i>	<i>Na-</i>	<i>Mg-</i>	<i>Al-</i>	<i>Si-</i>	<i>P-</i>	<i>S-</i>	<i>K-</i>	<i>Ca-</i>	<i>Ti-</i>	<i>Mn-</i>	<i>Fe-</i>	<i>Cu-</i>	<i>Zn-</i>	<i>Mo-</i>	<i>Ba-</i>
	<i>K</i>	<i>K</i>	<i>K</i>	<i>K</i>	<i>K</i>	<i>K</i>	<i>K</i>	<i>K</i>	<i>K</i>	<i>K</i>	<i>K</i>	<i>K</i>	<i>K</i>	<i>K</i>	<i>K</i>	<i>K</i>	<i>L</i>	<i>L</i>
<i>Jiaxig-L4b(2)_pt1</i>	C	O	F	Na	Mg	Al	Si	P	S	K	Ca	Ti	Mn	Fe	Cu	Zn		Ba
<i>Jiaxig-L4b(2)_pt2</i>	C	O	F		Mg	Al	Si	P		K	Ca	Ti	Mn	Fe	Cu	Zn	Mo	Ba
<i>Jiaxig-L4b(2)_pt3</i>	C		F			Al	Si	P			Ca	Ti	Mn	Fe				
<i>Jiaxig-L4b(2)_pt4</i>	C	O				Al	Si	P			Ca	Ti	Mn	Fe				

Compound %

	<i>C</i>	<i>O</i>	<i>F</i>	<i>Na</i>	<i>Mg</i>	<i>Al</i>	<i>Si</i>	<i>P</i>	<i>S</i>	<i>K</i>	<i>Ca</i>	<i>Ti</i>	<i>Mn</i>	<i>Fe</i>	<i>Cu</i>	<i>Zn</i>	<i>Mo</i>	<i>Ba</i>
<i>Jiaxig-L4b(2)_pt1</i>	39.16	24.30	0.00	0.05	0.07	0.21	0.50	3.48	0.68	0.13	13.90	0.16	4.43	10.41	0.38	1.54		0.59
<i>Jiaxig-L4b(2)_pt2</i>	24.56	22.39	0.00		0.06	0.36	0.43	0.38		0.07	3.83	0.09	29.74	13.58	0.60	2.87	0.33	0.71
<i>Jiaxig-L4b(2)_pt3</i>	96.65		0.00			0.04	0.09	0.07			0.31	0.04	1.34	1.46				
<i>Jiaxig-L4b(2)_pt4</i>	62.99	34.11				0.06	0.10	0.06			0.25	0.06	1.04	1.35				

